PSI Report No. 13-02
August 2013
ISSN 1019-0643

Modelling of air quality in Switzerland in the context of the revision of the Gothenburg Protocol

Final Report

Sebnem Aksoyoglu, Johannes Keller, Michel Tinguely, André S. H. Prévôt

General Energy Research Department

Laboratory of Atmospheric Chemistry
Paul Scherrer Institute, 5232 Villigen PSI

This project was financially supported by the Federal Office for the Environment, FOEN

Summary

In this project, we studied the changes in air quality due to emission reductions in Europe with a focus on Switzerland using an air quality model (CAMx). We performed the model simulations for the following entire years: 1990 (for retrospective analysis); 2005 (as the reference year); 2006 (for model validation) and 2020 (using three emission scenarios prepared by IIASA in the framework of the revision of the Gothenburg protocol). We used the same meteorology of the year 2006 (modelled by the WRF meteorological model) in all cases. The focus in this study was on ozone, PM2.5 and PM10. We analysed the model results as relative differences with respect to the reference year 2005. The investigated parameters were annual average concentrations of ozone, PM2.5 and PM10, indicators for ozone impacts on forests (AOT40) and health (SOMO35) as well as nitrogen deposition. We discuss the results for Switzerland only in this report; the figures for the rest of Europe can be found in the Appendix.

Comparisons of model results with various detailed measurement data suggest that the model reproduced the concentrations of the gaseous and particulate species quite well, except for a few discrepancies in winter that occurred mainly during periods with strong inversions, which are not well captured by the meteorological model.

Among the three scenarios BL (baseline), Mid and MTFR (Maximum Technically Feasible Reduction), the BL scenario is the closest to the recently revised Gothenburg Protocol. The predicted anthropogenic emissions for 2020 in Europe are lower than those in 2005 and the differences vary according to pollutant, source and country.

We chose 1990 for the retrospective analysis, because it was the reference year for the first Gothenburg Protocol. We simulated the air quality in 1990 using emission data for that year and compared the results with measurements. The modelled relative decreases of 35-45% in annual average concentrations of PM2.5 and PM10 between 1990 and 2005 agree quite well with those from measurements at various sites in Switzerland. The absolute values of modelled AOT40 and SOMO35 for 2005 also match the data obtained from measurements. The model results suggest a significant decrease in AOT40 since 1990. Observations however, show not only a decrease at some rural sites but also an increase at urban sites during that period. A similar discrepancy was also found for SOMO35. Since calculation of AOT40 and SOMO35 is very sensitive to the threshold values, the background ozone concentrations might affect the model results. We repeated the simulations for 1990 with lower background ozone concentrations and found that the discrepancy between the model results and measurements became smaller but did not disappear. Even though the background ozone concentrations used in the model for 1990 and 2005 were based on observations, they might need further revision to be addressed in a follow-up project.

The modelled PM2.5 concentrations in 2005 varied between 10 – 15 μg m^{-3} in Switzerland and PM2.5 / PM10 ratio was about 80%. Emission reductions according to the baseline scenario would lead to about a 30% decrease in PM2.5 concentrations in 2020. The largest decrease in PM2.5 was predicted to be about 45% using the MTFR scenario. On the other hand, the annual average ozone concentrations would decrease only by about 5% over the Alpine regions and would continue to increase in the Swiss Plateau. Further analysis of our results suggests

that although emission reductions do lead to a decrease in peak ozone concentrations, they also cause an increase in low ozone concentrations especially in urban areas due to less titration with NO. AOT40 values, which refer to ozone levels above 40 ppb, were predicted to decrease in 2020 by more than 50% during the vegetation period. The health-relevant indicator SOMO35 for 2020 was also predicted to be lower by about 30-40% with respect to the reference year 2005. However - as discussed above - these two indicators depend strongly on the background ozone concentration and its evolution.

In addition to the pollutant concentrations, we analysed the nitrogen deposition as well. We modelled both dry and wet deposition of all oxidized and reduced nitrogen species. The highest modelled nitrogen depositions are over the Swiss Plateau and in southern Switzerland (20-25 kg N $ha^{-1}.y^{-1}$). The depositions of the reduced nitrogen species ammonia and particulate ammonium in Switzerland were found to be larger than the deposition of the oxidized species and they occur mainly north of the Alps where ammonia emissions are the highest. The results of the retrospective study indicated a decrease of 10 – 30% in nitrogen deposition since 1990. Applying the baseline scenario, we found that the nitrogen deposition would decrease by about 25% in 2020 compared to 2005, mainly due to the reduction in the oxidized fraction.

The results obtained in this modelling study show the need for a detailed analysis of background ozone concentrations for use in calculating AOT40 and SOMO35 trends. These vegetation and health impact indicators are very sensitive to that parameter.

The modelled data obtained in this project for different years using various emission scenarios provide a valuable starting point for further, more detailed analyses of individual aerosol species, their trends, seasonal variations and deposition rates.

Table of Contents

1 Introduction

Air quality is important for the human health, crop growth and ecological system. Air pollution can affect our health in many ways such as irritation to the eye, nose and throat, chronic respiratory and cardiovascular diseases [*Pope and Dockery*, 2006]. One of Europe's main environmental concerns is the air pollution and current policy focuses mainly on ozone (O_3) and particulate matter (PM10 and PM2.5). In spite of the current legislation devoted to air pollution control, ozone and PM10 levels often exceed the ambient air quality standards in Europe (standard for ozone is 120 $\mu g\ m^{-3}$ maximum daily 8-hour mean, for PM10 50 $\mu g\ m^{-3}$ daily mean).

In an earlier study we calculated the effects of numerous regulations enforced in Europe since 1985 and predicted the effects of Gothenburg protocol targets for 2010 on ozone [*Andreani-Aksoyoglu et al.*, 2008]. Our results suggested that the decrease in local ozone production due to emission reductions might have been partly or completely compensated by the simultaneous increase in the background ozone, indicating that the further development of the background ozone concentrations in Europe would be very important for tropospheric ozone levels. The ozone precursor emissions in Europe and in North America have decreased significantly since 1980s while NO_x emissions increased dramatically in Asia in the last decade [*Zhang et al.*, 2010]. Ozone concentrations in Europe can therefore be affected by emissions from other continents due to its sufficiently long lifetime.

In 2007, the Convention on Long-Range Transboundary Air Pollution initiated the revision of its Gothenburg multi-pollutant/multi-effect protocol [*UNECE*, 1999]. In the revised protocol, fine particulate matter (PM2.5) was included. The EMEP Centre for Integrated Assessment Modelling (CIAM) at IIASA prepared various emission control scenarios for cost-effective improvements of air quality in Europe in 2020 using the GAINS (Greenhouse gas – Air pollution Interactions and Synergies) model.

In this study, we used the CAMx air quality model with a horizontal resolution higher than the EMEP model to simulate the air quality for 2020 using various emission scenarios. We investigated the effects of emission reductions on ozone and particulate matter in Europe with a focus on Switzerland. We also performed model simulations for 1990 and evaluated the changes in air quality since then. In this report, we discussed the changes in annual average concentrations of pollutants, nitrogen deposition and damage indicators AOT40 and SOMO35 between the reference year 2005 and 2020 as well as between 1990 and 2005.

2 Method

In this project we used the 3-dimensional air quality model CAMx (Comprehensive Air quality Model with extensions, http://www.camx.com) and meteorological model WRF (Weather Research and Forecasting Model, http://wrf-model.org/index.php). Details of these two models are given in the Appendix 1.

The coarse model domain covered whole Europe with a horizontal resolution of 0.250º x 0.125º (Fig. 2.1). A second, nested domain with three times higher resolution covered Switzerland. There were 31 layers in WRF of which 14 were used in CAMx. The lowest CAMx layer (surface layer) was 20 m above ground and the top of the model was at about 7 km a.s.l. Details on model parameterization can be found in *Aksoyoglu et al.*, [2011]. The model results in the lowest layer of the nested domain with higher resolution were discussed in this report.

The meteorological model WRF was reinitialized every four days while we ran the chemical transport model CAMx continuously for the entire year. We calculated the meteorological fields for 2006 with the WRF model and used them for all the CAMx simulations with different emission scenarios shown in Table 2.1. The details of emissions are given in Chapter 3. We performed the model validation using available data from measurement campaigns (with aerosol mass spectrometer, AMS) and monitoring networks (NABEL) for the year 2006. The reference year is 2005 for comparison with various future emission scenarios.

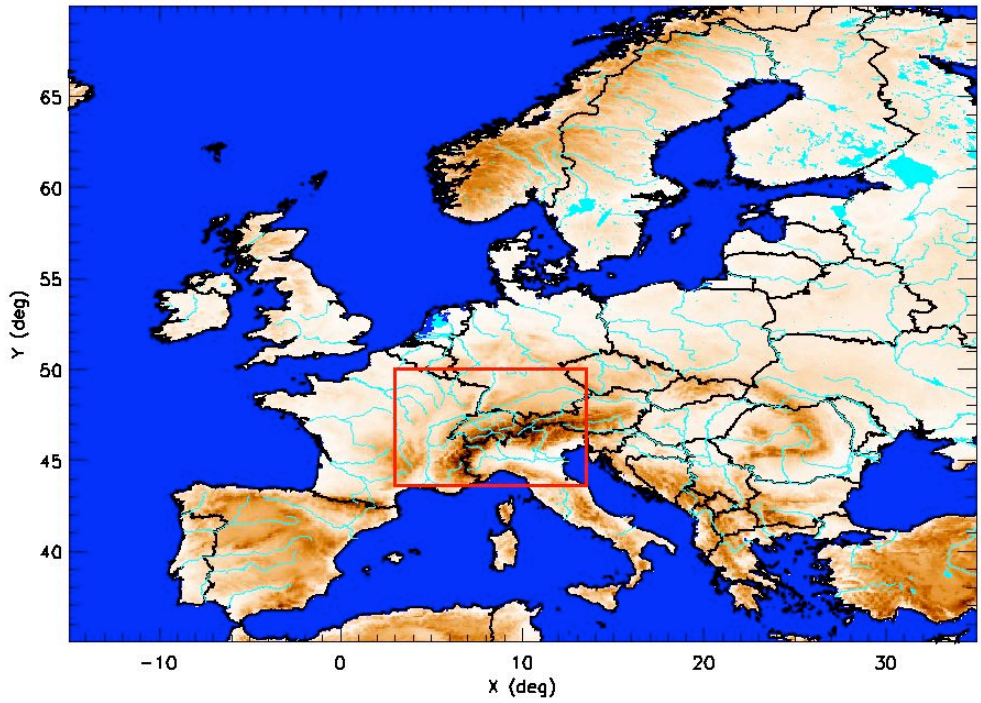

Figure 2.1: Model domains in latitude-longitude coordinates. Horizontal resolution: Domain 1: 0.250º x 0.125º, Domain 2 (in red): 0.083º x 0.042º

Table 2.1 Description of emission scenarios

Name	year	Description	CEIP / GAINS scenario
V	2006	model validation	CEIP 2006
RC:	2005	Reference case	CEIP 2005,CIAM4-PRIMES-baseline
BL	2020	Baseline	GAINS CIAM4-PRIMES-baseline
Mid	2020	Mid	GAINS CIAM4-PRIMES-Mid
MTFR	2020	Maximum technically feasible reduction	GAINS CIAM4-PRIMES-MTFR
Retro 1	1990	Retrospective analysis with lower background ozone than in 2005	CEIP 1990, Goth_NAT_July2011 (for PM2.5 and PM10)
Retro 2	1990	Retrospective analysis with same background ozone as in 2005	Same as Retro 1

Initial and boundary concentrations for the reference year (2005) were extracted from the output of the global model MOZART [*Horowitz et al.*, 2003]. The choice of the background ozone is crucial in air quality simulations and for predicting the effect of emission reductions [*Andreani-Aksoyoglu et al.*, 2008]. A recent analysis of various ozone observation data in Europe showed that ozone increased in the 1980s and 1990s but started decreasing slowly in summer in the 2000s with no significant changes in other seasons [*Logan et al.*, 2012]. Authors indicate the inconsistencies in various data sets leading to different trends. It is therefore very difficult to choose a realistic background ozone concentration for the model domain and for the period of interest. In this work, we kept the background ozone concentrations constant for the period between 2005 and 2020 (see Table 2.2) based on observations [*Wilson et al.*, 2012; *Logan et al.*, 2012]. We performed simulations for 1990 however with two different background ozone concentrations. In Retro 1 scenario, background ozone concentration in 1990 is 5 ppb lower than those in the other scenarios for 2005 and later. In Retro 2, we kept ozone concentrations the same as in the other scenarios assuming that background ozone did not change anymore between 1990 and 2005.

Table 2.2: Ozone concentrations (ppb) used in the initial and boundary concentrations for various seasons (DJF: December, January, February, MAM: March, April, May, JJA: June, July, August, SON: September, October, November).

Scenario	DJF	MAM	JJA	SON
V 2006	40	45	50	45
RC 2005	40	45	50	45
BL, Mid, MTFR 2020	40	45	50	45
Retro 1 (1990)	35	40	45	40
Retro 2 (1990)	40	45	50	45

3 Emissions

Emissions originate from both biogenic and anthropogenic sources. We calculated the biogenic emissions using our own model (see Chapter 3.4). Raw anthropogenic emission data for air quality models are usually available as gridded annual emission totals of a set of species released by specific source categories. In general, the species are restricted to explicit inorganic pollutants (NO_x, SO_2, CO etc.), non-methane volatile organic compounds (NMVOC) and particulate matter (PM10, PM2.5). The data provider specifies the projection of the grid, which is adapted to the domain of interest (e.g. lat / lon for global or European emissions, oblique Mercator projection for Switzerland). Hence, this data has to be transformed to the requirements of the chemical mechanism for the model domain of interest. In the current set-up of CAMx, NMVOC are split into lumped species according to the chemical reaction scheme CB05 (Carbon Bond Mechanism 5) [*Yarwood et al.*, 2005]. This lumped mechanism is based on chemical bonds. Each of the CB05 species is characterized by specific properties such as the reaction rate constant.

Particulate matter is usually reported as total PM10 and PM2.5. To split those emissions into primary elemental carbon (PEC) and primary organic aerosols (POA), we estimated the ratio POA / (POA+PEC) as 0.6 on the basis of published measurements [*Szidat et al.*, 2006; *Alfarra et al.*, 2007]. The authors found that the observed ratio varies substantially with time, emission source and location.

Gridded emissions refer to a specific year. In order to harmonize data from different sources and reference years, emissions have to be converted to a common reference year. We normalized the data using annual emission totals for each country. There are two data sources available. The first one is the Centre of Emission Inventories and Projections (CEIP) of the European Monitoring and Evaluation Programme (EMEP) that manages a database of annual emissions until 2009 submitted by the European countries (http://www.ceip.at/webdab-emission-database/emissions-as-used-in-emep-models/). The second data source is the International Institute for Applied Systems Analysis (IIASA) that runs the GAINS model (Greenhouse Gas and Air Pollution Interactions and Synergies) for emission projections until 2020 on the basis of the economic development assumed for each country (http://gains.iiasa.ac.at/gains/EUN/index.login). Numerous scenarios for different economy and technology related assumptions are available.

.

3.1 European Anthropogenic Emissions

We used the gridded TNO/MACC emission inventory (http://www.gmes-atmosphere.eu/) for 2006 as the basic anthropogenic emission inventory [*Denier van der Gon et al.*, 2010]. It was also used to prepare gridded, hourly emissions for other years by scaling it with annual data from CEIP and GAINS. Information on the TNO / MACC inventory is given in Table 3.1. Each grid cell may contain emissions from different source areas (see Table 3.2). For instance, grid cells located on the borderline of two countries contain two contributions. Ship emissions are reported as off-road (SNAP 8) emissions for the 5 major water bodies Atlantic Ocean, Baltic Sea, North Sea, Mediterranean Sea and Black Sea. Note that grid cells within coastal areas usually have contributions from international shipping and from off-road traffic of the respective country. Annual, weekly and diurnal time variations are provided as well. The diurnal dependence refers to the civil time of each country, e.g. Central European Summer Time (CEST) for France or British Summer Time (BST) for UK in summer. Hence, for each country the diurnal time function has to be shifted to UTC

specified as the standard time for the whole domain, which is also the common time zone in WRF and CAMx.

The NMVOC of each SNAP category into the species of the CB05 mechanism are split according to the rules suggested by TNO. As an alternative, the CB05 species can be calculated on the basis of the explicit compound distribution for each SNAP category as proposed by Passant [2002] and the conversion rules provided by ENVIRON [*Yarwood et al.*, 2005].

Table 3.1: Features of the European anthropogenic emission inventory TNO/MACC

projection	geographic (lat / lon)
longitude range	-15 to 35 deg E
latitude range	35 to 70 deg N
longitude grid cell size	0.125 deg (9.5 km at 47 deg N)
latitude grid cell size	0.0625 deg (6.9 km)
no. WE grid cells	400
no. SN grid cells	560
species	NOx, SO2, CO, NH3, NMVOC, CH4, PM10, PM2.5
Unit	t $year^{-1}$ grid $cell^{-1}$
source categories of land emissions	according to SNAP (Tab. 3.2)
source category of ship emissions	SNAP 8 (off-road)
reference year	2006

Table 3.2: SNAP categories of the European emissions

SNAP	Description
1	public power, cogeneration and district heating plants
2	commercial, institutional and residential combustion
3	industrial combustion and processes with combustion
4	non-combustion production processes
5	extraction and distribution of fossil fuels
6	solvent use
71	road transport gasoline
72	road transport diesel
73	road transport, liquefied petroleum gas (LPG)
74	road transport evaporation
75	road transport, brake-wear
8	other mobile sources and machinery (off-road)
9	waste treatment and disposal
10	agriculture

3.2 Swiss Anthropogenic Emissions

The gridded Swiss anthropogenic emissions are not available as a single harmonised data set but are provided by different partners. They are not classified according to a common scheme such as the SNAP emission categories. Moreover, the reference years and the grid projections, resolutions and offsets may differ. As described below, the data sets delivered refer either to a common emission source or a single

pollutant. These data therefore, were scaled to a common structure as described in Chapter 3.3.

Road traffic

Annual road traffic emissions of NO_x, CO, NMVOC, toluene, benzene, xylene, PM10 and PM2.5 were prepared by INFRAS on the basis of the "Handbook of Emission Factors for Road Transport (HBEFA) [*INFRAS*, 2010]. Data are split into link and zone emissions. The co-ordinates are based on the Swiss co-ordinate system. The spatial resolution is 250 m for NO_x, toluene, benzene, xylene, and 200 m for NMVOC, CO, PM10 and PM2.5. Reference year is 2005 for NMVOC and CO and 2000 for the remaining species. Temporal variations were provided as well [*Heldstab and Wuethrich*, 2006].

Since cars in Switzerland have to fulfil the same emission standards as those of EU (Euro standards), the total NMVOC emission was split into the CB05 species following the rules of Passant [2002] for the SNAP category 7 and of ENVIRON as described above.

Industrial and Residential Sources

Annual NO_x, PM2.5 and PM10 emissions from residential activities, heating, industry, off-road traffic, rail transport (PM only) and agriculture / forestry on a 200 m resolution have been provided in gridded form by Meteotest, based on the national inventory. Reference year of this data set is 2000. Annual totals of PM10 emissions have been split into numerous sub-categories according to *Kropf* [2001] and *Heldstab et al.* [2003]. PM emissions of wood combustion are supposed to be released entirely as PM2.5. INFRAS and Meteotest provided the gridded PM2.5 wood burning emissions from residential and industrial sources. It is important to mention that wood burning emissions have already been included in the 2000 data source, but the spatial distribution was not as detailed as they are now.

Spatial distributions of total annual NMVOC emissions from industry and household were also provided by INFRAS [*Heldstab and Wuethrich*, 2006]. The split into the explicit speciation according to the scheme of Passant and the conversion to CB05 were performed on the basis of a survey of different sources such as paint production, paint use, printing industry, solvent use, etc. [*Schneider*, 2007].

NH_3 Sources

Meteotest provided annual NH_3 emissions for 2000 and 2007 on a 1 km grid. This data includes the sum of emissions from household, industry, road traffic, waste treatment and disposal, agriculture, and natural sources [*Kupper et al.*, 2010].

SO_2 Sources

Sulphur dioxide is mainly emitted by industrial and residential combustion. Electric power generation from thermal plants is negligible in Switzerland. However, emissions in SNAP category 1 are due to district heating plants (including municipal waste incineration plants). Since no gridded SO_2 emission inventory is available, synthetic grids have been created. Those grids have the same spatial distribution as NO_x from industrial and residential sources and the annual total for Switzerland as provided by BAFU (http://www.ceip.at/webdab-emission-database/emissions-as-used-in-emep-models/).

3.3 Scaling emissions for different years and scenarios

The European emission grids for the reference year *yyyyscem* of a given emission scenario were calculated by scaling the raw data (reference year *yyyyref* = *2006* for the European TNO/MACC emissions) using annual emission totals for each country, species and SNAP category. There are 2 cases to be distinguished:

a. *yyyyscem* < *2010*. The annual emissions for each SNAP category are extracted from the EMEP / CEIP database, which includes emissions of the past as submitted by the EMEP member states. Emissions E_{raw} of all grid cells associated to a common country are scaled with the ratio $E_{CEIP}(yyyyscem) / E_{CEIP}(yyyyref)$. This procedure has been applied to calculate the data sets for 2005 (reference scenario) and 1990 (retro scenario).

   PM data are available only for years later than 2000. For the Retro case (1990) a data set was created by scaling 2005 data with GAINS simulations [*Wagner*, 2012]. For countries with missing data for 1990, emissions are supposed to be constant until the first year of submission.

   Ship emissions are available from CEIP back to 1990.

b. *yyyyscem* ≥ *2010*. For the 2020 scenarios the 2005 data were scaled to 2020 using the GAINS CIAM4 / 2011 simulations of the Reference Case RC (2005), BL, MTFR and Mid scenarios (2020).

   For national and international maritime traffic in 2000 and various scenarios in 2020 emission data for NO_x, SO_2 and PM2.5 are compiled by [*Cofala et al.*, 2007]. However, international ship emissions are not subject to the revision of the Gothenburg Protocol. Therefore, those emissions were modified and kept constant for all 2020 scenarios [*Wagner et al.*, 2010].

In Appendix 2 the annual emissions of France, Germany, Austria, Italy, Switzerland and the 5 maritime areas are listed for the various scenarios. Note that for the reference year 2005 the GAINS emissions may substantially differ from those of provided by CEIP, depending on pollutant and SNAP category. There is no GAINS data for CO because it is not included in the Gothenburg Protocol.

Anthropogenic emissions for 2006 (calculated using TNO/MACC inventory) are also given in the tables for comparison.

3.4 Biogenic Emissions

The most abundant BVOC (biogenic volatile organic compounds) species in Switzerland are monoterpenes, which are emitted mainly by Norway spruce and fir trees. Less abundant, but much more reactive is isoprene emitted predominantly by oak trees and, to a lesser extend, by spruce and pasture. NO emissions are caused by bacteriological decomposition in soils. Monoterpene and NO emissions are temperature dependent, whereas the isoprene release is a function of both temperature and shortwave irradiance. Recently, sesquiterpene has also been identified as a relevant species. In [*Andreani-Aksoyoglu and Keller*, 1995] and [*Keller et al.*, 1995] a method for the estimation of biogenic emissions is given. We calculated the gridded biogenic emissions directly for each CAMx domain using the corresponding land use and meteorological data.

First, we converted the global USGS land use data on a 30'' grid, to our domains using the WRF / WPS pre-processors. We then replaced them by the GlobCover 2006 inventory [*ESA_GOFC-GOLD*, 2011]. For each European country the

deciduous and coniferous forest fractions were split into the tree species mentioned above according to *Simpson et al.* [1999]. Inside the Swiss border the global data were replaced by data of the land use statistics (100 m resolution) issued by the Federal office of Statistics [*BFS*, 1999] and by forest data (1 km resolution) taken from the national forest inventory [*Mahrer and Vollenweider*, 1983]. The latter includes the land cover of 10 different tree species, in particular spruce, fir and oak. About 24% of the Swiss area is covered with forests, of which 71% are coniferous. Norway spruce and fir are the most abundant species (67 and 20 % of the coniferous forests, respectively). Oak trees on the other hand, contribute only 8% to deciduous trees. Gridded temperature and shortwave irradiance data were extracted from the WRF output. The total BVOC emissions modelled for 2006 are 100.5 kt in Switzerland and they are composed of monoterpenes (95%), sesquiterpenes (3%) and isoprene (2%). The distribution of BVOC emissions on Swiss grid cells is shown in Fig. 3.1. The annual BVOC emissions for 2006 are comparable to the anthropogenic NMVOC emissions for 2005, but in 2020 anthropogenic emissions would be lower (see Table A2.5). This indicates the increasing importance of biogenic emissions with further reductions of anthropogenic NMVOC emissions.

Currently the biogenic emission inventory is being improved by extending the number of species and trees, using best available land use data, and including updated temperature and irradiance dependencies [*Oderbolz et al.*, 2013].

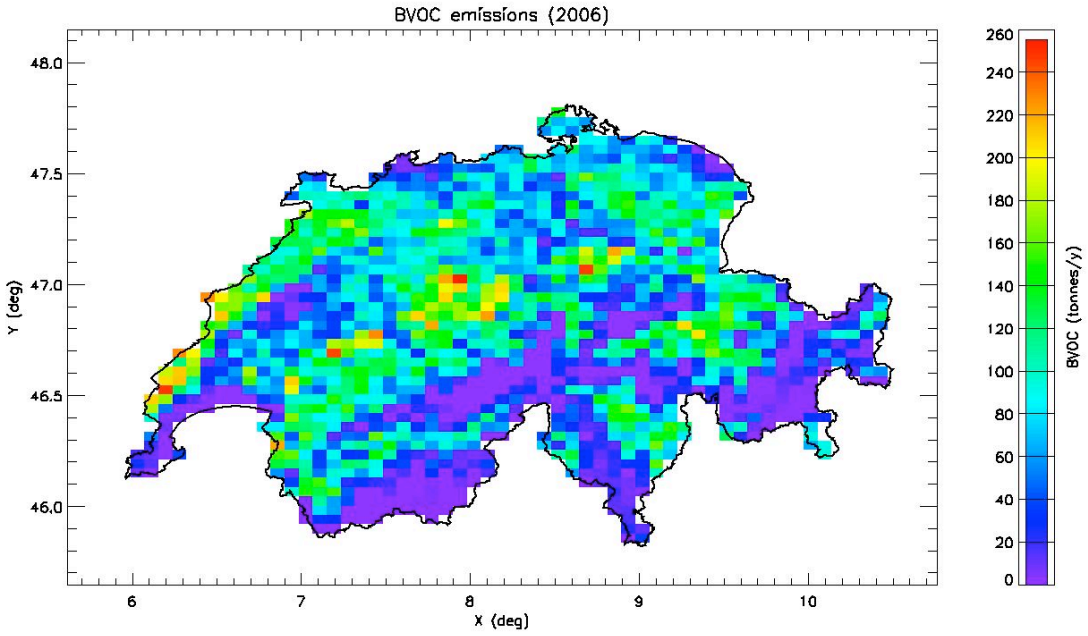

Figure 3.1. Total modelled biogenic VOC emissions (isoprene, monoterpenes and sesquiterpenes) in 2006.

3.5 Conversion of the emissions to the CAMx grids

First, we converted the European emission inventory to the CB05 mechanism as described in Chapter 3.1. Subsequently the geographic coordinates were transformed to the lon / lat coordinates of each CAMx domain. It is worth mentioning that the coarse domain (domain 1) is the same as the domain of the TNO/MACC emission inventory, but the grid cell size is increased by a factor of 2. For grid cells located within the Swiss boundaries, the European values were replaced by the Swiss emission data. Anthropogenic emissions of a given CAMx grid cell were calculated by computing the geographic (or Swiss) co-ordinates of the 4 corners and the totals of the European (or Swiss) emission rates within the respective polygons. Biogenic emissions do not need to be converted since they are already based on the meteorological grids.

3.6 Emission scenarios

We defined seven emission scenarios as shown in Table 2.1. Note that for all scenarios the meteorology is the same and refers to 2006. We chose 2006 for model validation because of the availability of various detailed measurements and the experience acquired in previous studies. The European emissions refer to that year as well. The reference year is the year for which the CEIP or GAINS emission data was extracted. The reference case (2005) is compared with the other scenarios. The baseline scenario (BL) assumes an emission development following the current legislation. The Mid is an emission scenario with moderate emission reductions between BL and MTFR scenarios where MTFR considers the maximum technically feasible reduction (MTFR) of emissions. It contains the lowest emissions for most of the source categories.

The retrospective scenario (retro) is not related to the revision of the Gothenburg Protocol but refers to the actual emissions in the past. Since data of PM2.5 and PM10 are only available for 2000 and later, 1990 data were calculated on the basis of 2005 data using GAINS simulations for that year. We performed the scenario for 1990 with two different background ozone concentrations (referred to as Retro 1 and Retro 2) as described in detail in Chapter 4.3.1. The results of Retro 1 (with lower background ozone in 1990 than in 2005) were used for comparisons with the reference case RC (2005).

In Fig. 3.2, we compared the relative changes in annual emissions with respect to the reference case RC (2005) for various scenarios in Switzerland (CH) and the surrounding countries Germany, France, Italy and Austria (D/F/I/A). We included emissions for the revised Gothenburg Protocol (2020 rev) in the figure although there was no GAINS scenario available during the time of this work. After the revised protocol was signed, it became clear that the committed reductions were very similar to those for the baseline (2020 BL) or in some cases even lower (see Fig. 3.2). In general, reductions in BL and Mid scenarios are similar for most of the pollutants except for NH_3. As expected, reductions in the MTFR case are the largest among all scenarios. The relative changes for Switzerland are usually lower than its neighbour countries Germany, France, Italy and Austria, except for PM2.5 for which reductions are comparable.

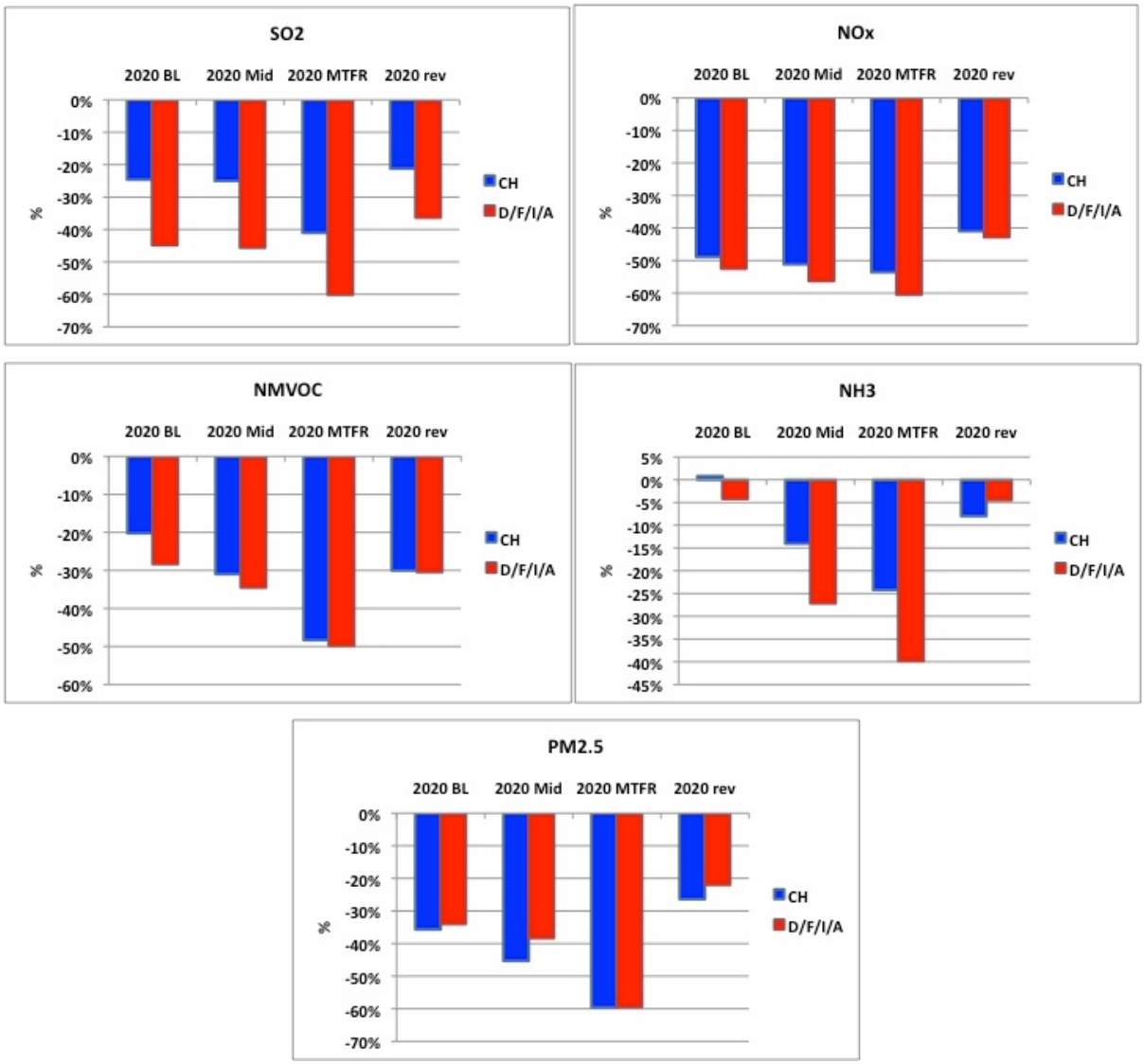

Figure 3.2. Relative changes (%) in annual emissions of SO_2, NO_x, NMVOC, NH_3 and $PM_{2.5}$ with respect to reference case RC (2005) for various scenarios in Switzerland (CH) and surrounding countries Germany, France, Italy and Austria (D/F/I/A).

4 Results and discussion

We discuss here only the model results for the area of Switzerland in the second domain. The results for the European domain are given in Appendix 3.

4.1 Model validation

Meteorological parameters

The meteorological parameters simulated by the WRF model were compared with measurements at 24 ANETZ stations in Switzerland (see Fig. 4.1.1 for some examples). In general, performance of WRF model using ECMWF data for initialization looks better than that of previously used MM5 model using COSMO7 for initialization for the same period of time [*Andreani-Aksoyoglu et al.*, 2009], especially for temperature, specific humidity and wind speed. As expected, model results for the meteorological parameters agree with observations better in summer than in winter.

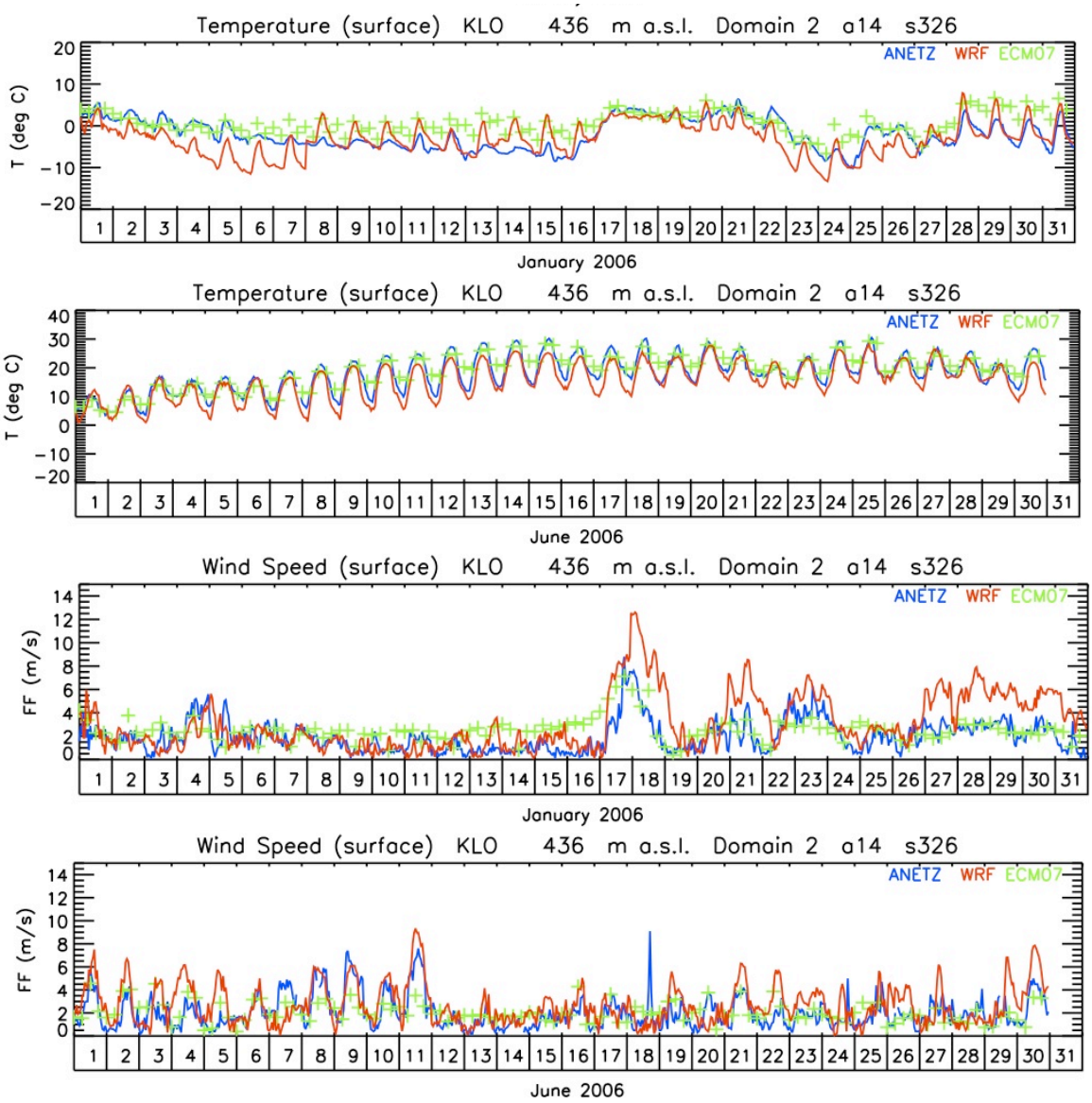

Figure 4.1.1: Measured and modelled surface temperature and wind speed at the ANETZ site Zurich Kloten (KLO) in January and June 2006. Blue: measurements, red: WRF model, green: ECMWF (used for initialization in model).

Gaseous species

We compared the CAMx model results with measurements from the field campaigns as well as from the national air pollution-monitoring network NABEL in 2006. Time series of gaseous species such as CO, SO_2, NO_x and O_3 at some NABEL stations are shown in Figs. 4.1.2 - 4.1.5. In general, model could reproduce the temporal variation of pollutants quite well. However, the model performance gets worse in winter because of the difficult meteorological conditions in winter 2006 when exceptionally cold inversion periods with extended fog layer occurred. Comparison with measurements suggests that the model performance for gaseous pollutants is better at locations with higher altitudes (i.e. Chaumont, Rigi, Davos). At urban sites where local emissions are relatively high, NO_x concentrations are usually underestimated because of the model resolution (see Fig. 4.1.4) leading to overestimation of ozone concentrations at night and in the morning. In addition to the horizontal resolution, representation of inversion layer at night and mixing layer during the day also plays an important role in the modelling of pollutant concentrations. In case of ozone, although the temporal variation is captured, maximum concentrations in summer are underestimated (Fig. 4.1.5).

The modelled and measured frequency distributions of ozone concentrations (histograms) in 2006 are shown in Fig. 4.1.6 together with the cumulative frequency distributions. The distributions at the rural site Laegern are similar for both measured and modelled ozone concentrations. They both have the highest number of points approximately in the middle of the graph. At urban sites such as Zurich and Lugano, on the other hand, the discrepancy between the measurements and model results at low concentrations can be clearly seen. These results show how difficult it can be to compare and interpret parameters such as ozone damage indicators AOT40 and SOMO35 that are calculated by summing measured or modelled ozone values above thresholds of 40 and 35 ppb, respectively. This point is discussed further in Section 4.2.2 and 4.2.3.

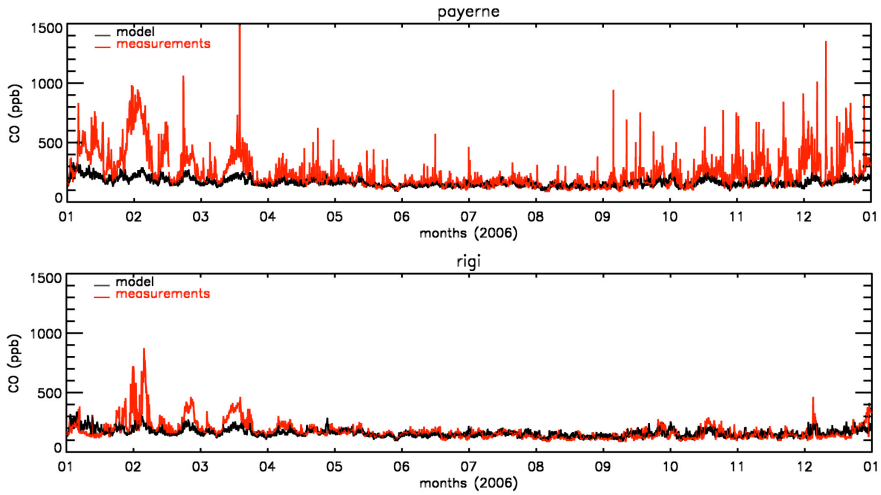

Figure 4.1.2: Measured (red) and modelled (black) hourly concentrations of CO (ppb) at Payerne (rural) and Rigi (mountainous) in 2006.

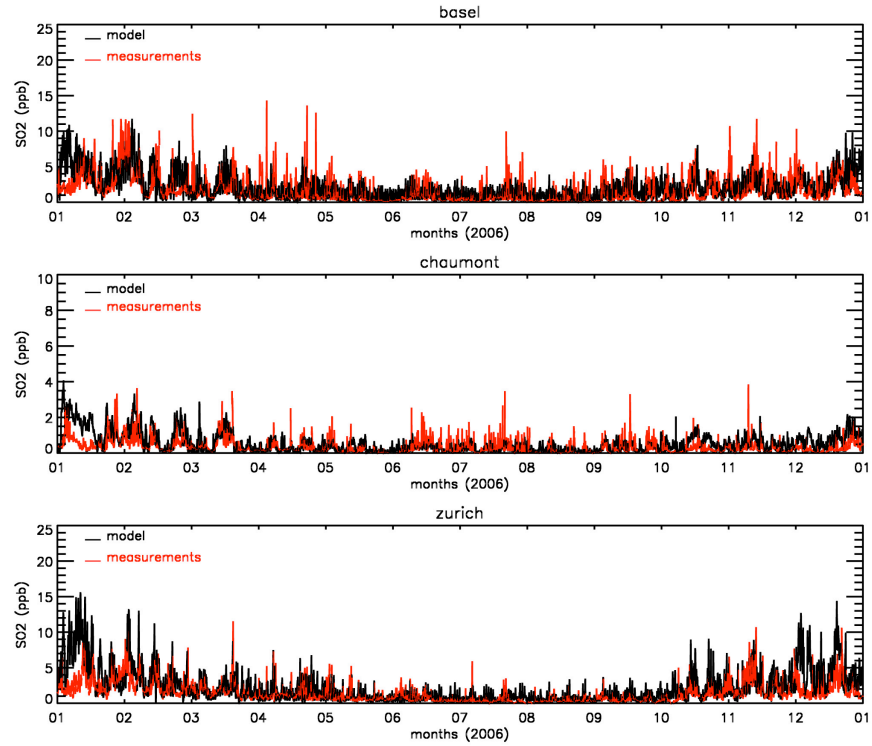

Figure 4.1.3: Measured (red) and modelled (black) hourly concentrations of SO_2 (ppb) at Basel (suburban), Chaumont (rural) and Zurich (urban) in 2006.

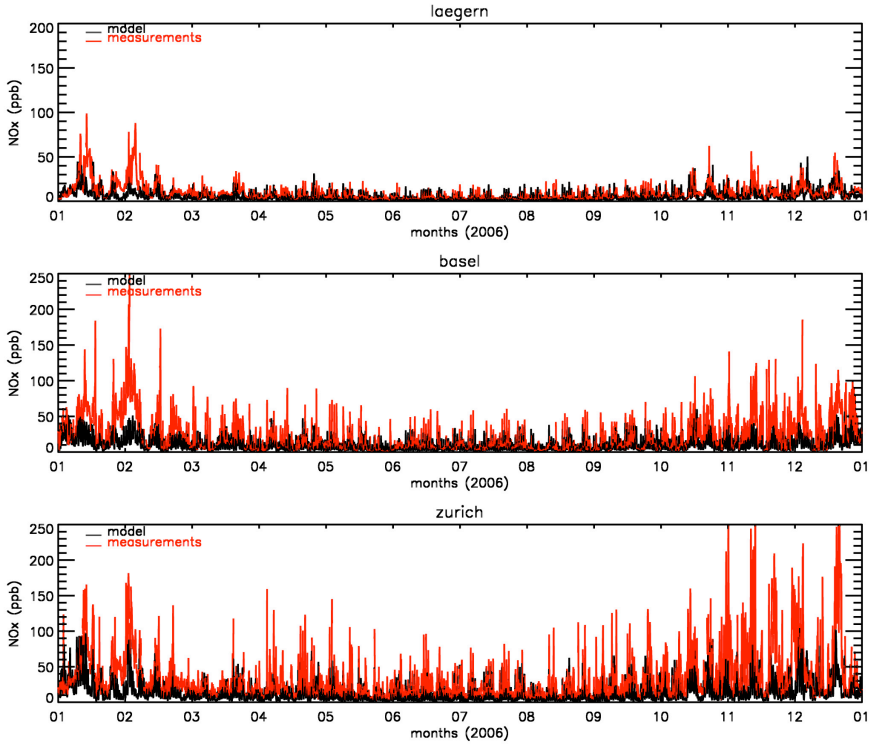

Figure 4.1.4: Measured (red) and modelled (black) hourly concentrations of NO_x (ppb) at Laegern (rural), Basel (suburban) and Zurich (urban) in 2006.

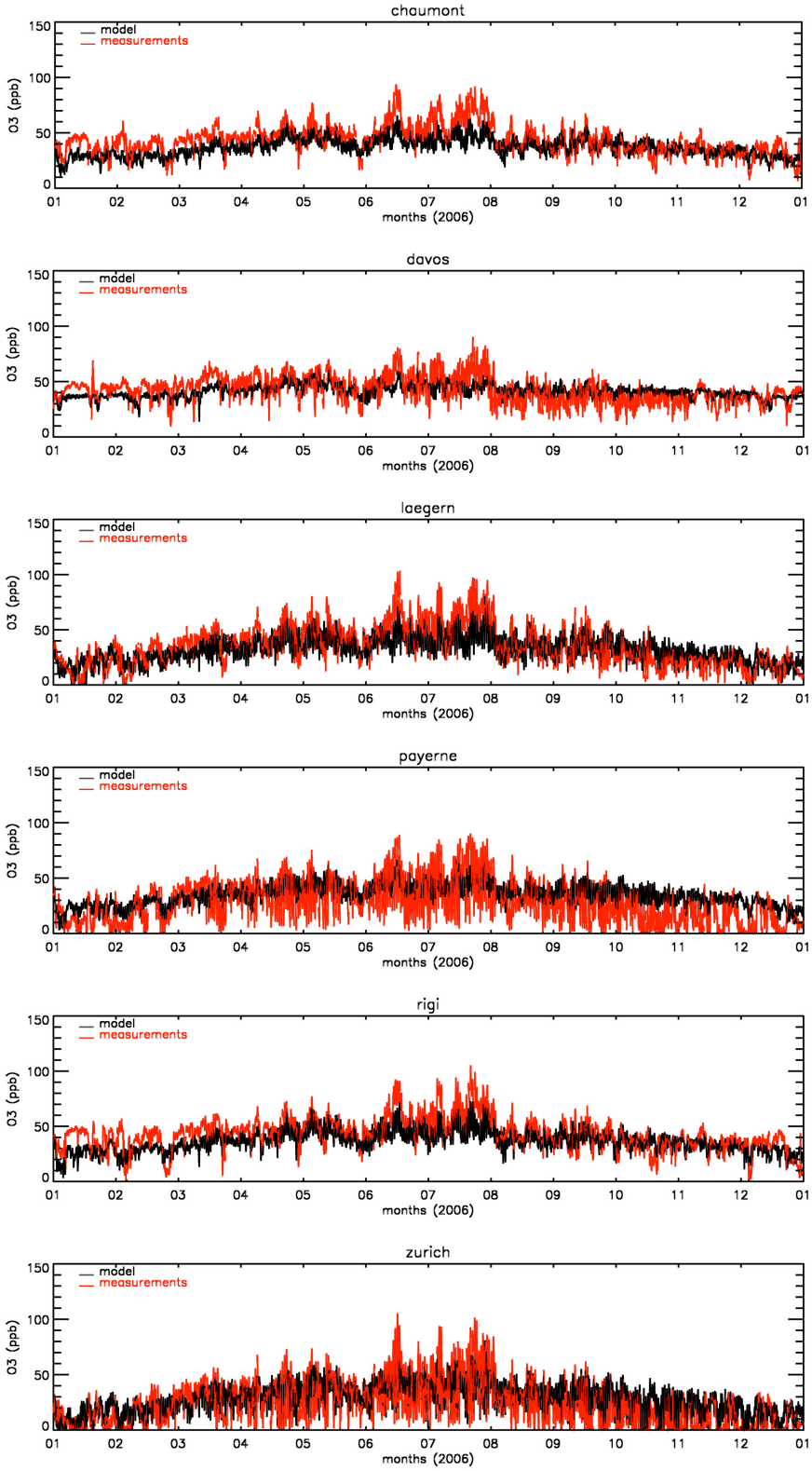

Figure 4.1.5: Measured (red) and modelled (black) hourly concentrations of O_3 (ppb) at Chaumont (rural), Davos (mountainous), Laegern (rural), Payerne (rural), Rigi (mountainous) and Zurich (urban) in 2006.

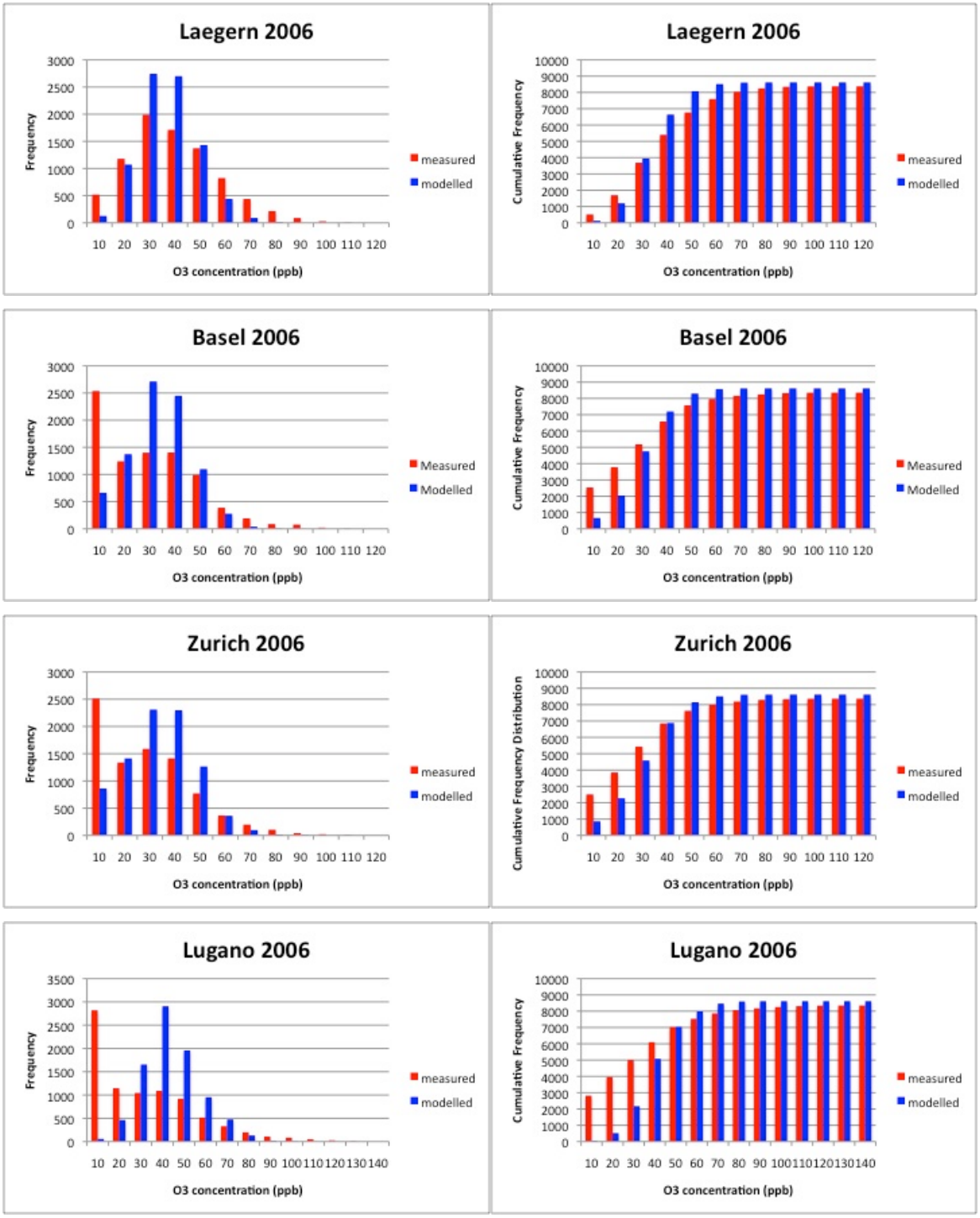

Figure 4.1.6: Frequency (left) and cumulative frequency (right) distribution for ozone concentrations at Laegern (rural, north), Basel (suburban, north), Zurich (urban, north) and Lugano (urban, south).

Aerosols

There were two aerosol measurement campaigns in 2006: one in January at Zurich and another in June at Payerne. Figs. 4.1.7 and 4.1.8 show the comparison of the modelled concentrations of particulate species with the measured ones during the two campaigns. Particulate nitrate, sulphate, ammonium, and organic aerosol measurements refer to AMS (Aerosol Mass Spectrometer) data [*Lanz et al.*, 2010].

Elemental carbon (EC) data are calculated from Aethalometer black carbon (BC) concentrations.

The winter period in 2006 was exceptionally cold and was characterized by strong inversion episodes. An extended fog layer over the Swiss Plateau persisted especially between 6 and 16 January and after 23 January. These conditions accompanied by low-wind speeds lead to difficulties for the meteorological models to reproduce correctly the meteorological parameters that are crucial for the air quality model, as we experienced earlier with the MM5 model [*Aksoyoglu et al.*, 2011]. Although we could reproduce the meteorological parameters much better than before, concentrations of particulate sulphate for the low-wind period in January are underestimated (Fig. 4.1.7). Sulphate is formed via aqueous chemistry using the cloud water content. Underestimation of sulphate during the period between 6 and 16 January is most likely due to the fog layer that cannot be reproduced in models correctly. The good agreement with measurements on fog-free days (17-24 January) and in June (Fig. 4.1.8) supports this explanation. Overestimation of SO_2 in January at Zurich (Fig. 4.1.3) also indicates insufficient formation of sulphate in the model. The modelled concentrations of the primary species such as EC are very close to the measurements both in January and June (Figs. 4.1.7 and 4.1.8). Modelling of organic aerosols is still quite demanding mainly due to the limited knowledge about the secondary organic aerosol formation. The CAMx model used in this study includes a SOA model based on the partitioning theory using various precursors such as anthropogenic and biogenic VOC species as well as the oligomerization process leading to an increase in aerosol concentrations. The recently developed VBS (volatility basis set) approach based on volatility has not yet been implemented in CAMx. The model performance for organic aerosols is reasonably well for relatively low concentrations, however, it becomes worse when formation of secondary organic aerosols increases. The overall PM2.5 (sum of inorganic and organic species) concentrations could be reproduced quite well in June whereas modelled PM2.5 is lower than the measurements for some days in January (Figs. 4.1.7 and 4.1.8).

We also compared the modelled PM2.5 and PM10 concentrations with measurements during the whole year at some NABEL stations as seen in Figs. 4.1.9 and 4.1.10, respectively (note that these PM2.5 measurements are not the same as those in Figs. 4.1.7 and 4.1.8). The average ratio of modelled PM2.5 / PM10 is about 80%. We could reproduce the temporal variation of particulate matter quite well. Agreement between the modelled and measured PM concentrations is reasonably good at the rural sites. The model performance is excellent at Chaumont which is 1136 m a.s.l. (see Fig. 4.1.9). On the other hand, measured PM2.5 concentrations at the other locations are higher than the modelled ones in winter months. It is clearly seen from the time series for PM2.5 and PM10 that model performance gets worse during the winter months. This is partly due to the difficult meteorological conditions prevailing during the cold days with strong inversions that lead to high uncertainties in calculated meteorological parameters. Another reason might be the underestimation of wood burning contribution to emissions. Histograms for measured and modelled PM10 concentrations in 2006 show a very similar distribution at the rural site Chaumont with a very good model performance whereas high concentrations at urban sites were underestimated (Fig. 4.1.11).

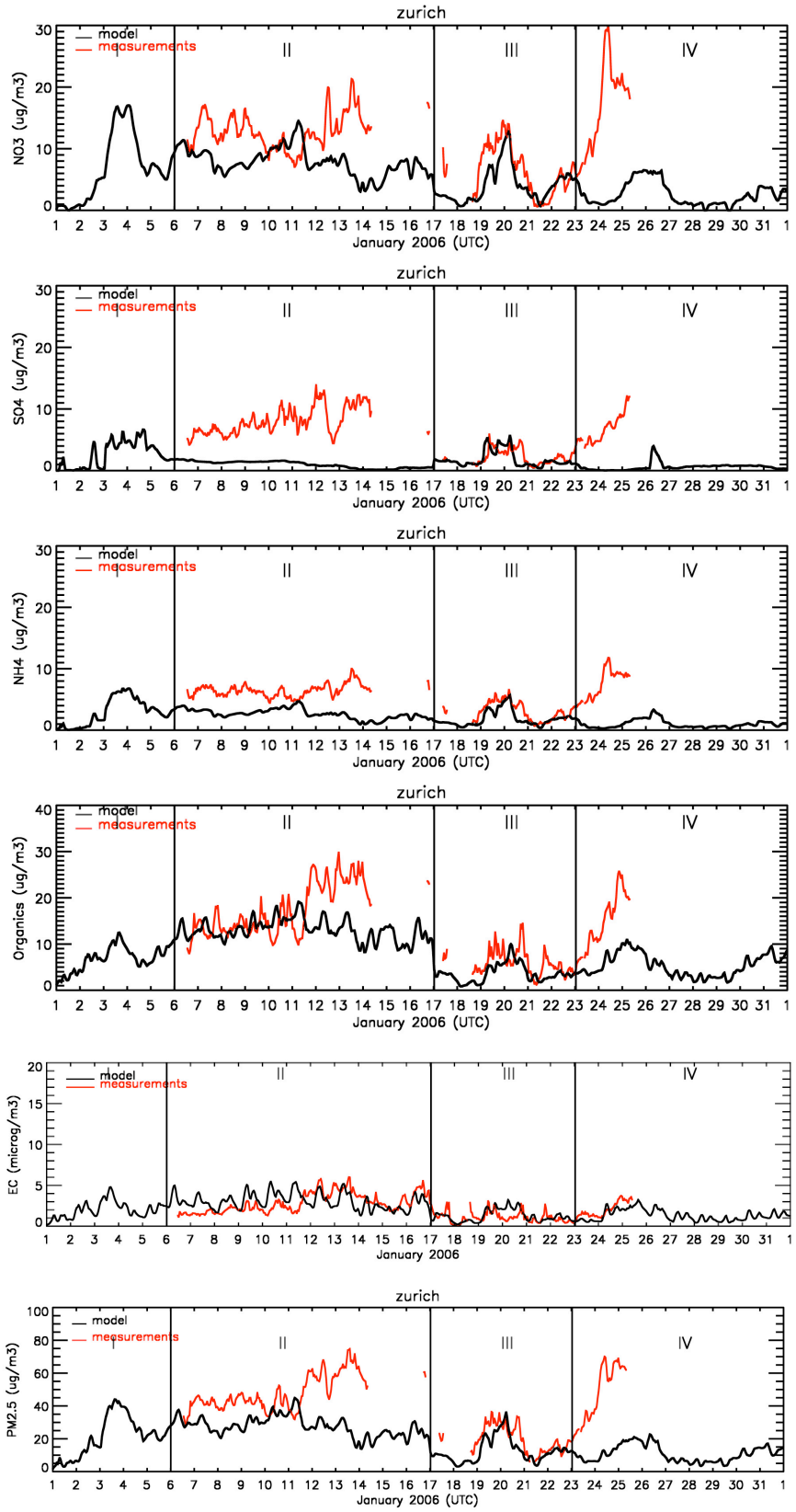

Figure 4.1.7: Measured (red) and modelled (black) hourly concentrations of particulate nitrate, sulphate, ammonium, organic aerosols, elemental carbon (EC) and PM2.5 (sum of all species shown above) at Zurich in January 2006.

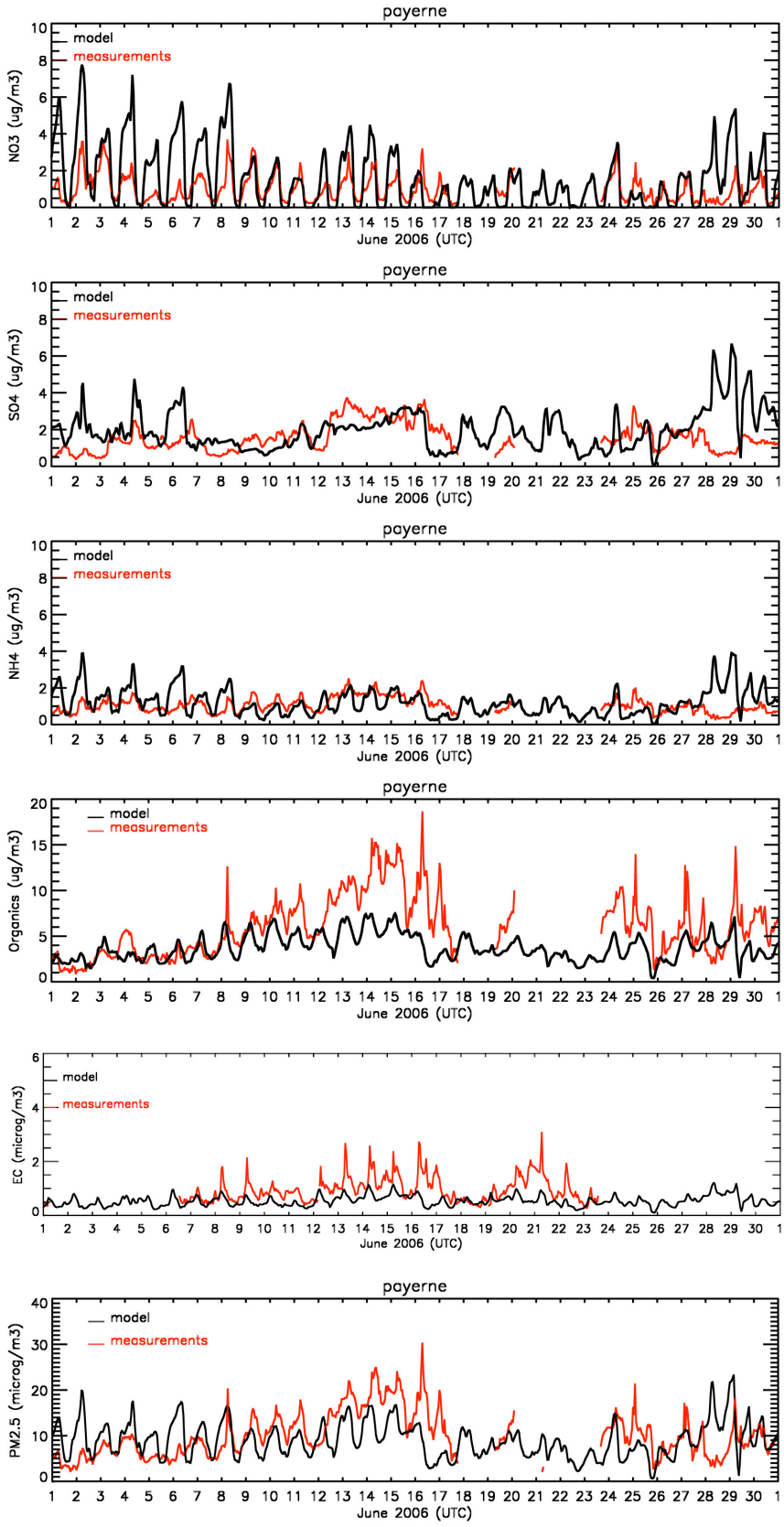

Figure 4.1.8: Measured (red) and modelled (black) hourly concentrations of particulate nitrate, sulphate, ammonium, organic aerosols, elemental carbon (EC) and PM2.5 (sum of all species shown above) at Payerne in June 2006.

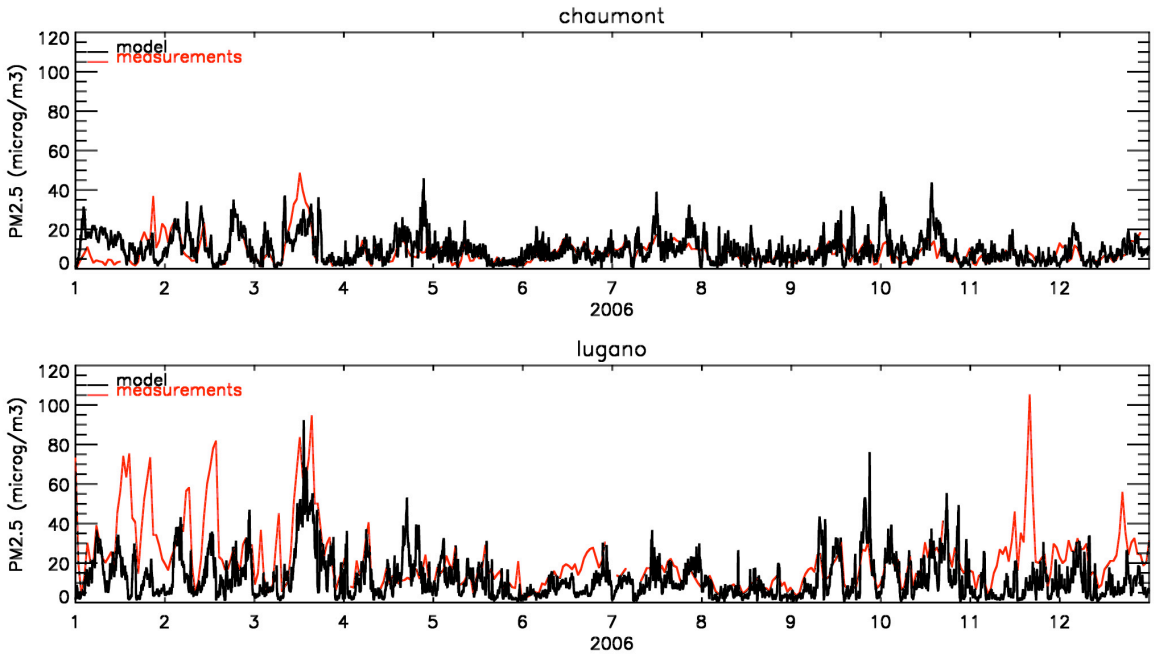

Figure 4.1.9: Time series of measured (red) and modelled (black) concentrations of PM2.5 at Chaumont (rural, elevated) and Lugano (urban) in 2006.

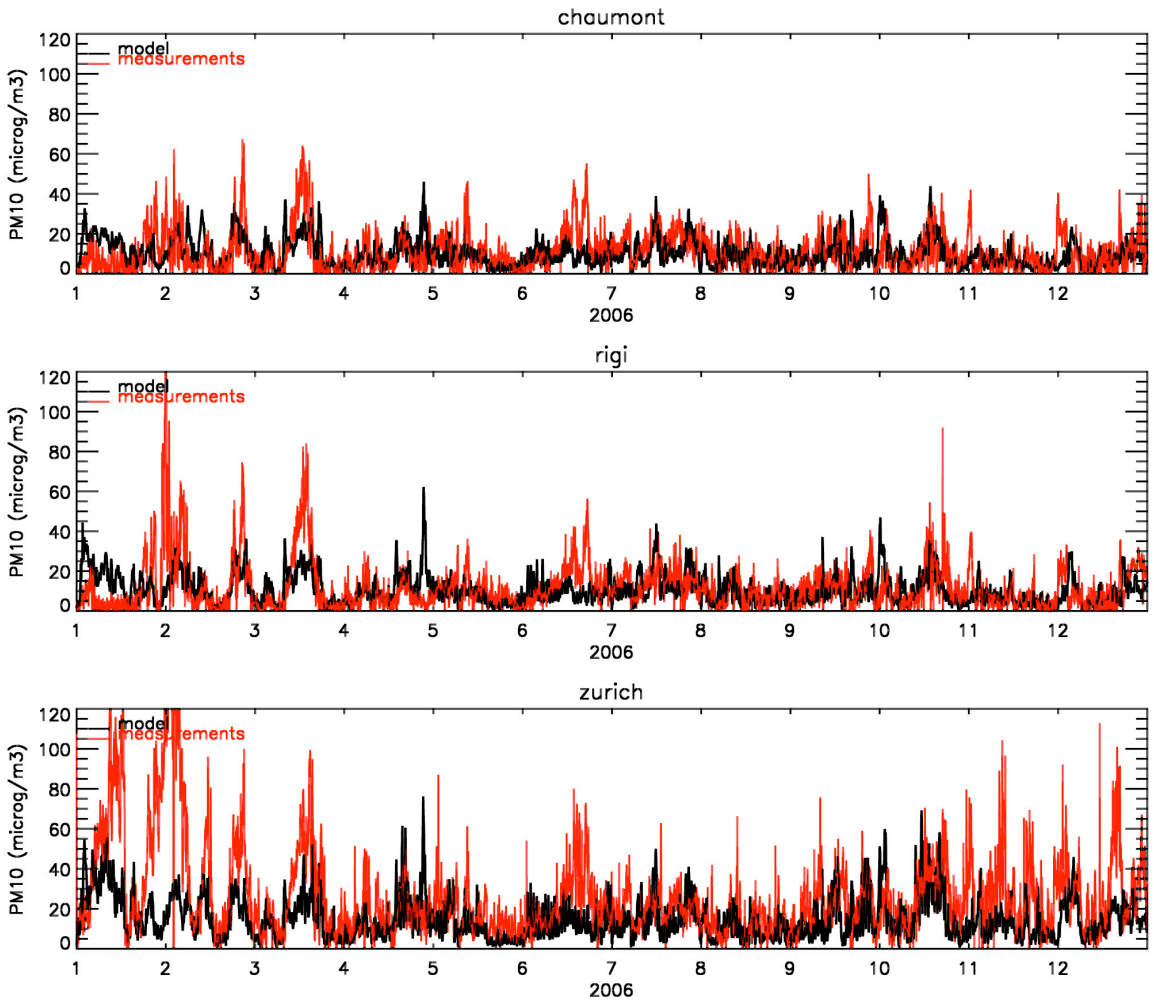

Figure 4.1.10: Time series of measured (red) and modelled (black) concentrations of PM10 at Chaumont (rural, elevated), Rigi (mountainous) and Zurich (urban) in 2006.

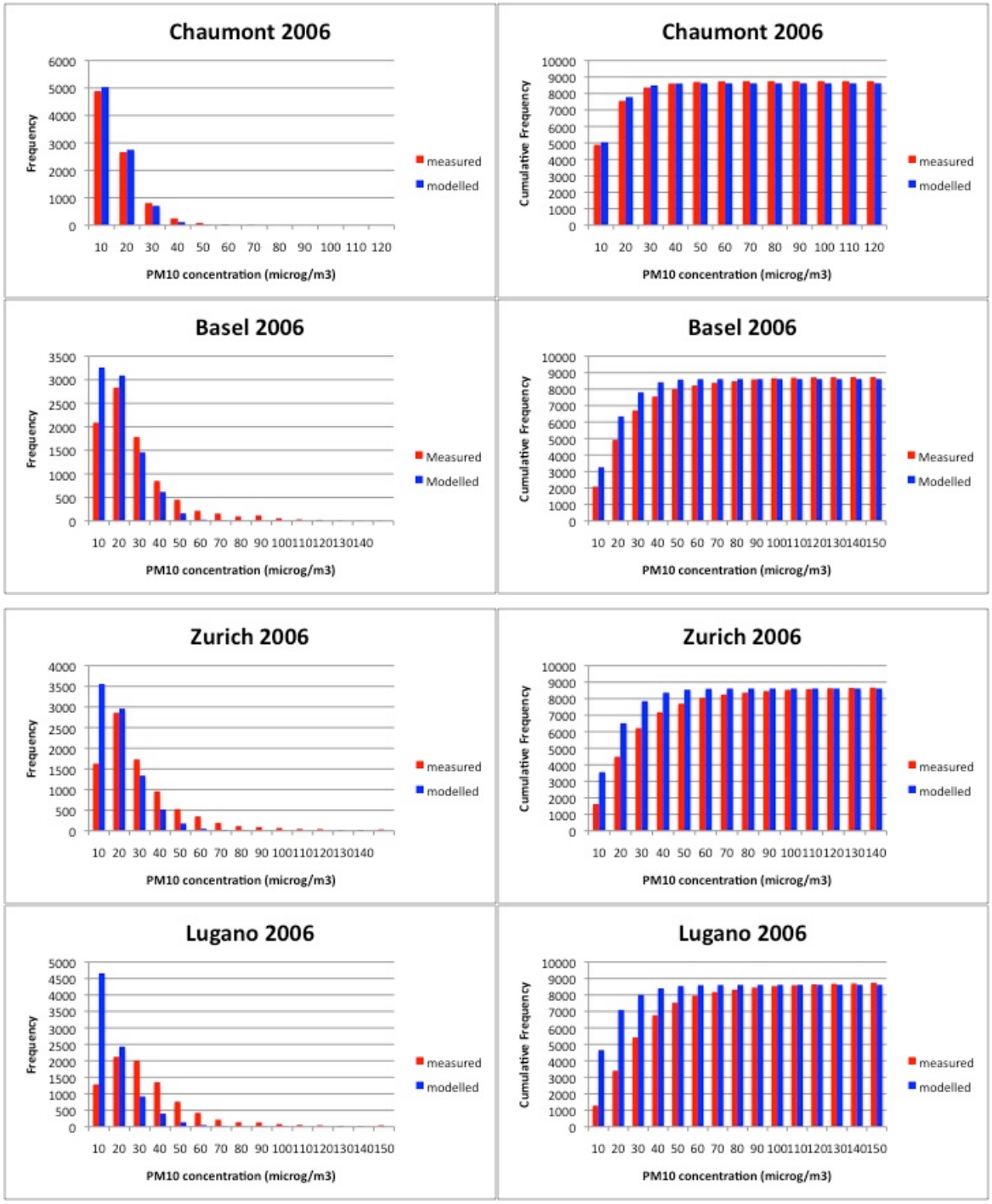

Figure 4.1.11: Frequency (left) and cumulative frequency (right) distribution of measured (red) and modelled (blue) PM10 at Chaumont (rural), Basel (suburban), Zurich (urban, north) and Lugano (urban, south).

We also compared the modelled and measured average concentrations of PM2.5 and PM10 using scatter plots for some NABEL stations where the data was available. There are more stations available for PM10 than PM2.5. As seen in Fig. 4.1.12, the model performance for PM2.5 looks better than that of PM10. The agreement between the measurements and model results is very good at rural and elevated sites such as Chaumont and Rigi. On the other hand, concentrations at urban sites such as Bern and Lugano are underestimated. The model performance gets better when the winter months are excluded as shown in the lower panel of Fig. 4.1.12.

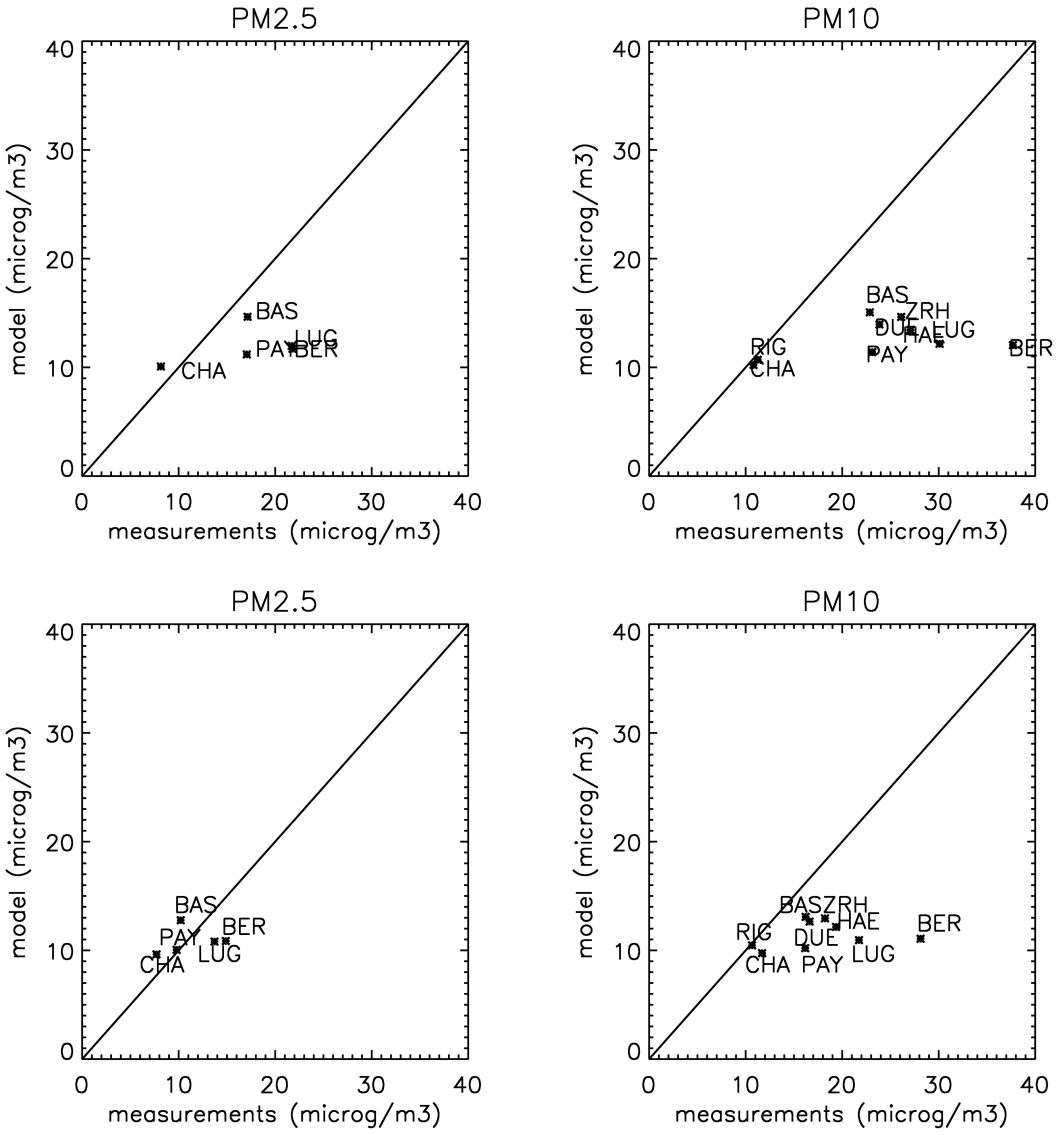

Figure 4.1.12: Measured versus modelled average concentrations of PM2.5 (left) and PM10 (right) at some NABEL stations for whole year (above) and for 1 April - 30 September 2006 (below).

4.2 Ozone

4.2.1 Annual average concentrations

In this section, we discuss the annual average ozone concentrations for the reference case in 2005 and compare with the results of emission scenarios in 2020 as well as with the retrospective case in 1990. On average, ozone concentrations for the reference case (RC 2005) are highest at elevated sites and lowest around urban locations (Fig. 4.2.1.1). The annual average ozone concentrations of about 30-35 ppb at rural sites in the north and around 40 ppb at elevated sites match the observations at NABEL stations such as Payerne (28.6 ppb), Laegern (35.3 ppb), Davos (36.1 ppb) and Jungfraujoch (38.1 ppb). At urban sites, the predicted annual average ozone concentrations are lower.

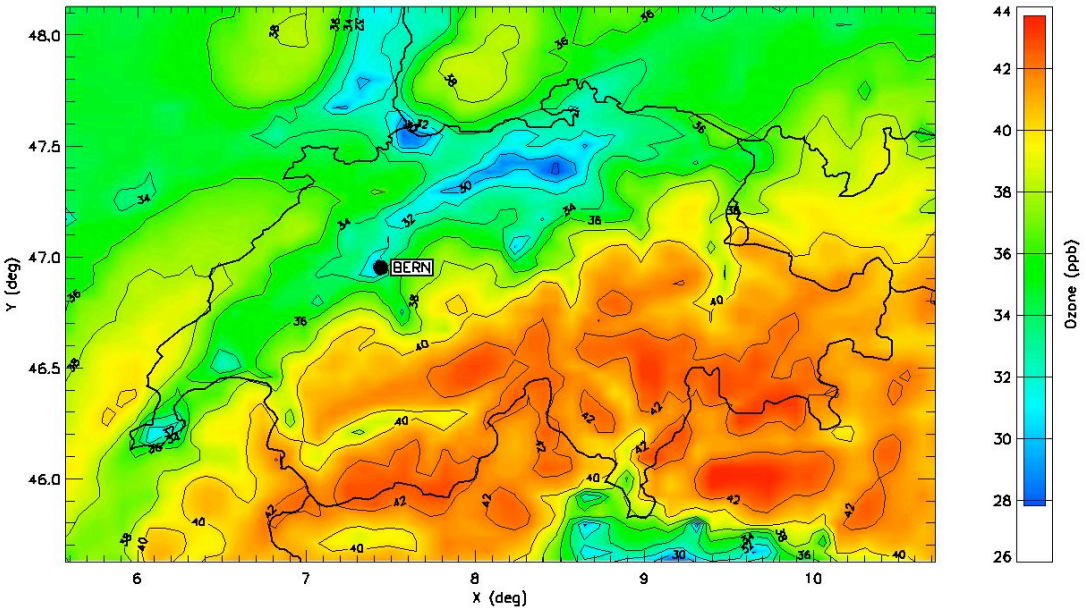

Figure 4.2.1.1: Annual average concentration of ozone (ppb) for the reference case (RC 2005)

The relative difference in annual average ozone concentrations between the RC and Baseline scenario (BL 2020) is shown in Fig. 4.2.1.2. There would be a decrease by 4-6 % over the Alpine regions and southern part of the Alps. On the other hand, annual average ozone concentrations would increase by 2-4 % at urban sites due to reduced destruction of ozone with NO. The relative differences in ozone for other future scenarios Mid and MTFR are similar for Switzerland (Figs. 4.2.1.3 and 4.2.1.4).

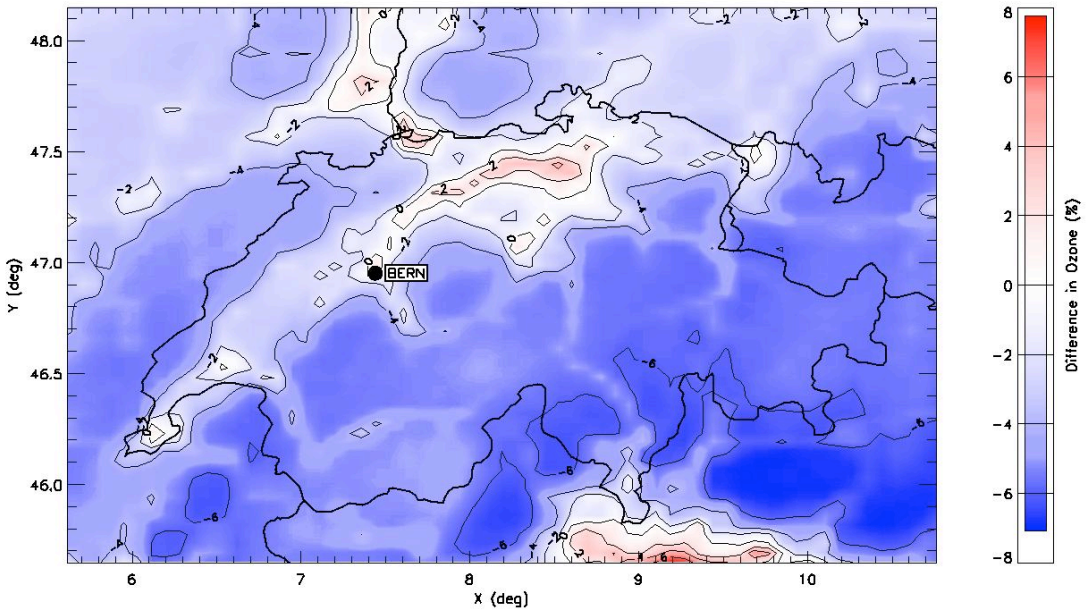

Figure 4.2.1.2: Difference in annual average of ozone (%), BL 2020- RC 2005.

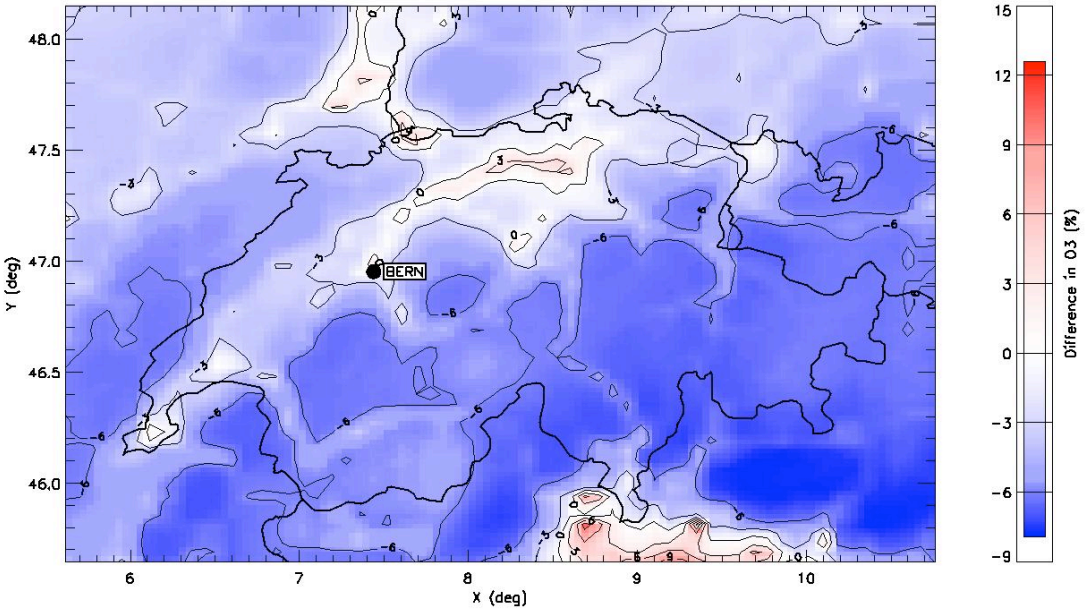

Figure 4.2.1.3: Difference in annual average of ozone (%), Mid 2020- RC 2005.

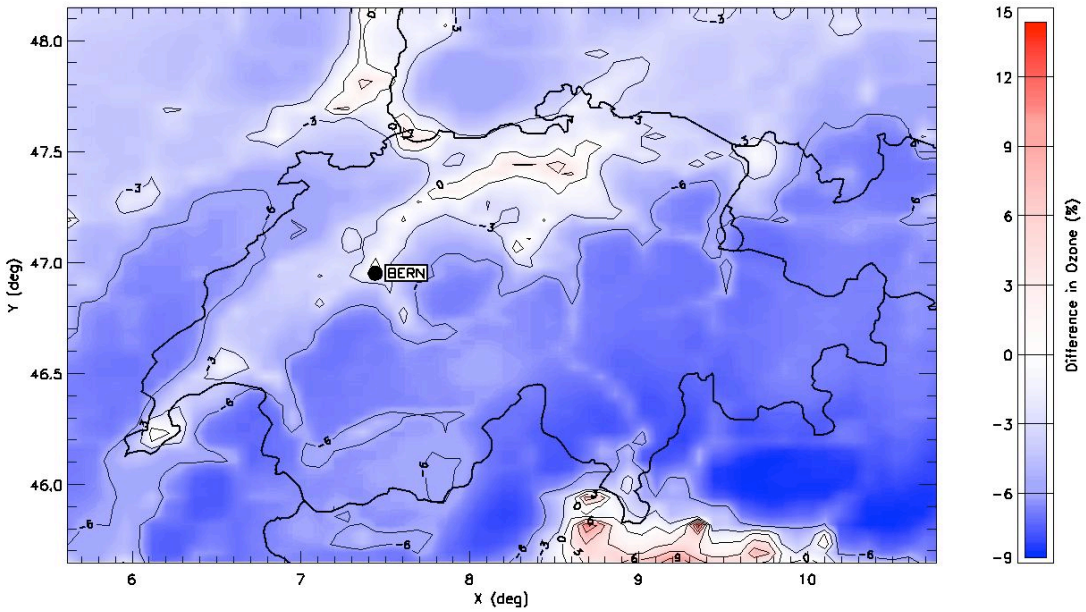

Figure 4.2.1.4: Difference in annual average of ozone (%), MTFR 2020- RC 2005.

Fig. 4.2.1.5 shows the annual average ozone concentrations for the retrospective case with two different background ozone concentrations. In general, ozone levels in Retro 1 (with lower background ozone) are lower than those in Retro 2 and they are closer to the observations in 1990 (15-30 ppb measured in the Swiss Plateau, ~ 35 ppb at elevated sites), although they might still be too high.

The relative difference in the annual average ozone concentrations between RC 2005 and Retro 1, 1990 is shown in Fig. 4.2.1.6 for the Swiss domain. These results indicate an increase in average ozone concentration by about 5-10 % over the Swiss Plateau between 1990 and 2005 whereas the change indicated by the observations is higher (10-40%). On the other hand, time series of both modelled and measured data show clearly that the peak ozone concentrations (in summer) decreased while low concentrations increased since 1990 (see Fig. 4.2.1.7).

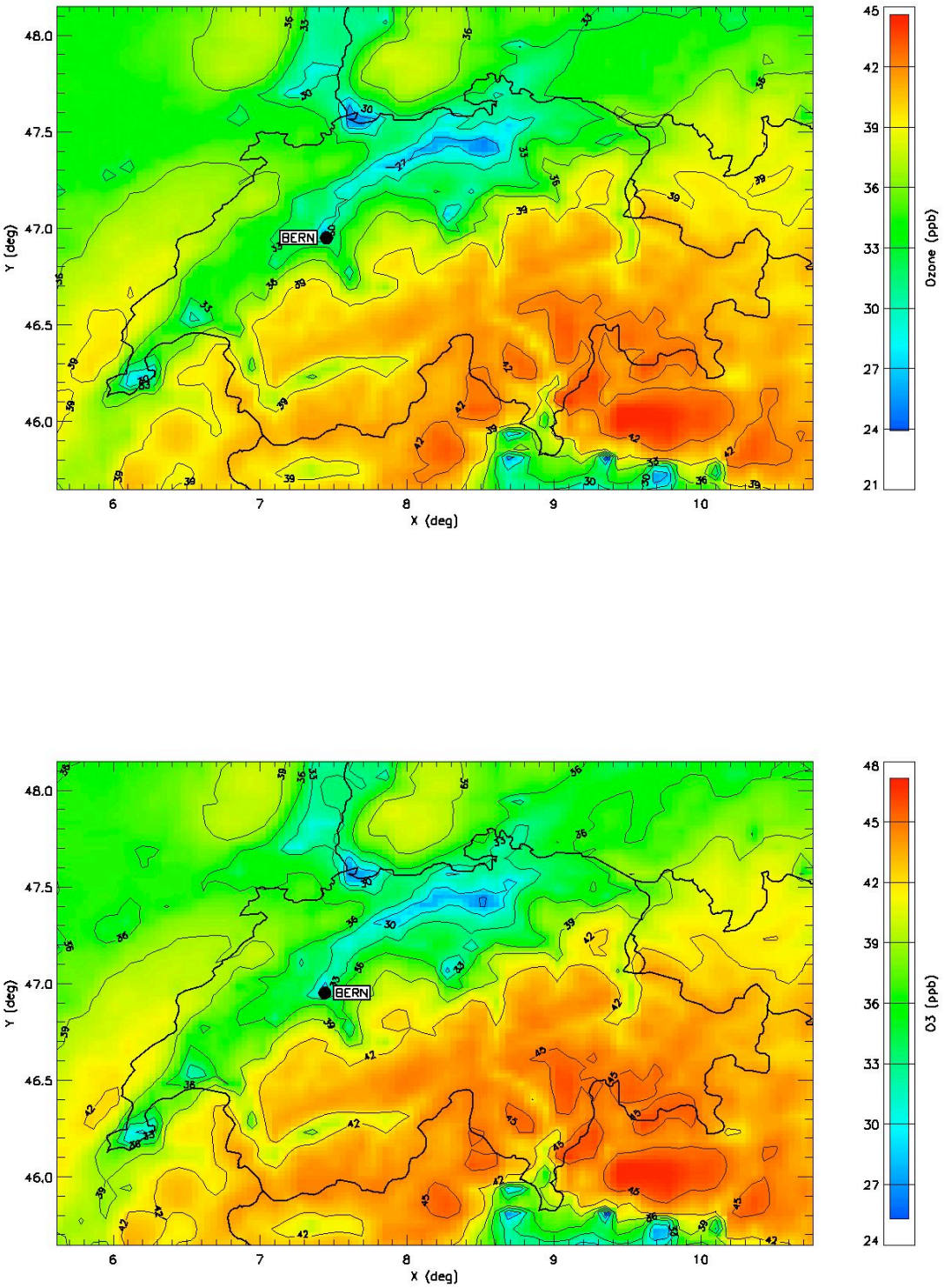

Figure 4.2.1.5: Annual average concentration of ozone (ppb) for Retro 1, 1990 (above) and Retro 2, 1990 (below)

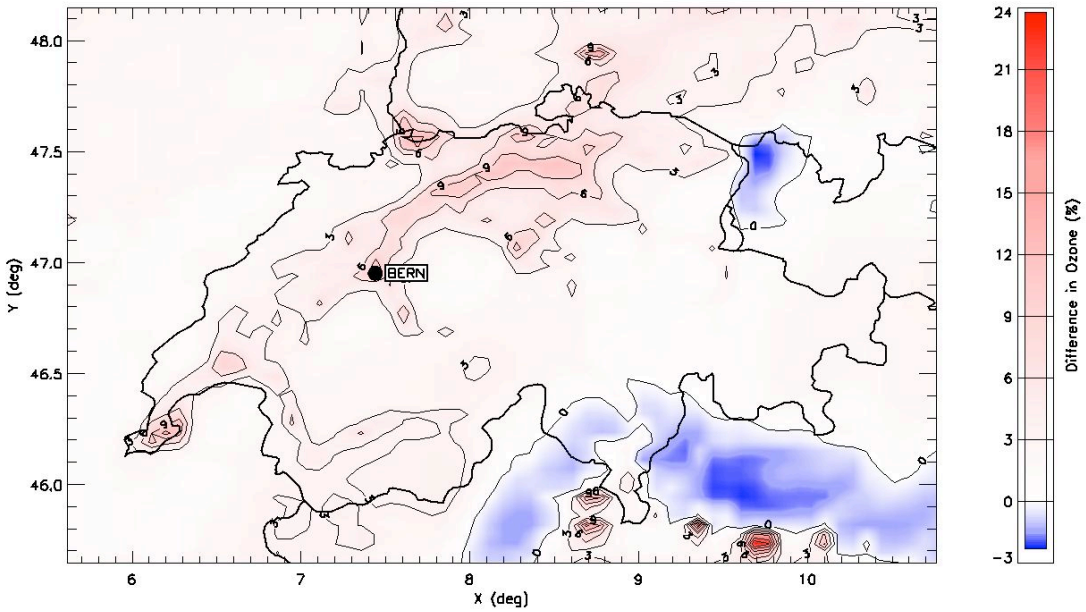

Figure 4.2.1.6: Difference in annual average of ozone (%), RC 2005 – Retro 1,1990.

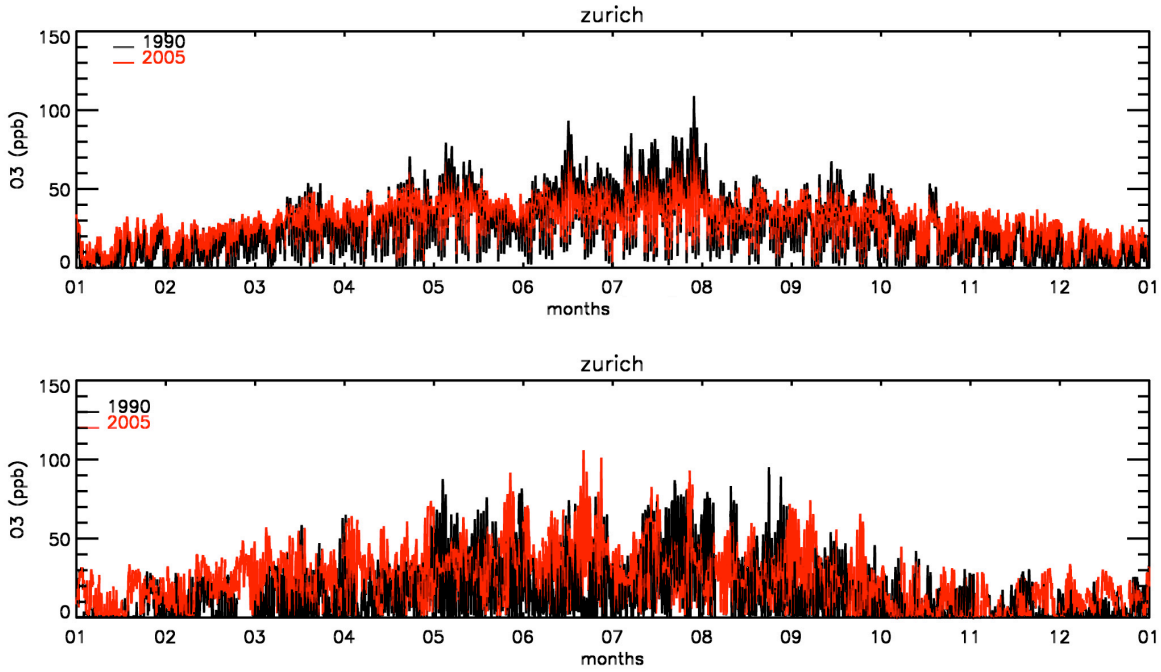

Figure 4.2.1.7: Comparison of ozone concentrations in 1990 (black) and 2005 (red) at Zurich from model (above) and measurements (below). The model data refer to Retro 1, 1990, RC 2005 and meteorology for 2006.

4.2.2 AOT40

AOT40 (Accumulated dose of ozone Over the Threshold of 40 ppb) is an indicator used to determine the damage on vegetation [*Ashmore and Wilson*, 1992]. AOT40 for forests was calculated from April to September, for the daytime hours (8:00 AM – 8:00 PM) for all scenarios. The corresponding unit is ppb.h. The modelled AOT40 results are given as ppm.h for convenience in this report.

The modelled AOT40 for the reference case (2005) range between 10-15 and 20-30 ppm.h in Switzerland, in the north and the south, respectively (Fig. 4.2.2.1). These results are in the same range as those from measurements for 2005 (Fig. 4.2.2.2).

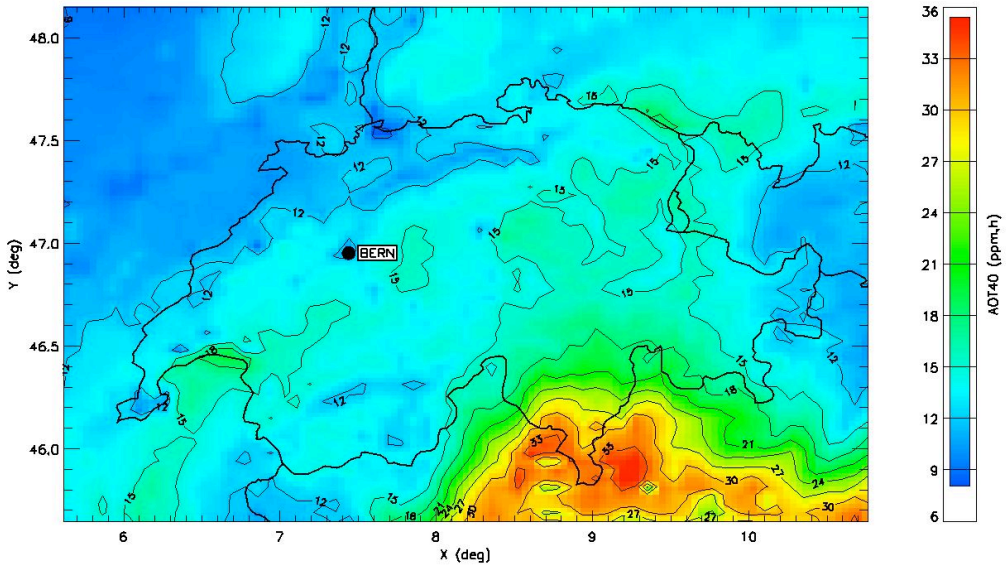

Figure 4.2.2.1: Modelled AOT40 (ppm.h) for the reference case (RC 2005)

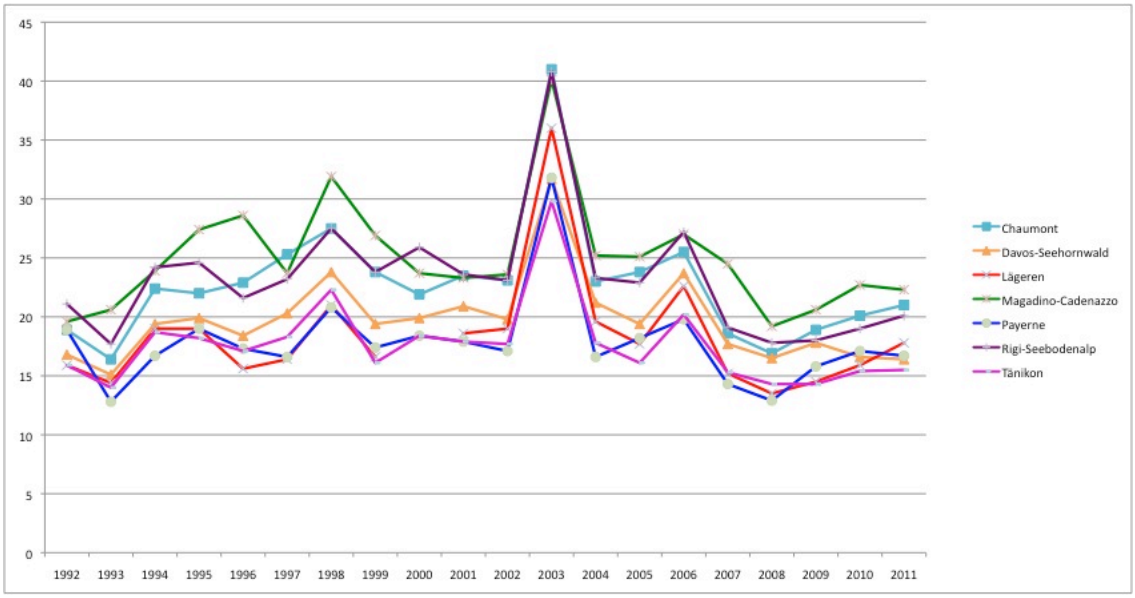

Figure 4.2.2.2: Trends in AOT40 (ppm.h) from measurements (from FOEN)

The relative changes in AOT40 for the future scenarios in 2020 are shown in Figs. 4.2.2.3 - 4.2.2.5. The predicted change for the BL case is 50% – 70% whereas it goes up to 75% for the MTFR case.

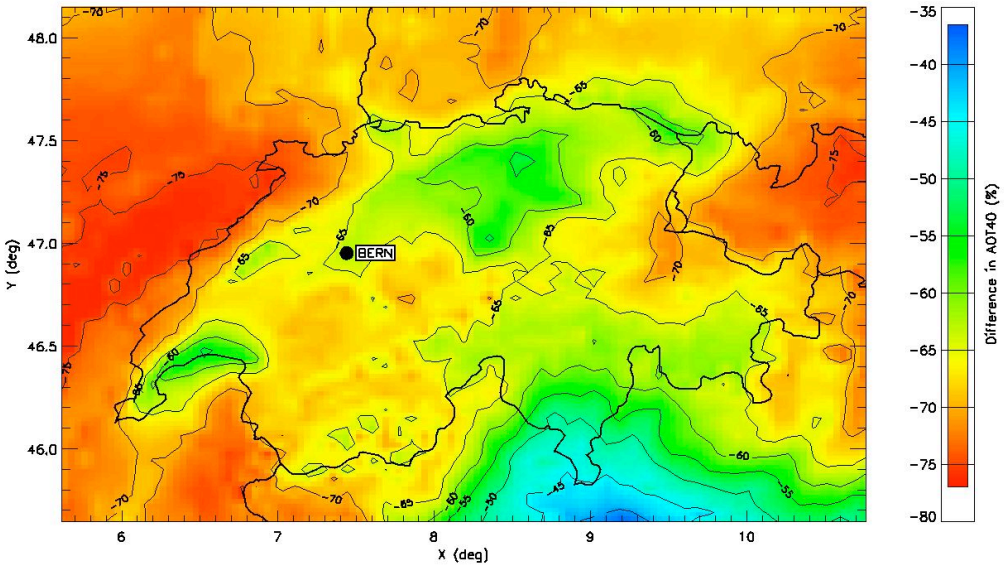

Figure 4.2.2.3: Difference in AOT40 (%), BL 2020- RC 2005.

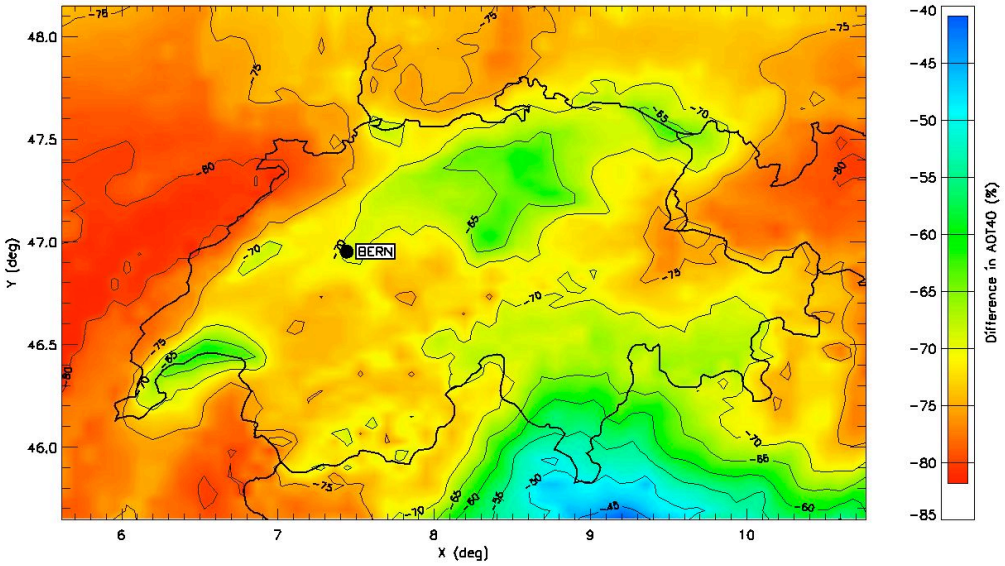

Figure 4.2.2.4: Difference in AOT40 (%), Mid 2020- RC 2005.

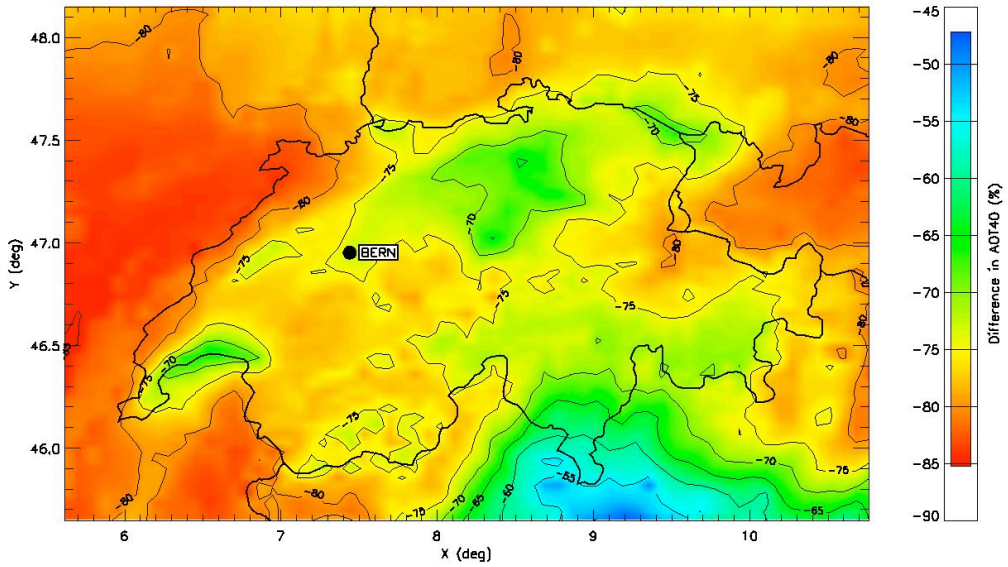

Figure 4.2.2.5: Difference in AOT40 (%), MTFR 2020- RC 2005.

In the retrospective case (1990) the calculated AOT40 values are shown in Fig. 4.2.2.6. The Retro 1 case with lower background ozone leads to a slightly lower AOT40 than Retro 2. AOT40 in both cases are higher than those in 2005. The model results suggest that AOT40 decreased since 1990 (by 25-40% in Retro 1, by 35-45% in Retro 2) (Fig. 4.2.2.7) although average annual ozone concentrations increased (see Fig. 4.2.1.6). This indicates that peak ozone values decreased due to emission reductions as shown in Fig. 4.2.1.7. On the other hand, measurements suggest that AOT40 decreased by about 20-25% at rural sites in the north but increased by 10-25% at urban sites between 1990 and 2005. This discrepancy between the model results and observations indicates the sensitivity of indicator parameters on threshold values. Changes in the background ozone levels might affect such calculations significantly. The Retro 1 case seems to give results closer to the observations although predicted changes are still larger than the observations. The change in the frequency distribution of ozone between 1990 and 2005 is shown in Fig. 4.2.2.8 for Zurich. The distribution of modelled ozone concentrations in 1990 and 2005 is clearly different. The most frequent levels were shifted from 10 ppb towards 30-40 ppb. On the other hand, histogram of measured concentrations looks different than the modelled ones. As discussed in Chapter 4.1 (see also Fig. 4.1.5) the model overestimates the low ozone concentrations at urban areas at night and in the morning. The histogram of measurements in Zurich for 1990 shows a steep curve decreasing with increasing concentration. In 2005 on the other hand, the distribution is shifted towards higher levels. Overestimation of ozone concentrations by regional models at night in the polluted, urban areas is a common problem. This alone however, cannot be responsible for the discrepancy between measured and modelled AOT40 because it is the sum of ozone concentrations above 40 ppb and calculated only during the daytime. The difference between modelled and measured ozone histograms above 40 ppb is relevant for understanding the changes in AOT40.

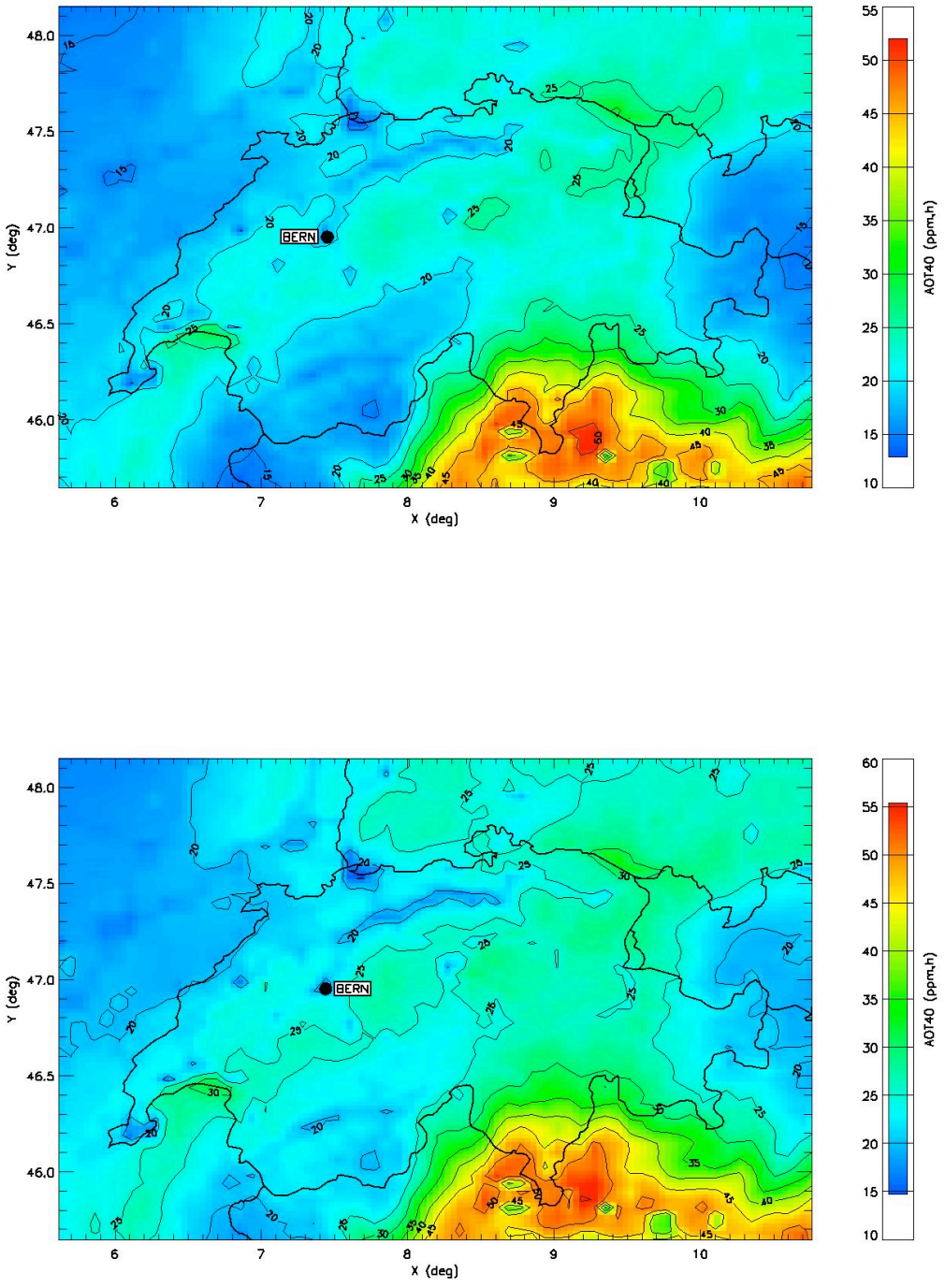

Figure 4.2.2.6: Modelled AOT40 (ppm.h) for Retro 1, 1990 (above) and Retro 2, 1990 (below)

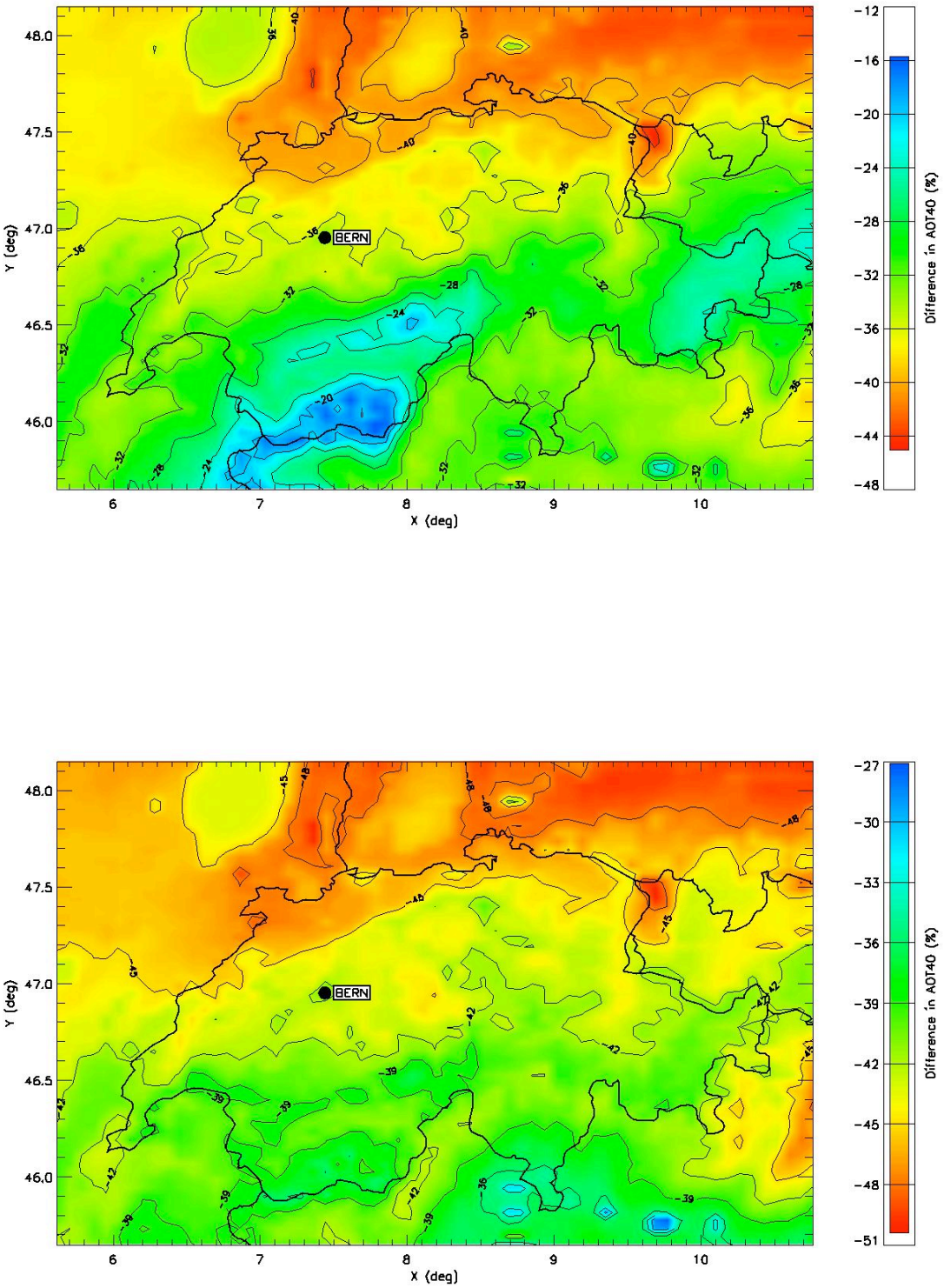

Figure 4.2.2.7: Difference in AOT40 (%), RC 2005 – Retro 1, 1990 (above) and RC 2005 – Retro 2, 1990 (below).

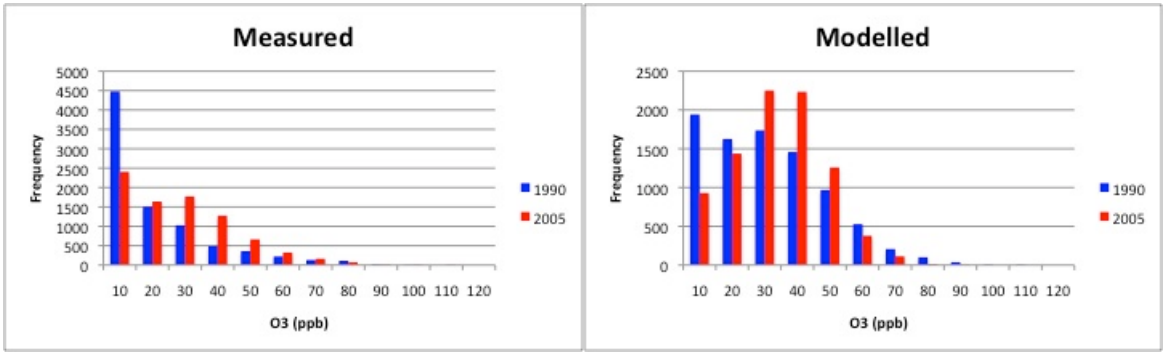

Figure 4.2.2.8: Change in frequency distribution of measured (left) and modelled (right) ozone between Retro 1, 1990 and RC 2005 at Zurich.

4.2.3 SOMO35

SOMO35 (Sum of Ozone Means Over 35 ppb) is an indicator for health impact assessment recommended by WHO [*Amann et al.*, 2008]. It is defined as the yearly sum of the daily maximum of 8-hour running average over 35 ppb. For each day the maximum of the running 8-hour average for O_3 is selected and the values over 35 ppb are summed over the whole year. The corresponding unit is ppb.days (ppb.d). The modelled SOMO35 values are between 2000 - 2500 ppb.d in the north and 3500 – 4500 ppb.d in the south for the reference case 2005 (Fig. 4.2.3.1). SOMO35 values calculated from measurements vary between 1000 (urban sites) and 5000 (southern and elevated sites) ppb.d. The modelled SOMO35 for 2005 therefore looks reasonably good. An EMEP model study for 2010 using a coarser resolution suggests 3000 (north) – 5000 (south) ppb.d [*M. Gauss et al.*, 2012].

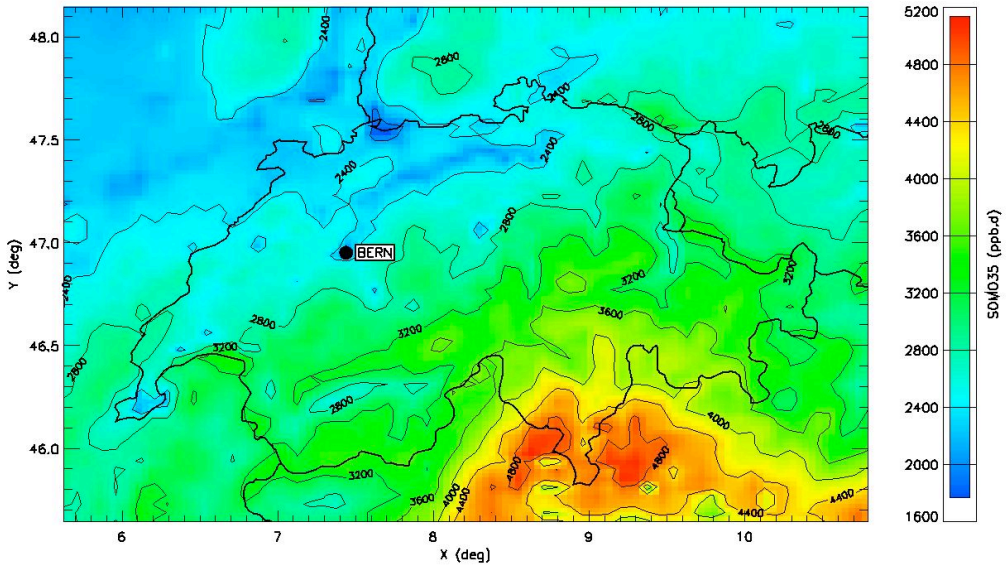

Figure 4.2.3.1: Modelled SOMO35 (ppb.d) for the reference case (RC 2005)

The model results suggest a decrease in SOMO35 by 30-50% depending on the emission scenario used for 2020 (Figs. 4.2.3.2 - 4.2.3.4). Baseline scenario yields a decrease of about 35% whereas the largest decrease (up to 50%) was predicted for the MTFR scenario.

We calculated SOMO35 for both Retro 1 and Retro 2 for 1990 (Fig. 4.2.3.6). The values vary between 3000 – 6000 ppb.d in Retro 1, and 3500 – 6500 ppb.d in Retro 2. Model results of Retro 1 case show a decrease of about 20-25 % in SOMO35 values in the north between 1990 and 2005 (Fig. 4.2.3.6). A small increase (5 %) was predicted at mountainous regions. Retro 2 simulations suggested a higher decrease (25-30%) in SOMO35. On the other hand, SOMO35 values based on measurements show about 15% decrease at rural sites in the north, but as in the case of AOT40, they show also an increase at urban and elevated sites (Fig. 4.2.3.7). Histograms shown in Fig. 4.2.2.8 can also be used for understanding the differences between modelled and measured SOMO35 values. As in the case of AOT40, the discrepancy between the modelled and measured relative change in SOMO35 is most likely due to the representation of the background ozone levels for 1990 and 2005, which needs further analysis.

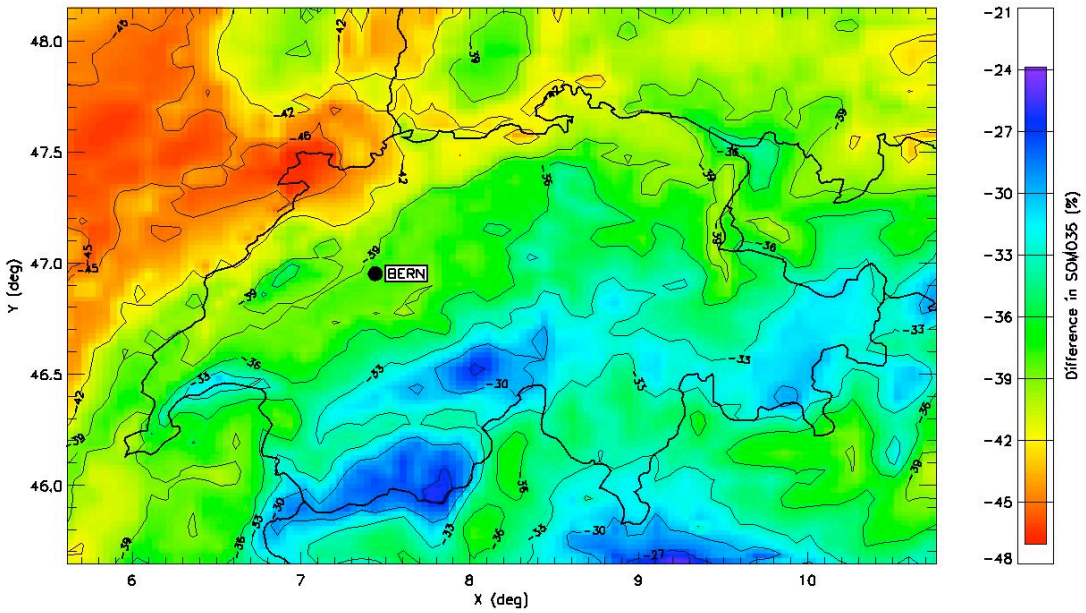

Figure 4.2.3.2: Difference in SOMO35 (%), BL 2020- RC 2005.

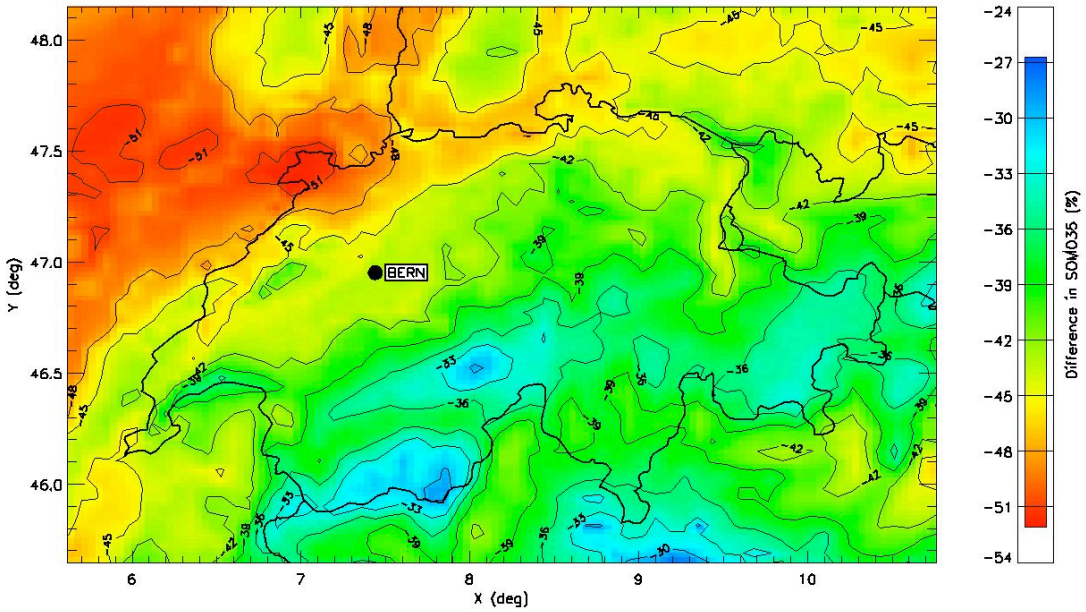

Figure 4.2.3.3: Difference in SOMO35 (%), Mid 2020- RC 2005.

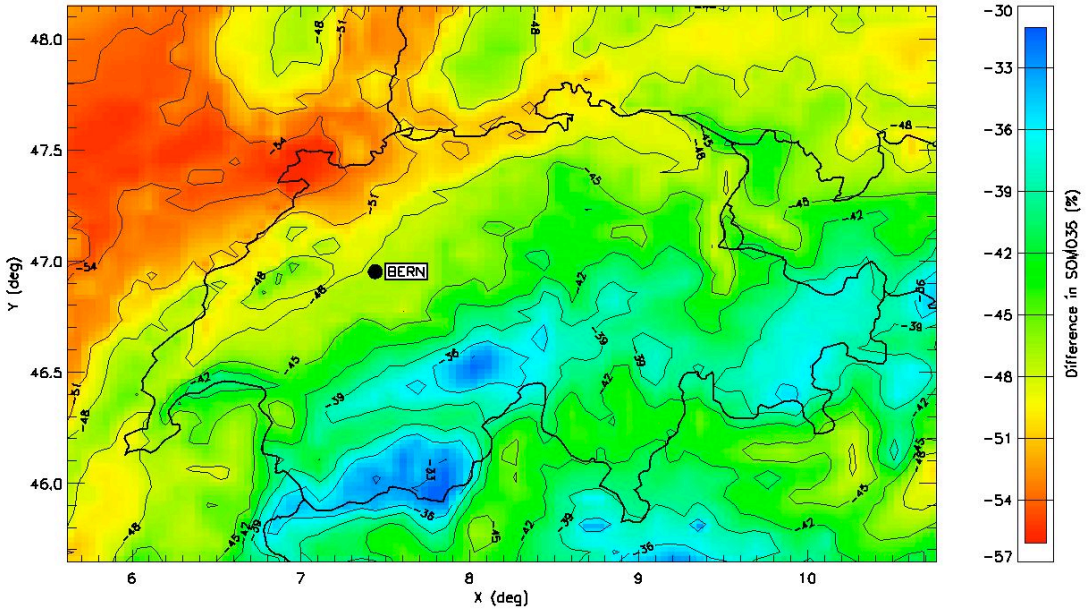

Figure 4.2.3.4: Difference in SOMO35 (%), MTFR 2020- RC 2005.

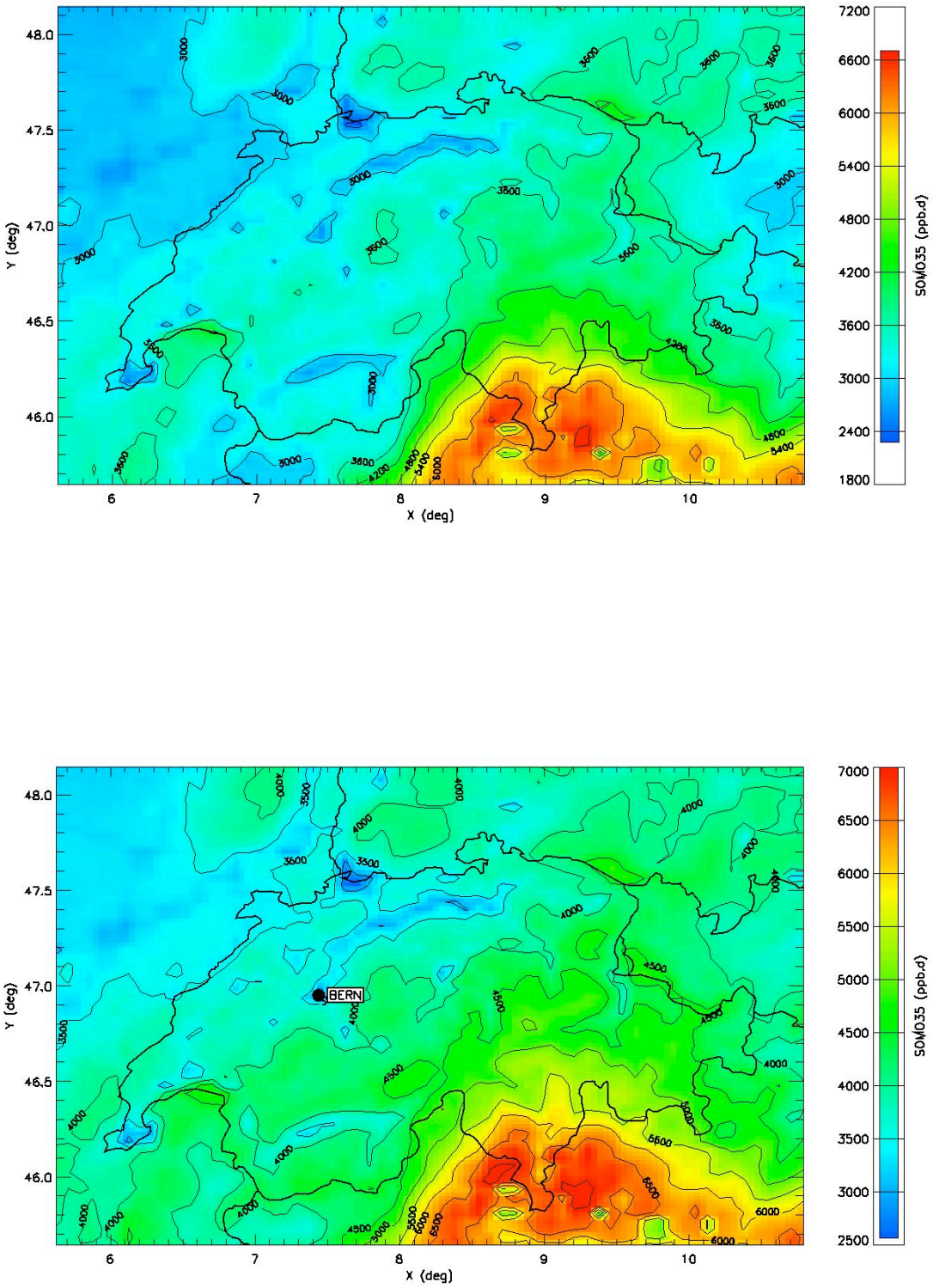

Figure 4.2.3.5: Modelled SOMO35 (ppb.d) for Retro 1,1990 (above) and Retro 2, 1990 (below)

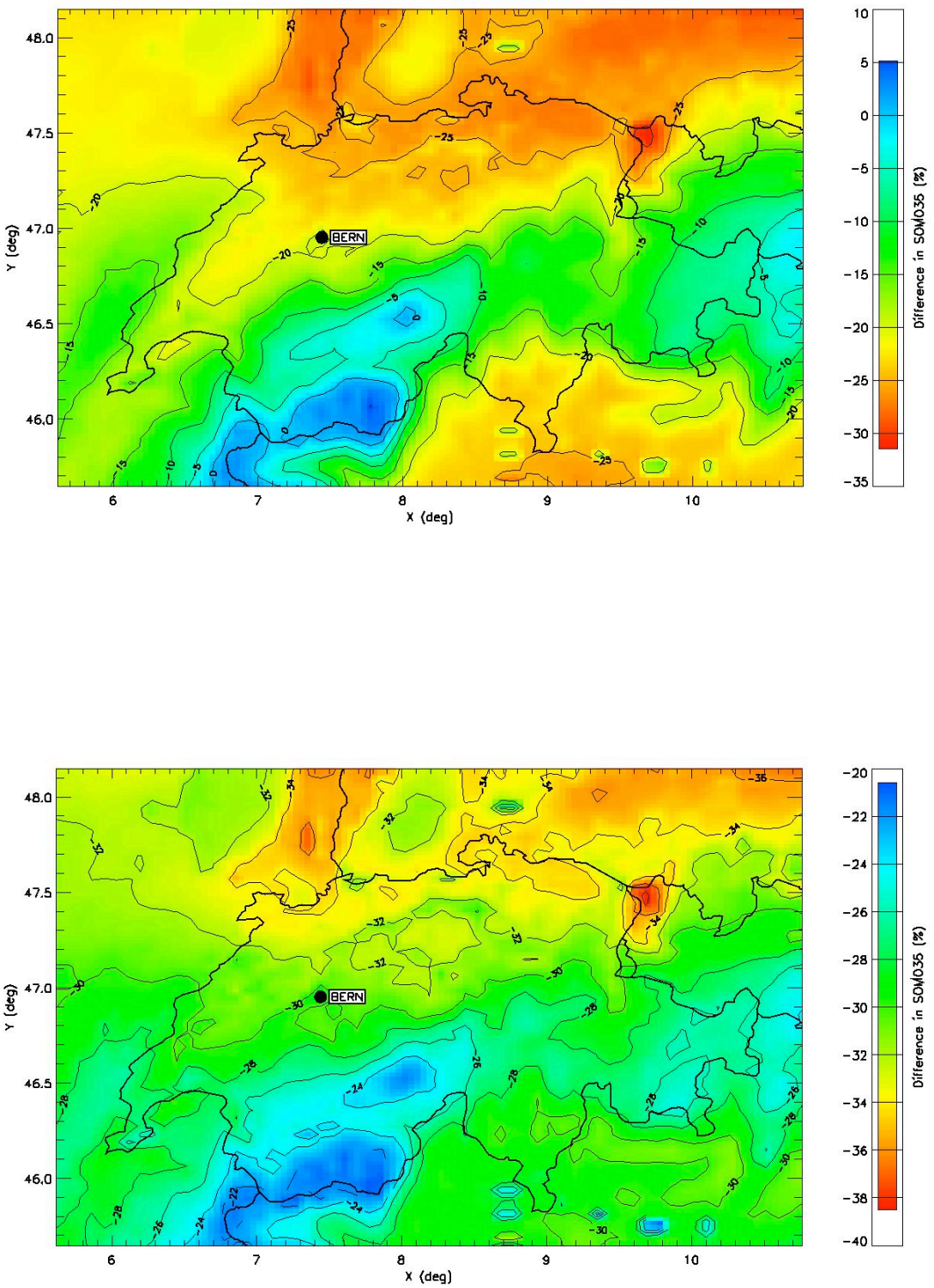

Figure 4.2.3.6: Difference in SOMO35 (%), RC 2005 – Retro 1, 1990 (above) and RC 2005 – Retro 2, 1990 (below).

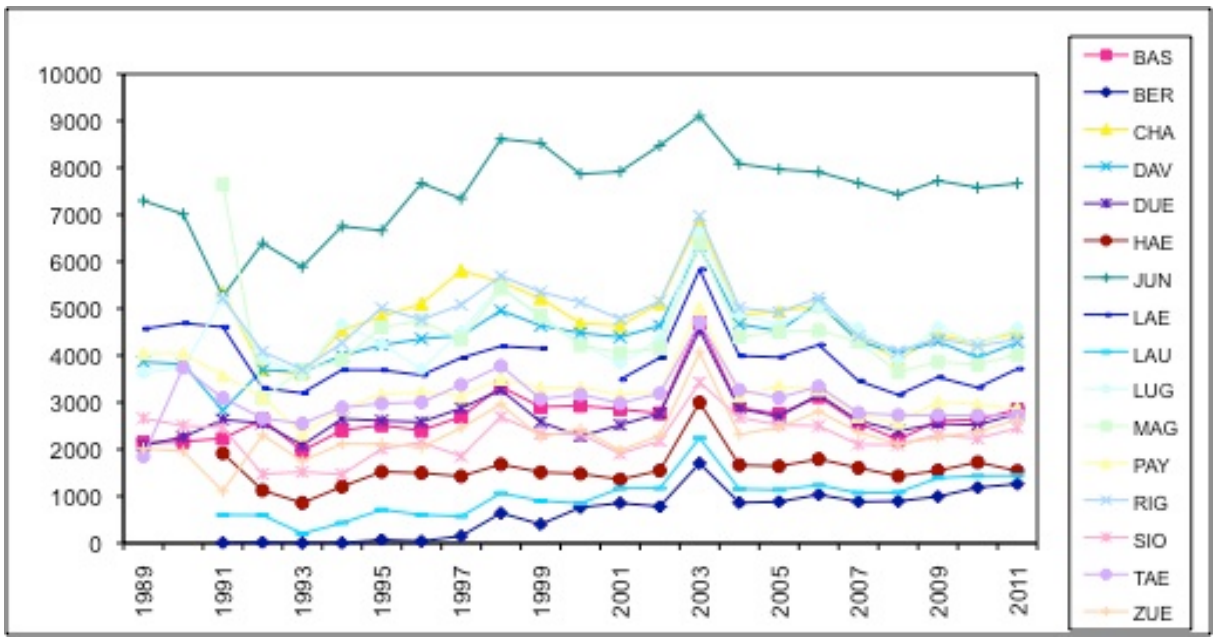

Figure 4.2.3.7: Trends in SOMO35 (ppb.d) from measurements (from FOEN)

4.3 Particulate matter

4.3.1 PM2.5

In this section, annual average PM2.5 concentrations of various emission scenarios will be compared with the reference case. The absolute values for RC 2005 vary between 10-15 $\mu g.m^{-3}$ over the Swiss Plateau and in southern Switzerland (Fig. 4.3.1.1). The measured annual average PM2.5 concentrations lie between 9 and 24 $\mu g.m^{-3}$ and the highest values are from urban traffic sites.

Simulations with various emission scenarios for 2020 suggest that a considerable reduction would be obtained with the BL scenario (30%) (Fig. 4.3.1.2). The predicted reduction in PM2.5 using the Mid and MTFR scenarios are about 35% and 45%, respectively (Figs. 4.3.1.3 - 4.3.1.4). The largest reductions were predicted in the southern part of the Alps.

The annual concentrations were predicted to be much higher in 1990 (Fig. 4.3.1.5). The model results suggest that PM2.5 concentrations decreased by about 40% between 1990 and 2005 in Switzerland (Fig. 4.3.1.6).

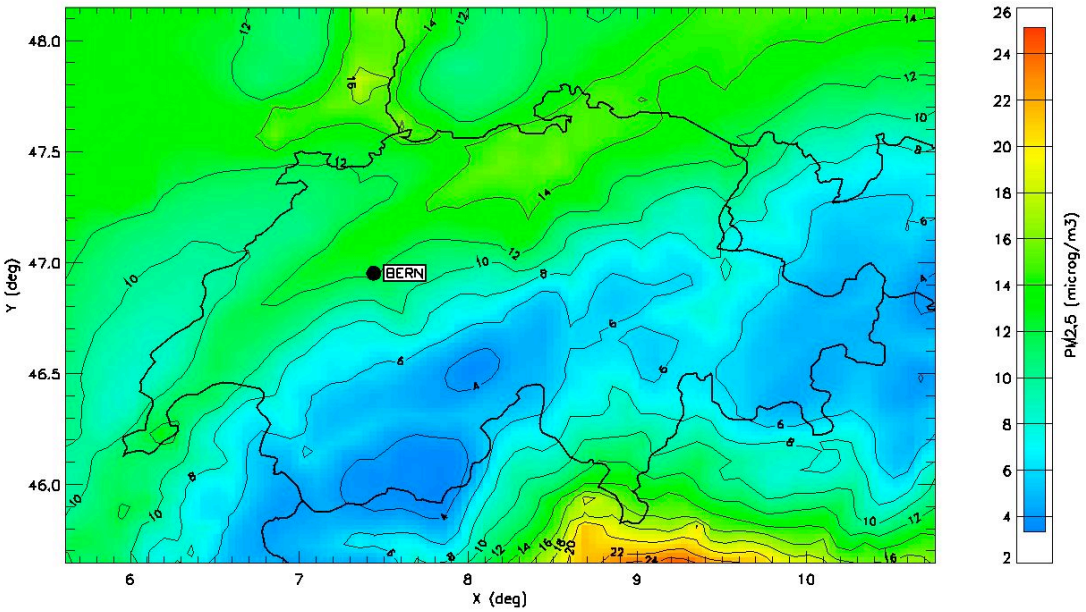

Figure 4.3.1.1: Annual average of PM2.5 ($\mu g.m^{-3}$) for the reference case (RC 2005).

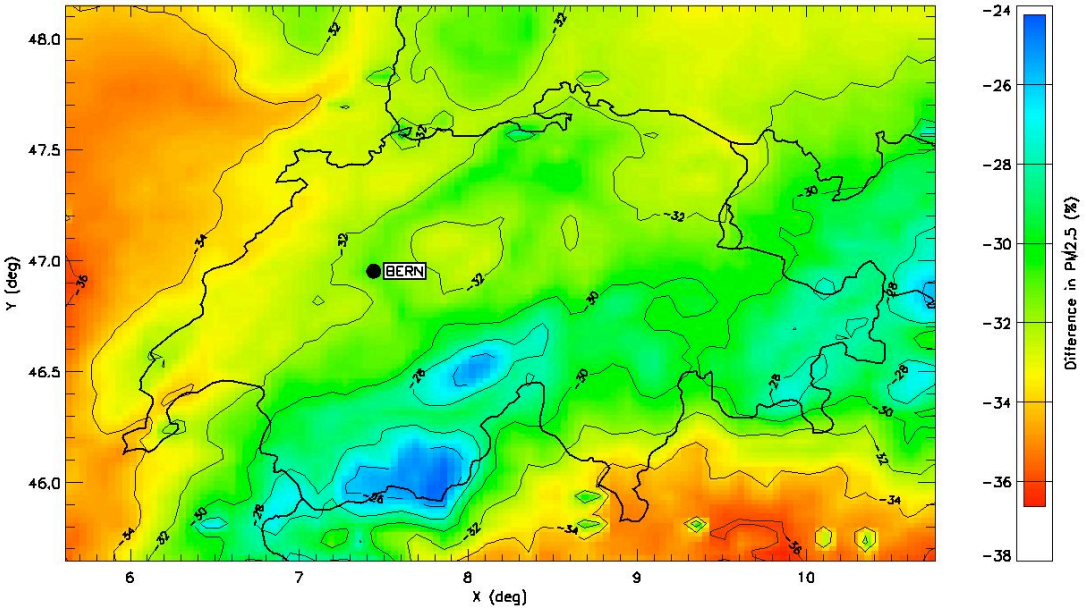

Figure 4.3.1.2: Difference in annual average of PM2.5 (%), BL 2020 - RC 2005

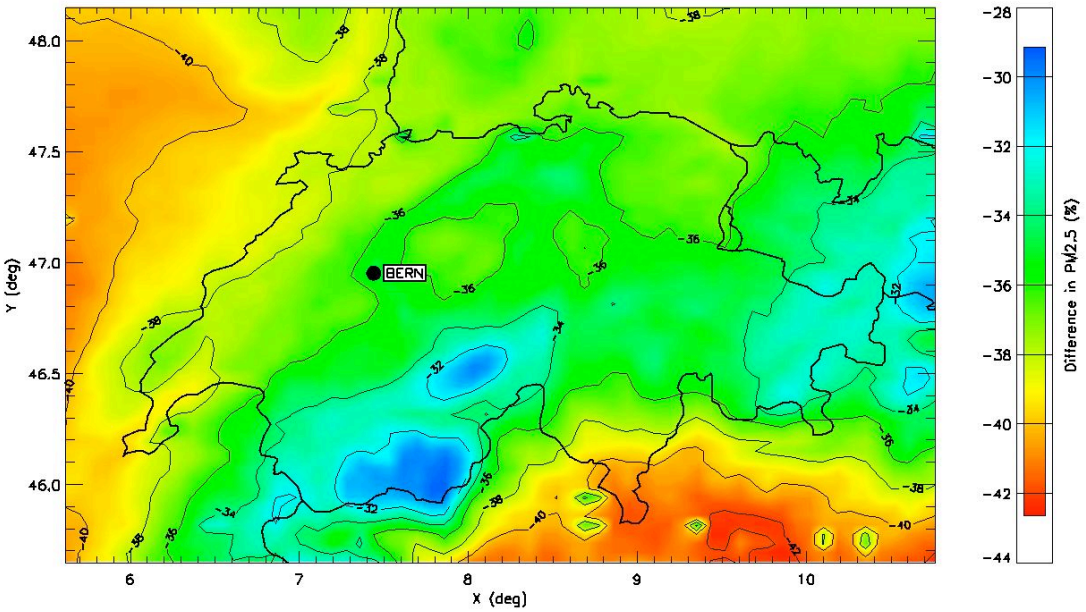

Figure 4.3.1.3: Difference in annual average of PM2.5 (%), Mid 2020- RC 2005.

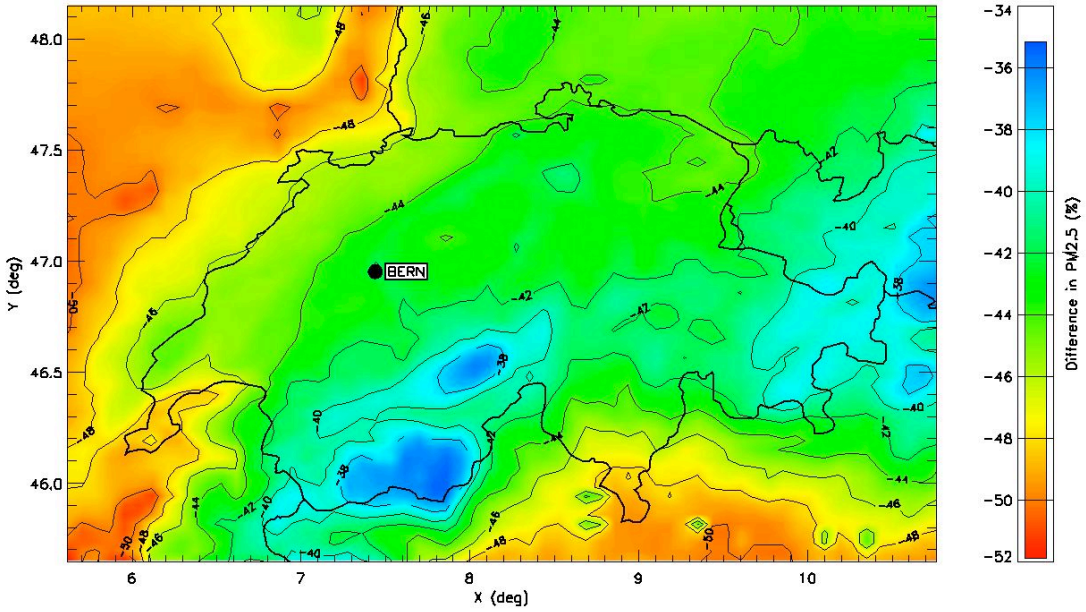

Figure 4.3.1.4: Difference in annual average of PM2.5 (%), MTFR 2020 - RC 2005.

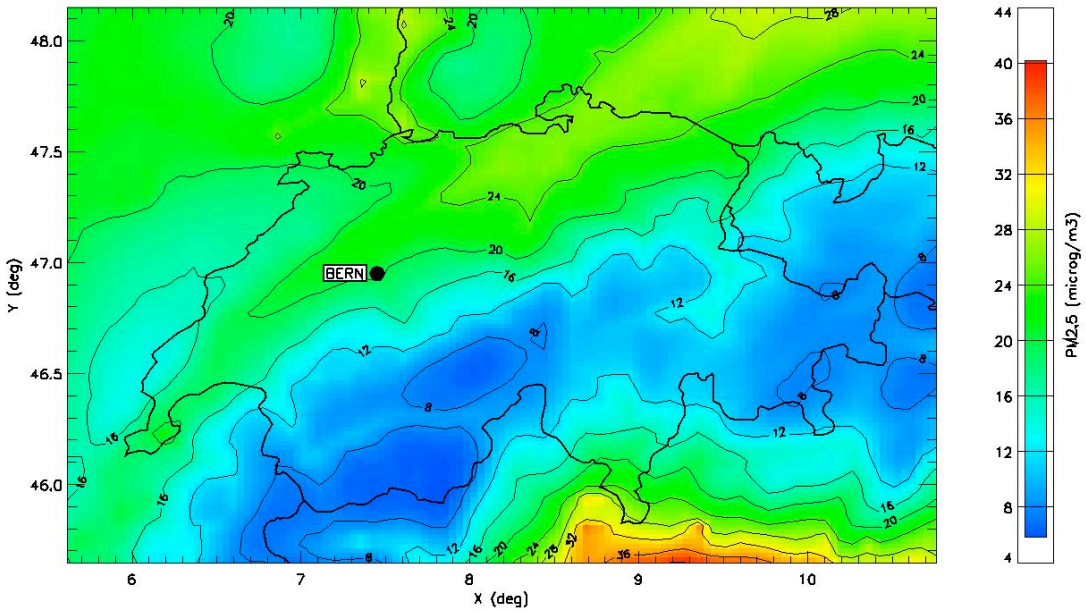

Figure 4.3.1.5: Annual average of PM2.5 ($\mu g.m^{-3}$) for Retro 1, 1990.

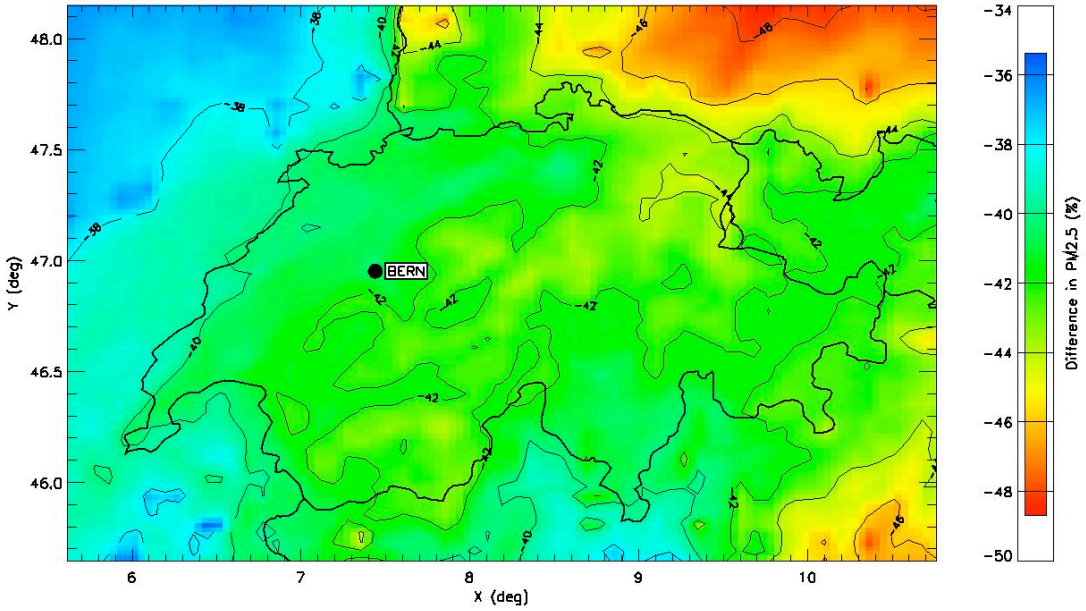

Figure 4.3.1.6: Difference in annual average of PM2.5 (%), RC 2005 – Retro 1, 1990.

4.3.2 PM10

In this section, annual average PM10 concentrations of various emission scenarios will be compared with the reference case. The model predictions show elevated levels of PM10 in 2005 over the Swiss Plateau and in the southern part of the Alps. The absolute values (12 – 18 μg.m^{-3}) are slightly higher than those for PM2.5 (Fig. 4.3.2.1). Comparison with measurements (see Fig. 4.3.2.2) suggests that the model underestimates PM10 concentrations at the urban traffic sites (as also discussed in Chapter 4.1).

A considerable reduction would be obtained in 2020 applying the Gothenburg Protocol scenarios (Figs. 4.3.2.3 - 4.3.2.5). The results suggest that the lowest change would be 30-35% with the BL scenario while MTFR would lead to the largest decrease of about 40-45%.

The modelled average PM10 concentrations in 1990 are shown in Fig. 4.3.2.6. As in the case of PM2.5 (see Chapter 4.3.1), about 40% decrease in PM10 concentrations was predicted between 1990 and 2005 in Switzerland (Fig. 4.3.2.6). The long-term PM10 measurements are available at various NABEL stations (Fig. 4.3.2.2). The relative change in the measured annual average PM10 concentrations vary between 30% and 45% depending on the type of the measurement site. The model results are very similar to the observed ones especially at the rural and elevated sites.

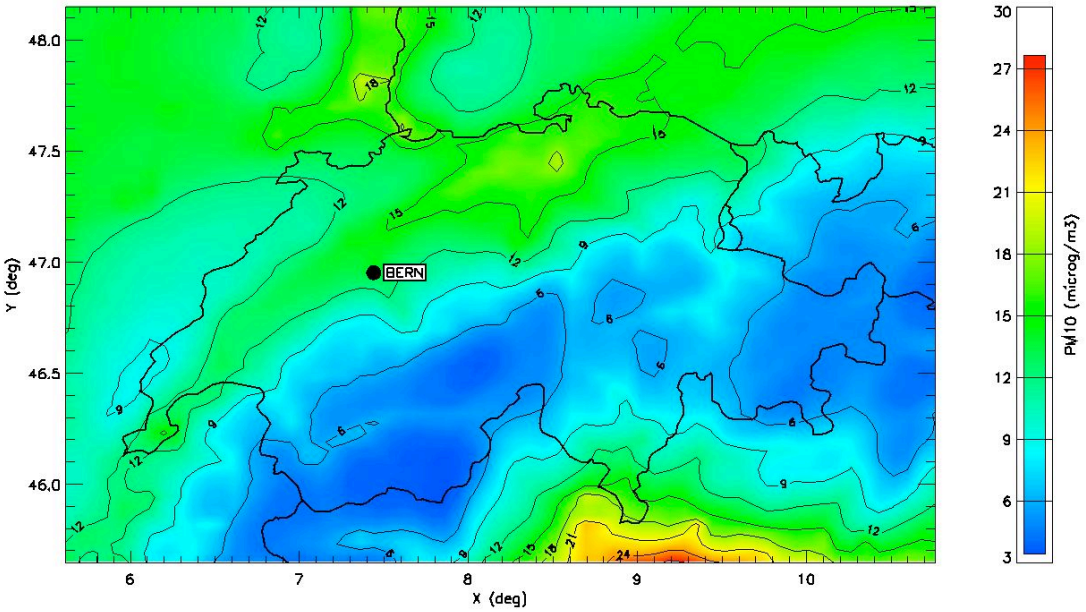

Figure 4.3.2.1: The modelled annual average of PM10 (μg.m^{-3}) for the reference case (RC 2005).

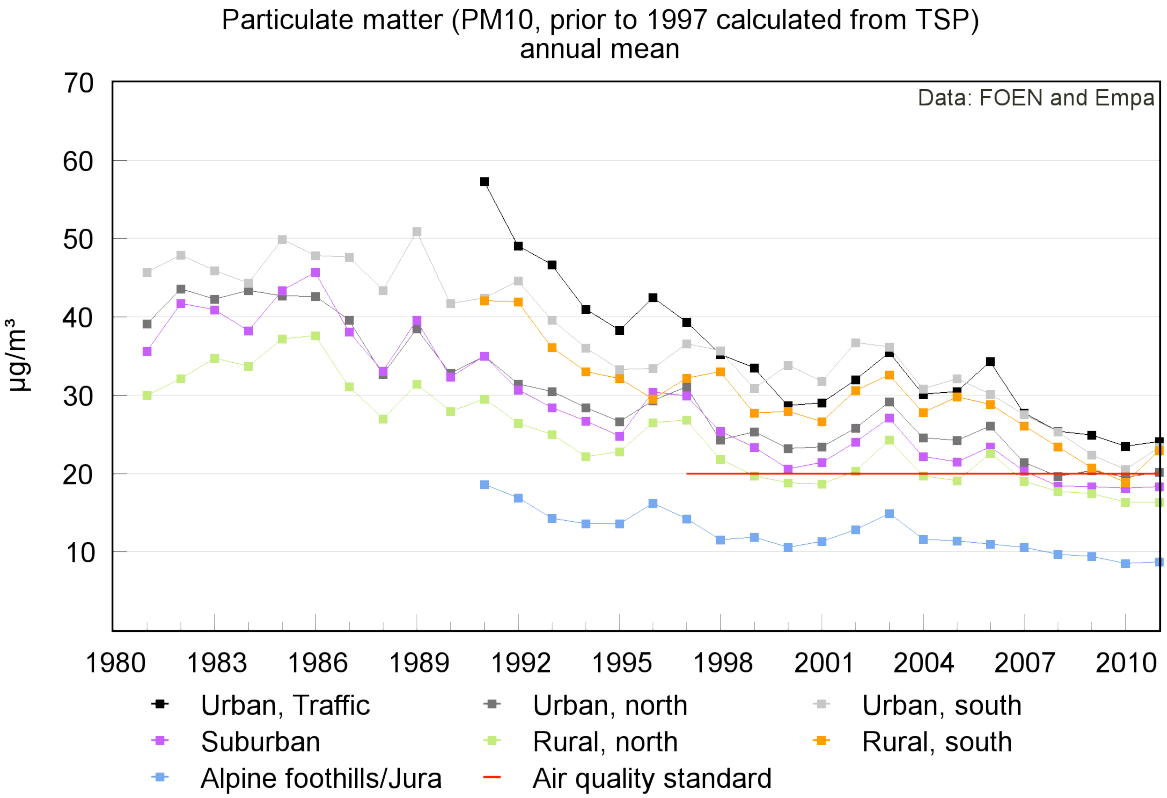

Figure 4.3.2.2: The measured annual average of PM10 (µg.m^{-3}) (from FOEN).

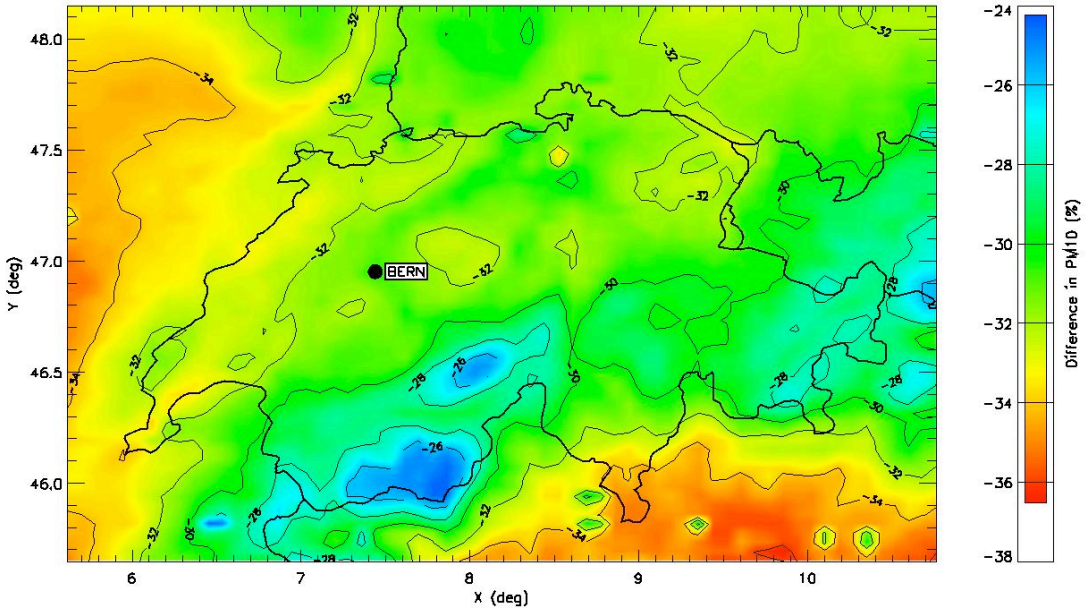

Figure 4.3.2.3: Difference in annual average of PM10 (%), BL 2020 - RC 2005.

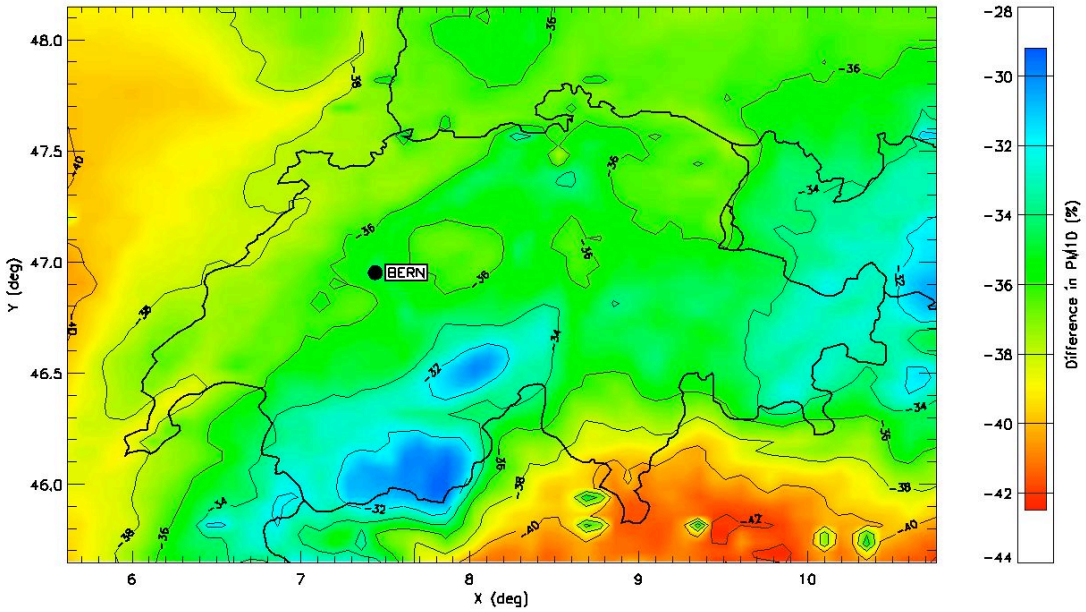

Figure 4.3.2.4: Difference in annual average of PM10 (%), Mid 2020- RC 2005.

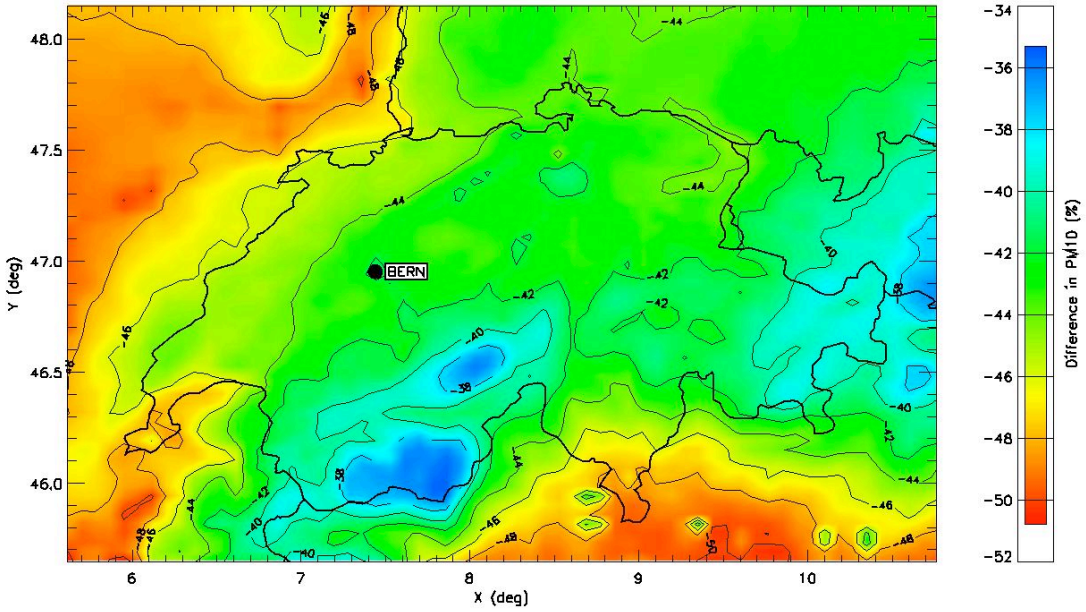

Figure 4.3.2.5: Difference in annual average of PM10 (%), MTFR 2020 - RC 2005.

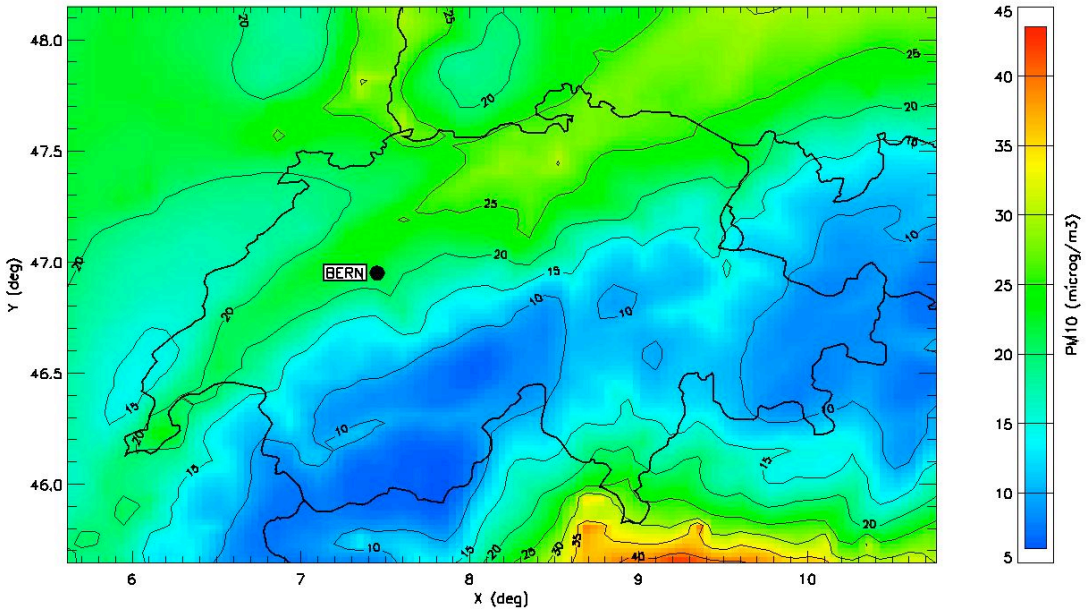

Figure 4.3.2.6: Annual average of PM10 ($\mu g.m^{-3}$) for Retro 1, 1990

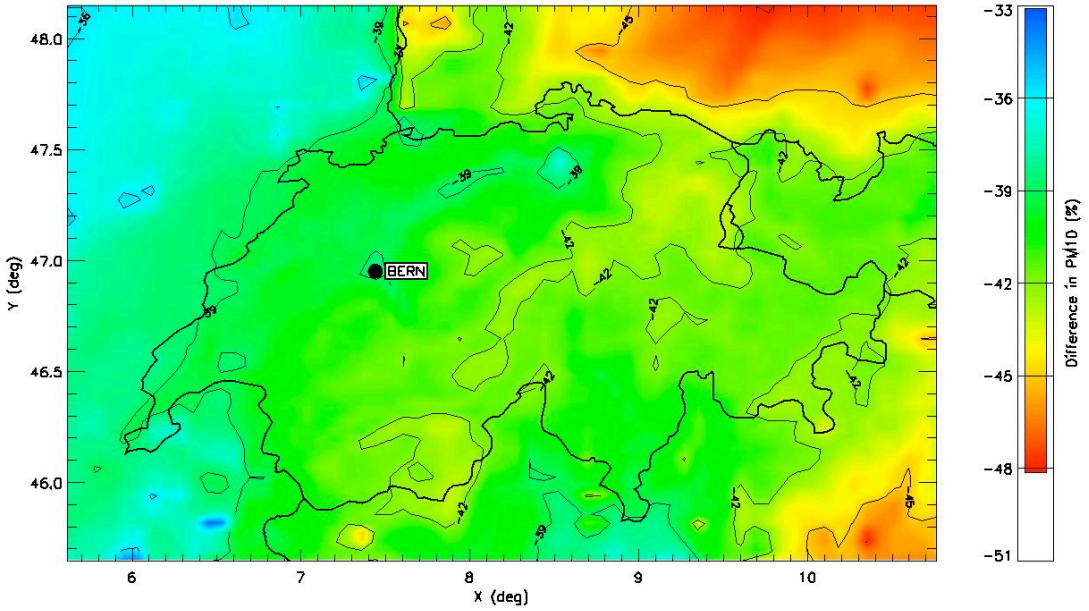

Figure 4.3.2.7: Difference in annual average of PM10 (%), RC 2005 – Retro 1, 1990

4.4 Deposition

Atmospheric deposition of pollutants on ecosystems raises serious concerns. In Switzerland, emissions of air pollutants such as sulphur dioxide and nitrogen oxides have been substantially reduced in the last couple of decades. While sulphur emissions are now stabilized at low levels, nitrogen oxides are still high. In this section, therefore, we focus on nitrogen deposition. In general, the main nitrogen sources are emissions of nitrogen oxides from combustion processes and ammonia from agricultural activities. The deposition of atmospheric nitrogen species constitutes a major nutrient input to the biosphere and enhances the forest growth. The increase of nitrogen inputs into terrestrial ecosystems however, represents a potential threat to forest ecosystems. Enhanced nitrogen deposition might cause soil acidification, eutrophication and nutrient imbalances and reduction in biodiversity. The deposition of atmospheric nitrogen compounds occurs via dry and wet processes. Nitrogen dioxide (NO_2), ammonia (NH_3), nitric acid (HNO_3), and nitrous acid (HONO) are the most important contributors to nitrogen dry deposition. Nitrogen wet deposition is a result of scavenging of atmospheric N constituents. In this section, we discuss the dry and wet deposition of total oxidized and reduced nitrogen compounds (see Table 4.4.1 for oxidized and reduced N species).

The annual deposition of oxidized and reduced nitrogen species for the reference year 2005 are shown in Figs. 4.4.1 and 4.4.2, respectively. The calculated deposition of reduced nitrogen species is higher than that of oxidized species. The modelled total nitrogen deposition for the reference case (2005) varies between 10 and 50 kg N ha^{-1} y^{-1} over the Swiss Plateau (Fig. 4.4.3). Elevated levels can also be seen in the south (10-20 kg N ha^{-1} y^{-1}). On the other hand, it is lower (about 5 kg N ha^{-1} y^{-1}) at high-altitude sites. These numbers are in the same range as those based on measurements at some locations in Switzerland [*Schmitt et al.*, 2005]. Deposition of reduced N species, especially NH_3 dry deposition is high in central Switzerland where ammonia emissions are the highest in Switzerland (Fig. 4.4.2). Combination of high ammonia concentrations with land use favourable for dry deposition leads to highest deposition of ammonia in a few grid cells in central Switzerland.

Model predictions for 1990 suggest that the nitrogen deposition decreased by about 25% between 1990 and 2005, mainly over the Alpine regions (Fig. 4.4.5). On the other hand, nitrogen deposition is predicted to decrease further by about 10-20% until 2020, assuming the baseline scenario (Fig. 4.4.6).

Table 4.4.1: Oxidized and reduced nitrogen species used in dry and wet deposition calculations

Oxidized N species	Deposition type	Reduced N species	Deposition type
NO_2 (nitrogen dioxide)	dry	NH_3 (ammonia)	dry, wet
HNO_3 (nitric acid)	dry, wet	NH_4 (particulate ammonium)	dry, wet
PAN (peroxy acetyl nitrate)	dry		
HONO (nitrous acid)	dry, wet		
PNO_3 (particulate nitrate)	dry, wet		

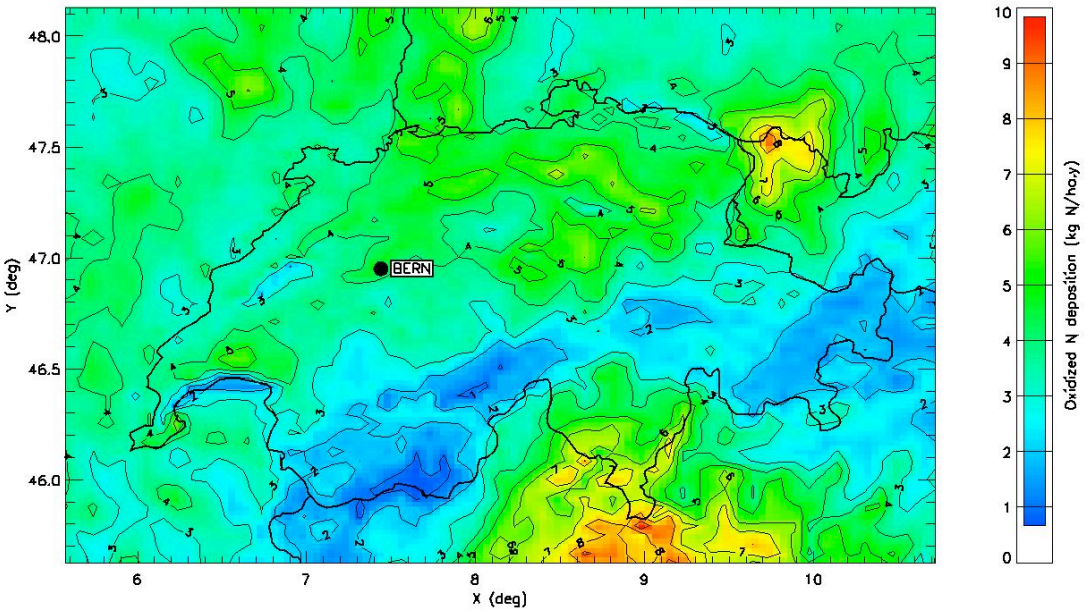

Figure 4.4.1: Deposition of oxidized nitrogen species (kg N $ha^{-1}.y^{-1}$) for the reference case (RC 2005)

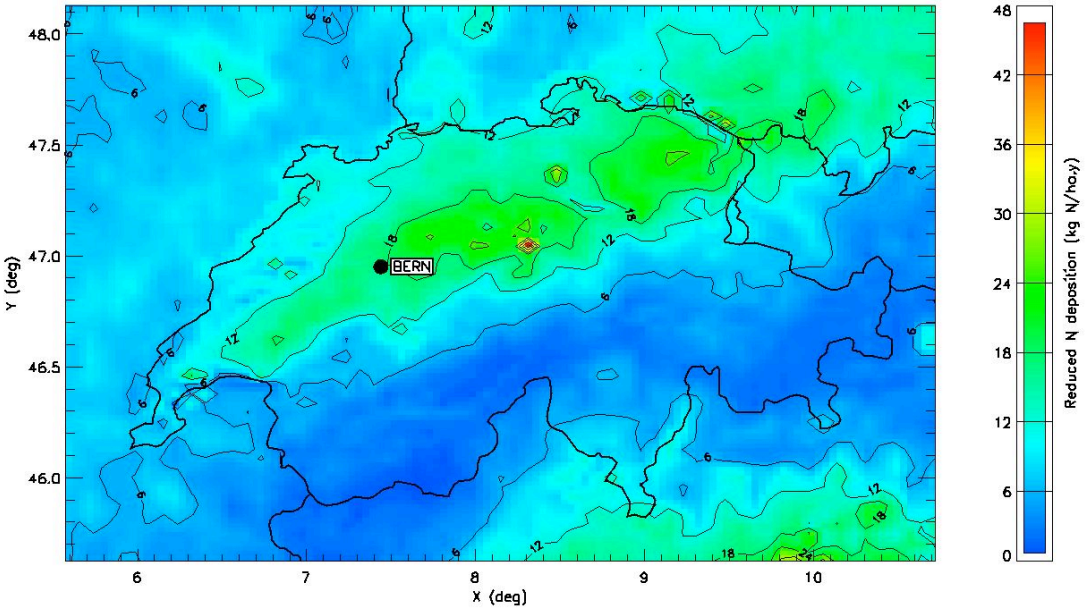

Figure 4.4.2: Deposition of reduced nitrogen species (kg N $ha^{-1}.y^{-1}$) for the reference case (RC 2005)

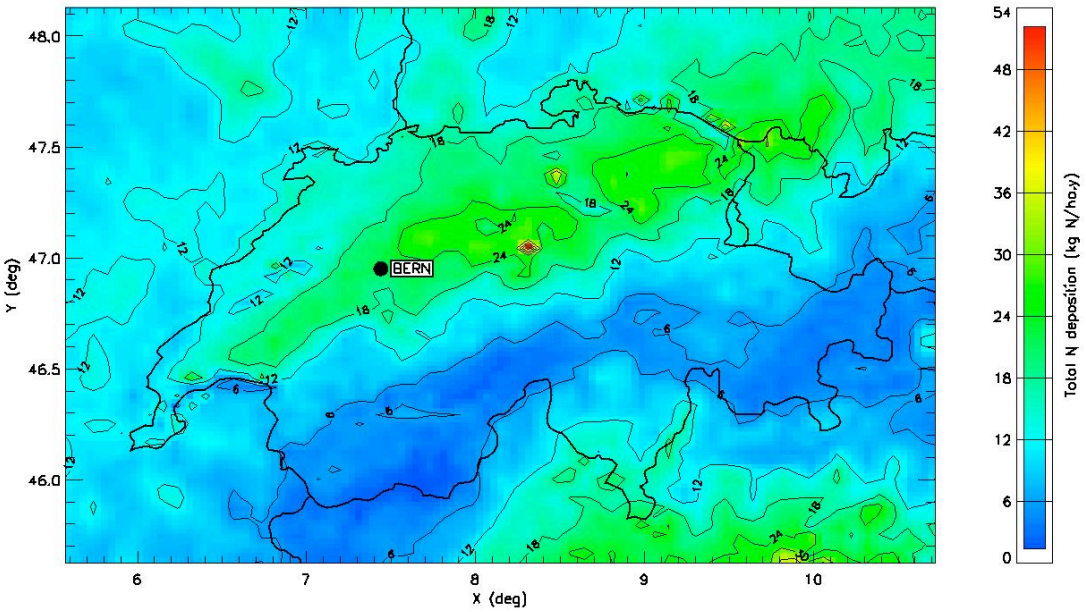

Figure 4.4.3: Deposition of oxidized and reduced nitrogen species (kg N $ha^{-1}.y^{-1}$) for the reference case (RC 2005)

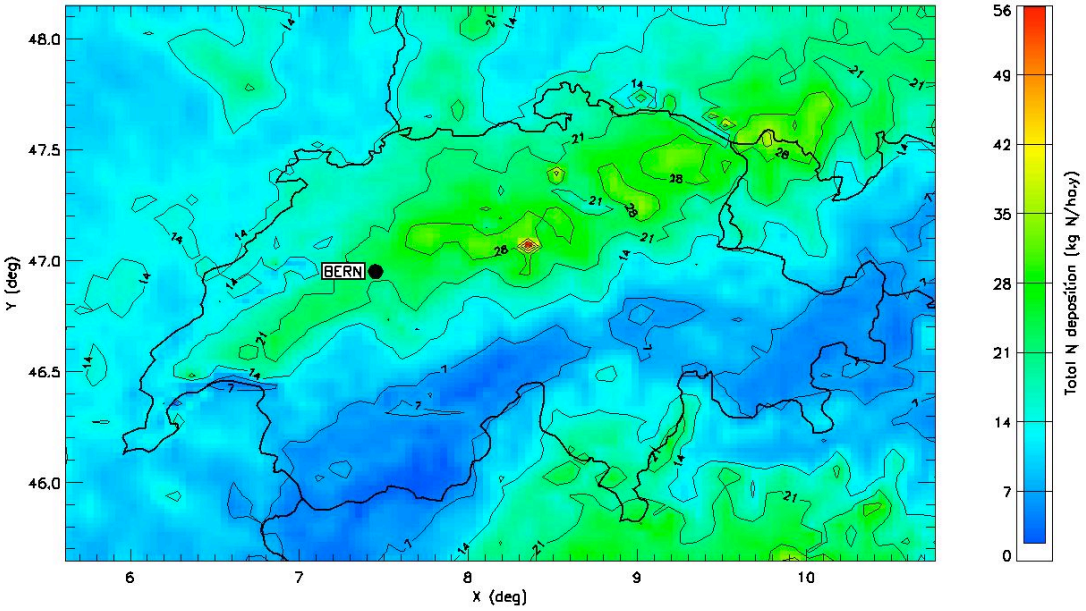

Figure 4.4.4: Deposition of oxidized and reduced nitrogen species (kg N $ha^{-1}.y^{-1}$) for Retro 1, 1990

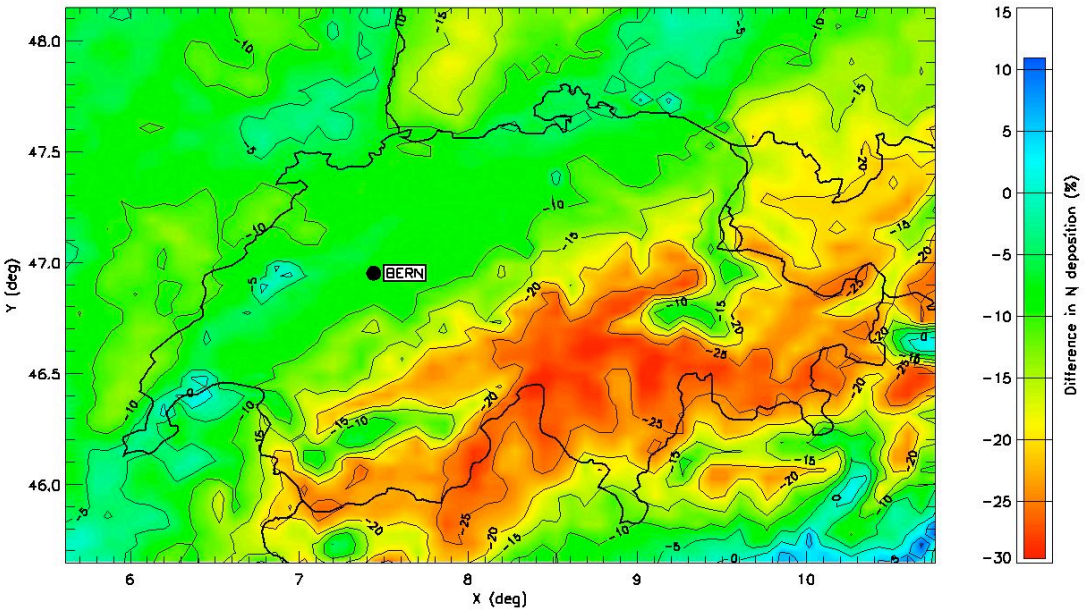

Figure 4.4.5: Difference in deposition of oxidized and reduced nitrogen species (%), RC 2005 – Retro 1, 1990

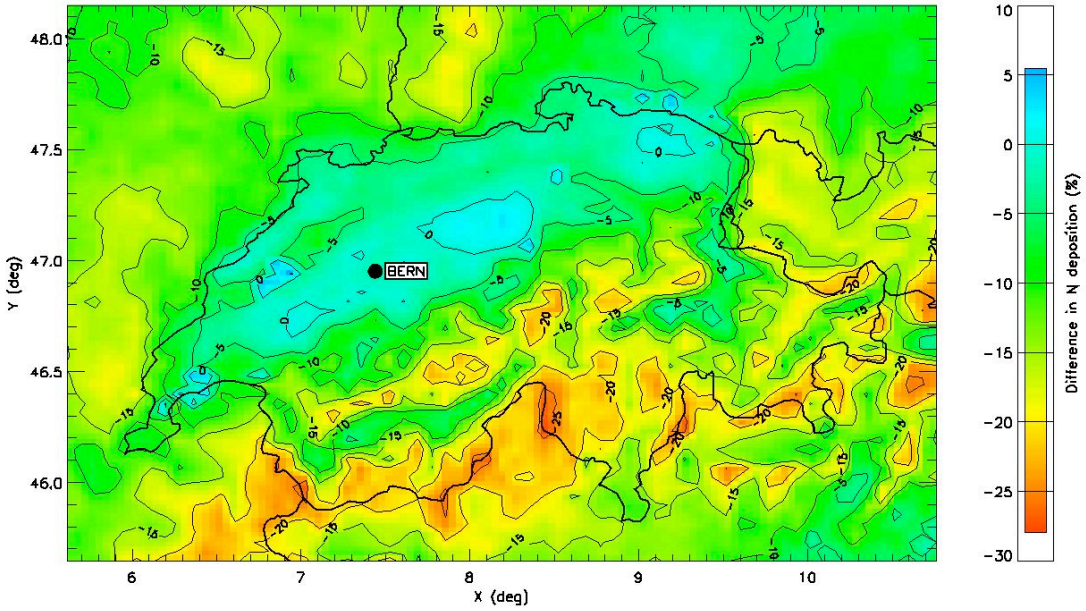

Figure 4.4.6: Difference in deposition of oxidized and reduced nitrogen species (%), BL 2020 – RC 2005

5 Conclusions

The results presented here give a general overview of how different emission scenarios for 2020 would affect the concentrations of ozone and particulate matter in Switzerland. They also indicate the importance of the background ozone concentrations in Europe for use in calculating AOT40 and SOMO35 trends.

Among the three Gothenburg scenarios BL (baseline), Mid and MTFR (Maximum Technically Feasible Reduction), the BL scenario is the closest to the recently revised Gothenburg Protocol. The reduction in Swiss emissions of gaseous species such as NO_x, SO_2, NMVOC and NH_3, is less than those of the neighbouring countries Germany, France, Italy and Austria. Reductions in PM2.5, on the other hand, are comparable.

The modelled PM2.5 concentrations in 2005 varied between 10 – 15 µg m^{-3} in Switzerland and PM2.5 / PM10 ratio was about 80%. Our results show that the application of emission reductions according to the BL scenario would lead to a significant decrease of PM2.5 (30%) in 2020. We also found that the effects of BL and Mid scenarios would be very similar. The maximum technically feasible reduction (MTFR) scenario would lead to the largest decrease (45%); its application, however, is unlikely.

We have also shown that under the BL scenario, the annual average ozone concentrations would decrease only by about 5% over the Alpine regions and would continue to increase in the Swiss Plateau. Further analysis of our results suggests that although emission reductions do lead to a decrease in peak ozone concentrations, they also cause an increase in the lower ozone concentrations, especially in urban areas due to less titration with NO. AOT40 values (which refer to ozone levels above 40 ppb) were predicted to decrease in 2020 by a large amount (50%) during the vegetation period. The health-relevant indicator SOMO35 for 2020 was also predicted to be lower by about 30-40% with respect to the reference year 2005.

The modelled relative changes of 35-45% in annual average concentrations of PM2.5 and PM10 between 1990 and 2005 agree very well with those from measurements at various stations in Switzerland. The absolute values of modelled AOT40 and SOMO35 for 2005 also match the data obtained from measurements reasonably well. The model results suggest a significant decrease in AOT40 since 1990 whereas observations show not only a decrease at some rural sites but also an increase at urban sites during that period. A similar discrepancy was found for SOMO35. Since calculation of AOT40 and SOMO35 is very sensitive to the threshold values, the background ozone concentrations might affect the model results. Although simulations with lower background ozone concentrations in 1990 improved the agreement between the model results and measurements, there was still some discrepancy. We conclude that even though the background ozone concentrations used in the model are based on recent observations, they might need further revision.

We also analysed the model results for both dry and wet deposition of all oxidized and reduced nitrogen species. We found the highest nitrogen depositions in 2005 over the Swiss Plateau and in the southern part of the Alps (20 - 25 kg N $ha^{-1}.y^{-1}$). These results are in the same range as a few reported measurement data available. Our results indicate that the deposition of the reduced nitrogen species ammonia and

particulate ammonium is larger than the deposition of the oxidized species. We also showed that the deposition of reduced N species (ammonia and particulate ammonium) occurred mainly in the northern part of the Alps where ammonia emissions are the highest.

We predicted that the nitrogen deposition decreased by 10 – 30% between 1990 and 2005. Further reductions in emissions until 2020 according to the baseline scenario would lead to 25% lower nitrogen deposition mainly due to the reduction in the oxidized fraction.

The results obtained in this modelling study show the need for a detailed analysis of background ozone concentrations, which are important in the calculation of AOT40 and SOMO35 trends, since these vegetation and health impact indicators are very sensitive to that parameter.

In this study, the focus was on annual averages of PM and ozone in Switzerland and the relative differences between various emission-scenarios. In order to achieve these results however, we modelled hourly, 3-dimensional, gridded concentrations of 35 gaseous and particulate species as well as their dry and wet depositions for entire 1990, 2005, 2006 and 2020 (with three different emission scenarios for 2020). The extensive model data generated in this way provide a very valuable dataset for further detailed analyses of individual gaseous and aerosol species, their trends, seasonal variations and deposition rates.

6 Acknowledgements

This study was financially supported by the Swiss Federal Office of Environment, FOEN.

We are grateful to the following people and institutions for providing weather, emission and air quality data: ECMWF, TNO, AQMEII, IIASA, INFRAS, Meteotest, NABEL/EMPA. We appreciate the availability of CAMx model developed by ENVIRON.

Our thanks extend to G. Theis and R. Weber (FOEN) for the fruitful co-operation throughout this project.

7 Acronyms

AOT40	Accumulated dose of ozone Over the Threshold of 40 ppb
BUWAL	Bundesamt fuer Umwelt, Wald und Landschaft
CAMx	Comprehensive Air Quality Model with EXtensions
CEST	Central European Summer Time (daylight saving time for Switzerland, 2 h ahead of UTC)
ECMWF	European Centre for Medium-Range Weather Forecasts
EMEP	European Monitoring and Evaluation Programme
	(Cooperative Programme for Monitoring and Evaluation of the Long-range Transmission of Air Pollutants in Europe
GAINS	The greenhouse gas and air pollution interactions and synergies model
IIASA	International Institute for Applied Systems Analysis
MM5	Meso-scale Model 5
MOZART	Model for OZone And Related chemical Tracers
NMVOC	non-methane volatile organic compounds
SNAP	Selected Nomenclature for Air Pollution
SOMO35	Sum of Ozone Means Over 35 ppb
TNO	The Netherlands Organisation for Applied Scientific Research
UTC	Universal Time Coordinated

8 References

Aksoyoglu, S., J. Keller, I. Barmpadimos, D. Oderbolz, V. A. Lanz, A. S. H. Prévôt, and U. Baltensperger (2011), Aerosol modelling in Europe with a focus on Switzerland during summer and winter episodes, *Atmos. Chem. Phys.*, *11* (14), doi:10.5194/acp-5111-7355-2011, 7355-7373.

Alfarra, M. R., A. S. H. Prevot, S. n. Szidat, J. Sandradewi, S. Weimer, V. A. Lanz, D. Schreiber, M. Mohr, and U. Baltensperger (2007), Identification of the Mass Spectral Signature of Organic Aerosols from Wood Burning Emissions, *Environmental Science & Technology*, *41*(16), 5770-5777.

Amann, M., D. Derwent, B. Forsberg, O. Hänninen, F. Hurley, M. Krzyzanowski, F. de Leeuw, S. J. Liu, C. Mandin, J. Schneider, P. Schwarze, and D. Simpson (2008), Health risks of ozone from long-range transboundary air pollution *Rep.*, WHO, Copenhagen, Denmark.

Andreani-Aksoyoglu, S., and J. Keller (1995), Estimates of monoterpene and isoprene emissions from the forests in Switzerland, *Journal of Atmospheric Chemistry*, *20*, 71-87.

Andreani-Aksoyoglu, S., J. Keller, C. Ordonez, M. Tinguely, M. Schultz, and A. S. H. Prevot (2008), Influence of various emission scenarios on ozone in Europe, *Ecological Modelling*, *217*, doi:10.1016/j.ecolmodel.2008.1006.1022, 1209-1218.

Andreani-Aksoyoglu, S., J. Keller, I. Barmpadimos, D. Oderbolz, M. Tinguely, A. S. H. Prévôt, R. Alfarra, and J. Sandradewi (2009), Modelling of air quality for winter and summer episodes in Switzerland, *PSI Report Nr. 09-06, 09-06*, Paul Scherrer Institute.

Ashmore, M. R., and R. B. Wilson (1992), Critical levels of air pollutants for Europe. Background papers prepared for the United Nations Economic Commission for Europe Workshop on Critical Levels. Egham, United Kingdom, 23-26 March 1992 *Rep.*

BFS (1999), *GEOSTAT Benuetzerhandbuch*, Bern.

Cofala, J., M. Amann, C. Heyes, F. Wagner, Z. Klimont, M. Posch, W. Schoepp, L. Tarasson, J. E. Jonson, C. Whall, and A. Stavrakaki (2007), Analysis of Policy Measures to Reduce Ship Emissions in the Context of the Revision of the National Emissions Ceilings Directive. Final Report, IIASA Contract No. 06-107.

Denier van der Gon, H., A. Visschedijk, H. van de Brugh, and R. Droege (2010), A high resolution European emission data base for the year 2005. A contribution to UBA-Projekt: “Strategien zur Verminderung der Feinstaubbelastung” – PAREST: Partikelreduktionsstrategien –Particle Reduction Strategies *Rep. TNO-034-UT-2010-01895_RPT-ML*, TNO, Utrecht (NL).

ESA_GOFC-GOLD (2011), The GlobCover Project, edited.

Gauss, M., A. Nyiri, B.M. Steensen, and H. Klein (2012), Transboundary air pollution by main pollutants (S, N, O3) and PM in 2010 *Rep. ISSN 1890-0003*, Norway.

Heldstab, J., and P. Wuethrich (2006), Emissionsmuster. Raeumliche Verteilung und Ganglinien fuer CO- /NMVOC-Emissionen *Rep.*, 15 pp, BAFU, Bern / Zürich.

Heldstab, J., P. de Haan van der Weg, T. Kuenzle, M. Keller, and R. Zbinden (2003), Modelling of PM10 and PM2.5 ambient concentrations in Switzerland 2000 and

2010*Rep. Environmental Documentation No. 169*, Bundesamt fuer Umwelt, Wald und Landschaft (BUWAL), Bern.

Horowitz, L. W., S. Walters, D. L. Mauzerall, L. K. Emmons, P. J. Rasch, C. Granier, X. Tie, J.-F. Lamarque, M. G. Schultz, G. S. Tyndall, J. J. Orlando, and G. P. Brasseur (2003), A global simulation of tropospheric ozone and related tracers: Description and evaluation of MOZART, version 2. , *J. Geophys. Res.*, *108*, 4784, doi:4710.1029/2002JD002853.

INFRAS (2010), HBEFA. Handbuch Emissionsfaktoren des Strassenverkehrs. Version 3.1, edited, INFRAS, UBA Berlin, UBA Wien, BAFU, Bern.

Keller, J., S. Andreani-Aksoyoğlu, and U. Joss (1995), Inventory of natural emissions in Switzerland, paper presented at Air Pollution III, Computational Mechanics Publications, Porto Carras, Greece.

Kropf, R. (2001), Massnahmen zur Reduktion der PM10-Emissionen*Rep. Umwelt-Materialien Nr. 136, Luft*, 112 pp, Bundesamt fuer Umwelt (BAFU), Bern.

Kupper, T., C. Bonjour, B. Achermann, F. Zaucker, B. Rihm, A. Nyfeler-Brunner, C. Leuenberger, and H. Menzi (2010), Ammoniakemissionen in der Schweiz: Neuberechnung 1990-2007 Prognose bis 2020 *Rep.*, BAFU.

Lanz, V. A., A. S. H. Prevot, M. R. Alfarra, S. Weimer, C. Mohr, P. F. DeCarlo, M. F. D. Gianini, C. Hueglin, J. Schneider, O. Favez, B. D'Anna, C. George, and U. Baltensperger (2010), Characterization of aerosol chemical composition with aerosol mass spectrometry in Central Europe: an overview, *Atmos. Chem. Phys.*, *10* (21), 10453-10471.

Logan, J. A., J. Staehelin, I. A. Megretskaia, J. P. Cammas, V. Thouret, H. Claude, H. De Backer, M. Steinbacher, H. E. Scheel, R. St¸bi, M. Frˆhlich, and R. Derwent (2012), Changes in ozone over Europe: Analysis of ozone measurements from sondes, regular aircraft (MOZAIC) and alpine surface sites, *J. Geophys. Res.*, *117*(D9), D09301.

Mahrer, F., and C. Vollenweider (1983), *Landesforstinventar LFI*, Eidgenössische Forschungsanstalt für Wald, Schnee und Landschaft (WSL), Birmensdorf.

Oderbolz, D. C., S. Aksoyoglu, J. Keller, I. Barmpadimos, R. Steinbrecher, C. A. Skjøth, C. Plaß-Dülmer, and A. S. H. Prévôt (2013), A comprehensive emission inventory of biogenic volatile organic compounds in Europe: improved seasonality and land-cover, *Atmos. Chem. Phys.*, *13* (4), 1689-1712.

Passant, N. R. (2002), Speciation of UK emissions of non-methane volatile organic compounds*Rep.*, 289 pp, AEA Technology, Culham.

Pope, C. A., and D. W. Dockery (2006), Health Effects of Fine Particulate Air Pollution: Lines that Connect, *Journal of the Air & Waste Management Association*, *56* (6), 709-742.

Schmitt, M., L. Thöni, P. Waldner, and A. Thimonier (2005), Total deposition of nitrogen on Swiss long-term forest ecosystem research (LWF) plots: comparison of the throughfall and the inferential method, *Atmospheric Environment*, *39* (6), 1079-1091.

Schneider, A. (2007), Branchenspezifische VOC-Profile *Rep. 129.17*, BAFU, Bern / Basel.

Simpson, D., W. Winiwarter, G. Börjesson, S. Cinderby, A. Ferreiro, A. Guenther, N. C. Hewitt, R. Janson, M. A. K. Khalil, S. Owen, T. E. Pierce, H. Puxbaum, M.

Shearer, U. Skiba, R. Steinbrecher, L. Tarrasón, and M. G. Öquist (1999), Inventorying emissions from nature in Europe, *Journal of Geophysical Research*, *104* (D7), 8113-8152.

Szidat, S., T. M. Jenk, H.-A. Synal, M. Kalberer, L. Wacker, I. Hajdas, A. Kasper-Giebl, and U. Baltensperger (2006), Contributions of fossil fuel, biomass burning, and biogenic emissions to carbonaceous aerosols in Zurich as traced by 14C, *J. Geophys. Res.*, *111, D07206*, doi:10.1029/2005JD006590.

UNECE (1999), Protocol to Abate Acidification, Eutrophication and Ground-level Ozone, edited by UNECE.

Wagner, F. (2012), personal communication, IIASA, edited, IIASA / GAINS.

Wagner, F., M. Amann, B. Imrich, J. Cofala, C. Heyes, Z. Klimont, P. Rafaj, and W. Schoepp (2010), Baseline Emission Projections and Further Cost-effective Reductions of Air Pollution Impacts in Europe - A 2010 Perspective*Rep.*, IIASA Contract No. 070307/2009/531887/SER/C4.

Wilson, R. C., Z. L. Fleming, P. S. Monks, G. Clain, S. Henne, I. B. Konovalov, S. Szopa, and L. Menut (2012), Have primary emission reduction measures reduced ozone across Europe? An analysis of European rural background ozone trends 1996–2005, *Atmos. Chem. Phys.*, *12* (1), 437-454.

Yarwood, G., S. Rao, M. Yocke, and G. Z. Whitten (2005), Updates to the Carbon Bond chemical mechanism: CB05 *Rep. RT-04-00675*, Yocke & Company, Novato, CA 94945.

Zhang, Y., S. C. Olsen, and M. K. Dubey (2010), WRF/Chem simulated springtime impact of rising Asian emissions on air quality over the U.S, *Atmospheric Environment*, *44* (24), 2799-2812.

Appendix 1 : Models

Meteorological Model, WRF

Eulerian chemical transport models (often called air quality models) require 3-dimensional fields of numerous time dependent meteorological quantities, e.g. air temperature, specific humidity, air pressure, wind velocity components, etc. In so-called off-line coupled models a meteorological pre-processor, usually a weather forecast model, provides those fields. An interface program is then used to convert the meteorological fields to the format required by the air quality model.

The Weather Research & Forecasting Model (WRF-ARW) Version 3.2.1 (http://www.wrf-model.org) was taken as the meteorological pre-processor and a modified version of WRFCAMx Version 3.1 as the interface.

WRF domains 1 and 2 were defined in geographical coordinates as follows:

Coarse grid (domain 1):

longitude: -15 to 35 deg E
latitude: 35 to 70 deg N
longitude grid cell size: 0.2500 deg
latitude grid cell size: 0.1250 deg
no. WE cells: 200
no. SN cells: 280
no. vertical layers: 31

Fine grid (domain 2):

longitude: 3.0 to 13.5 deg E
latitude: 43.5 to 50.0 deg N
longitude grid cell size: 0.0833 deg
latitude grid cell size: 0.0417 deg
no. WE cells: 126
no. SN cells: 156
no. vertical layers: 31

WRF Domain 1 is equal to the CAMx Domain 1. Domain 2 for WRF, however, is slightly larger than the corresponding CAMx domain to avoid numerical artefacts at the CAMx boundaries. CAMx Domain 2, including buffer cells, is extended by 2 cells at each of the 4 borders to get WRF Domain 2.

We used the data from ECMWF (*http://www.ecmwf.int*) data every 6 hours) to provide initial and boundary conditions for the WRF model.

In order to validate the meteorological model, we compared the simulated parameters such as temperature, wind direction, wind speed, solar irradiance, specific humidity, and the precipitation rate with measurements at various ANETZ stations as well as the data from ECMWF.

Air Quality Model, CAMx

The Comprehensive Air Quality Model with Extensions (CAMx) is an Eulerian photochemical dispersion model that allows for an integrated "one-atmosphere" assessment of gaseous and particulate air pollution over many scales ranging from urban to regional *(http://www.camx.com)*. CAMx simulates the emission, dispersion, chemical reactions, and removal of pollutants in the lower troposphere by solving the pollutant continuity equation for each chemical species on a system of nested three-dimensional grids. The model incorporates two-way grid nesting, which means that pollutant concentration information propagates into and out of all grid nests. This feature allows CAMx to be run with coarse grid spacing over a wide regional domain in which high spatial resolution is not particularly needed, while within the same run, applying fine grid nests in areas where high resolution is needed.

The CAMx simulations used a subset of 14 of the WRF σ-layers, of which the lowest had a thickness of about 20 m at a surface pressure of 950 hPa. The model top was set at σ=0.55 which corresponds to a geometric layer top of about 7000 m above sea level. The initial and boundary concentrations for the first domain were obtained from the global model MOZART [*Horowitz et al.*, 2003]. The photolysis rates were calculated using the TUV photolysis pre-processor [*Madronich*, 2002]. The required ozone column densities were extracted from TOMS data (*http://toms.gsfc.nasa.gov/ozone/ozone.html*). Dry deposition of gases was based on the resistance model of [*Zhang et al.*, 2003]. Surface deposition of particles occurs via diffusion, impaction and/or gravitational settling. Separate scavenging models for gases and aerosols were implemented in CAMx to calculate the wet deposition [*Environ*, 2006]. The gas-phase mechanism used in this work was CB05 [*Yarwood et al.*, 2005]. There are 51 species and 156 chemical reactions included in the CB05 mechanism.

Simulated aerosol species with particle sizes smaller than 2.5 μm included sulphate, nitrate, ammonium, POA, SOA and elemental carbon (EC). The condensable organic gases (CG) are formed from the oxidation of the aromatic precursors TOL (toluene) and XYL (xylene), as well as of the biogenic precursors isoprene, monoterpenes and sesquiterpenes (see Table 1 for the SOA precursor reactions). Partitioning of condensable organic gases to secondary organic aerosols was calculated using a semi-volatile equilibrium scheme called SOAP [*Strader*, 1999]. Properties of CG/SOA pairs used in CAMx are given in Table 2. It was assumed that the SOA oligomerized to a non-volatile form with a lifetime of about 1 day [*Kalberer et al.*, 2004]. Oligomerization slowly forms organic aerosol oligomers called SOPA (anthropogenic) and SOPB (biogenic), and it was shown to increase SOA yields [*Morris et al.*, 2006]. Aqueous sulphate and nitrate formation in cloud water were calculated using the RADM aqueous chemistry algorithm [*Chang et al.*, 1987]. Partitioning of inorganic aerosol constituents between the gas and aerosol phases was modelled with ISORROPIA [*Nenes et al.*, 1998].

There are two main output files in CAMx; 1) hourly average concentrations of each gaseous and particulate species in each grid cell, for each layer, and for each domain, 2) hourly surface deposition of all species.

Table 1: SOA precursor reactions included in CAMx [*Environ*, 2006].

Precursor	Reaction	CG Products[1]	K_{298} [2] (ppm^{-1} min^{-1})
Anthropogenic			
Toluenes	TOLA + OH	0.044 CG1+ 0.085 CG2	8.75E+03
Xylenes	XYLA + OH	0.027 CG1+ 0.118 CG2	3.71E+04
Biogenic			
Isoprene	ISP + O	none	5.32E+04
	ISP + OH	0.015 CG3 + 0.12 CG4	1.47E+05
	ISP + O_3	none	1.90E-02
	ISP + NO_3	none	9.96E+02
Terpenes	TRP + O	0.065 CG5 + 0.29 CG6	4.12E+04
	TRP + OH	0.065 CG5 + 0.29 CG6	7.76E+04
	TRP + O_3	0.065 CG5 + 0.29 CG6	1.33E-01
	TRP + NO_3	0.065 CG5 + 0.29 CG6	9.18E+03
Sesquiterpenes	SQT + OH	0.85 CG7	2.91E+05
	SQT + O_3	0.85 CG7	1.71E+01
	SQT + NO_3	0.85 CG7	2.81E+04

[1] : Yield values are in ppm/ppm

[2]: Rate constants are shown for 298 K and 1 atmosphere in ppm^{-1} min^{-1}.

References

Chang, J. S., R. A. Brost, I. S. A. Isaksen, S. Madronich, P. Middleton, W. R. Stockwell, and C. J. Walcek (1987), A three-dimensional eulerian acid deposition model : Physical concepts and formulation, *Journal of Geophysical Research*, *92*, 14,681-614,700.

Kalberer, M., D. Paulsen, M. Sax, M. Steinbacher, J. Dommen, A. S. H. Prévôt, R. Fisseha, E. Weingartner, V. Frankevic, R. Zenobi, and U. Baltensperger (2004), Identification of polymers as major components of atmospheric organic aerosols, *Science*, *303*, 1659-1662.

Madronich, S. (2002), The Tropospheric Visible Ultra-violet (TUV) model web page. , *National Center for Atmospheric Research, Boulder, CO.* , http://www.acd.ucar.edu/TUV/.

Morris, R. E., B. Koo, A. Guenther, G. Yarwood, D. McNally, T. W. Tesche, G. Tonnesen, J. Boylan, and P. Brewer (2006), Model sensitivity evaluation for organic carbon using two multi-pollutant air quality models that simulate regional haze in the southeastern United States, *Atmospheric Environment*, *40*(26), 4960-4972.

Nenes, A., S. N. Pandis, and C. Pilinis (1998), ISORROPIA: A new thermodynamic equilibrium model for multiphase multicomponent inorganic aerosols, *Aquatic Geochemistry*, *4*, 123-152.

Strader, R., F. Lurmann, S.N. Pandis (1999), Evaluation of secondary organic aerosol formation in winter, *Atmospheric Environment*, *33*, 4849-4863.

Zhang, L., J. R. Brook, and R. Vet (2003), A revised parameterization for gaseous dry deposition in air-quality models, *Atmos. Chem. Phys.*, *3*(6), 2067-2082.

Appendix 2: Annual emissions of France, Germany, Austria, Italy and Switzerland (data sources CEIP, GAINS)

Table A2.1 : Annual Emissions (National Totals) of France (kt yr^{-1})

France	(kt yr^{-1})								
species	SNAP	1990 CEIP Retro	2005 CEIP Reference	2005 GAINS Baseline	2020 GAINS Baseline	2020 GAINS Low-star	2020 GAINS Mid	2020 GAINS MTFR	2006 TNO-MACC
SO2	1	497.22	182.32	162.39	27.67	27.67	27.67	22.36	162.80
	2	130.16	60.36	63.02	38.58	38.58	38.58	25.97	57.89
	3	406.95	111.15	134.02	84.99	84.99	80.14	44.11	117.10
	4	81.68	53.81	77.80	42.34	42.34	41.68	36.69	11.64
	5	38.69	16.45	0.00	0.00	0.00	0.00	0.00	58.61
	6	0.00	0.00	0.00	0.00	0.00	0.00	0.00	0.00
	7	139.50	4.12	4.08	0.74	0.74	0.74	0.74	4.13
	8	30.17	26.80	23.89	4.00	4.00	4.00	1.90	19.55
	9	8.34	7.09	0.24	0.22	0.00	0.00	0.00	1.35
	10	0.00	0.00	0.00	0.00	0.00	0.00	0.00	0.00
	total	1332.70	462.09	465.43	198.54	198.31	192.81	131.77	433.10
NOx	1	144.36	149.34	134.01	37.08	34.14	33.15	26.01	123.80
	2	95.95	111.06	108.05	98.56	98.56	98.21	63.97	102.50
	3	184.87	132.98	152.32	110.36	83.42	67.19	59.36	148.20
	4	26.33	14.09	17.70	15.84	15.84	12.93	12.93	7.08
	5	0.00	0.00	0.00	0.00	0.00	0.00	0.00	5.04
	6	0.00	0.00	0.00	0.00	0.00	0.00	0.00	0.00
	7	1092.54	752.68	665.24	182.66	182.66	182.66	182.66	529.60
	8	201.25	258.30	224.76	123.31	123.31	123.31	123.31	166.90
	9	8.10	5.89	0.53	0.50	0.00	0.00	0.00	4.59
	10	75.39	0.00	0.00	0.00	0.00	0.00	0.00	64.60
	total	1828.79	1424.34	1302.61	568.32	537.93	517.44	468.24	1153.00
CO	1	30.14	25.87	0.00	0.00	0.00	0.00	0.00	24.41
	2	1902.21	1533.23	0.00	0.00	0.00	0.00	0.00	1608.00
	3	855.07	714.77	0.00	0.00	0.00	0.00	0.00	761.10
	4	1142.64	1089.95	0.00	0.00	0.00	0.00	0.00	753.30
	5	0.00	0.00	0.00	0.00	0.00	0.00	0.00	20.15
	6	0.00	0.01	0.00	0.00	0.00	0.00	0.00	0.00
	7	6260.15	1410.88	0.00	0.00	0.00	0.00	0.00	1389.00
	8	293.44	363.92	0.00	0.00	0.00	0.00	0.00	332.70
	9	227.78	272.63	0.00	0.00	0.00	0.00	0.00	256.60
	10	0.00	0.00	0.00	0.00	0.00	0.00	0.00	30.50
	total	10711.43	5411.26	0.00	0.00	0.00	0.00	0.00	5177.00
NMVOC	1	7.17	4.99	6.38	7.57	7.57	7.57	7.57	3.63
	2	207.37	267.58	326.68	144.57	144.57	144.57	26.83	273.50
	3	15.54	9.55	5.90	5.66	5.66	5.66	5.66	16.99
	4	111.62	105.62	92.32	90.61	84.48	81.53	63.66	88.33
	5	149.33	34.02	56.91	37.19	37.19	37.19	33.50	72.27
	6	651.04	440.05	427.51	322.74	315.20	306.41	232.11	432.70
	7	1051.39	251.79	235.97	38.28	38.28	38.28	38.28	219.10
	8	72.54	95.85	98.69	52.84	52.84	52.84	52.84	80.09
	9	16.55	16.06	16.49	13.00	12.01	12.01	12.01	15.68
	10	131.36	0.00	0.00	0.00	0.00	0.00	0.00	150.00
	total	2413.93	1225.51	1266.85	712.45	697.79	686.05	472.46	1352.00
NH3	1	0.00	0.04	0.64	0.71	0.71	0.72	0.91	0.05
	2	0.00	0.00	3.77	3.37	3.37	3.37	3.02	0.00
	3	0.90	0.66	0.33	0.58	0.57	0.86	0.95	0.72
	4	5.04	5.04	6.10	5.91	5.91	5.91	2.86	2.37
	5	0.00	0.00	0.00	0.00	0.00	0.00	0.00	0.00
	6	0.57	0.25	0.00	0.00	0.00	0.00	0.00	0.00
	7	0.80	10.54	13.99	7.60	7.60	7.60	7.60	12.63
	8	0.00	0.00	0.08	0.26	0.26	0.26	0.26	0.00
	9	7.69	13.18	16.69	16.83	16.83	16.83	16.83	9.64
	10	772.13	720.82	609.92	590.61	453.10	431.40	334.99	704.80
	total	787.13	750.53	651.53	625.86	488.35	466.95	367.42	730.20

Table A2.1 : Annual Emissions (National Totals) of France (kt yr^{-1}), cont'd

France	(kt yr^{-1})								
species	SNAP	1990 CEIP Retro	2005 CEIP Reference	2005 GAINS Baseline	2020 GAINS Baseline	2020 GAINS Low-star	2020 GAINS Mid	2020 GAINS MTFR	2006 TNO-MACC
PM2.5	1	0.00	5.87	3.61	0.44	0.44	0.44	0.24	4.77
	2	0.00	120.29	144.20	85.25	85.25	85.25	16.41	124.10
	3	0.00	13.60	12.39	10.28	10.28	10.28	6.51	11.43
	4	0.00	27.87	77.60	75.72	67.12	62.43	51.97	74.52
	5	0.00	40.10	0.19	0.05	0.05	0.05	0.05	1.21
	6	0.00	1.36	0.00	0.00	0.00	0.00	0.00	1.00
	7	0.00	37.99	39.01	8.09	8.09	8.09	8.09	38.88
	8	0.00	31.95	21.06	10.12	10.12	10.12	10.12	20.82
	9	0.00	13.53	10.30	10.87	8.30	8.30	7.81	12.45
	10	0.00	26.89	8.44	8.71	8.71	8.71	8.04	26.36
	total	0.00	319.44	316.78	209.53	198.36	193.67	109.25	315.60
PM10	1	0.00	9.97	6.05	0.63	0.63	0.63	0.27	8.47
	2	0.00	122.75	149.64	88.51	88.51	88.51	17.24	126.60
	3	0.00	16.56	18.56	15.74	15.74	15.74	7.53	15.48
	4	0.00	57.37	118.73	117.75	107.04	99.79	78.35	128.10
	5	0.00	57.04	1.71	0.49	0.49	0.49	0.49	1.73
	6	0.00	2.52	0.00	0.00	0.00	0.00	0.00	2.07
	7	0.00	52.75	48.13	18.28	18.28	18.28	18.28	53.78
	8	0.00	42.44	22.27	10.71	10.71	10.71	10.71	29.72
	9	0.00	15.82	10.66	11.24	8.30	8.30	7.81	14.95
	10	0.00	115.58	39.66	41.06	41.06	41.06	32.04	112.50
	total	0.00	492.81	415.42	304.40	290.75	283.50	172.72	493.50
PMcoarse	1	0.00	4.10	2.44	0.19	0.19	0.19	0.03	3.70
(PM10-PM2.5)	2	0.00	2.46	5.44	3.26	3.26	3.26	0.83	2.50
	3	0.00	2.97	6.17	5.46	5.46	5.46	1.02	4.05
	4	0.00	29.50	41.13	42.03	39.92	37.36	26.38	53.58
	5	0.00	16.93	1.52	0.44	0.44	0.44	0.44	0.53
	6	0.00	1.16	0.00	0.00	0.00	0.00	0.00	1.07
	7	0.00	14.76	9.12	10.19	10.19	10.19	10.19	14.90
	8	0.00	10.49	1.21	0.59	0.59	0.59	0.59	8.90
	9	0.00	2.29	0.36	0.37	0.00	0.00	0.00	2.50
	10	0.00	88.70	31.22	32.35	32.35	32.35	24.00	86.14
	total	0.00	173.36	98.64	94.87	92.39	89.83	63.47	177.90

Table A2.2 : Annual Emissions (National Totals) of Germany (kt yr^{-1})

Germany	(kt yr^{-1})								
species	SNAP	1990 CEIP Retro	2005 CEIP Reference	2005 GAINS Baseline	2020 GAINS Baseline	2020 GAINS Low-star	2020 GAINS Mid	2020 GAINS MTFR	2006 TNO-MACC
SO2	1	3098.85	297.54	253.13	166.64	166.64	164.79	155.08	282.90
	2	907.68	69.65	69.18	36.74	36.74	34.05	24.89	83.55
	3	907.65	50.95	103.78	48.58	48.58	48.58	43.37	63.14
	4	231.27	97.29	76.43	74.06	74.06	74.06	74.06	118.10
	5	26.88	9.45	0.00	0.00	0.00	0.00	0.00	15.13
	6	0.00	0.00	0.00	0.00	0.00	0.00	0.00	0.00
	7	90.20	0.81	4.89	0.95	0.95	0.95	0.95	0.80
	8	26.45	1.70	1.76	1.45	1.45	1.45	1.45	4.09
	9	0.00	11.29	0.46	0.39	0.22	0.22	0.18	0.02
	10	0.00	0.00	0.00	0.00	0.00	0.00	0.00	0.00
	total	5288.97	538.68	509.63	328.81	328.65	324.11	299.97	567.70
NOx	1	603.42	297.92	289.91	234.03	231.58	203.11	162.39	288.00
	2	149.38	92.80	113.29	104.86	104.85	104.85	104.21	104.40
	3	347.32	86.14	115.79	89.11	75.50	73.64	62.11	69.98
	4	30.82	107.73	17.25	16.63	16.63	16.63	16.63	94.32
	5	0.00	0.00	0.00	0.00	0.00	0.00	0.00	0.00
	6	0.00	0.00	0.00	0.00	0.00	0.00	0.00	0.00
	7	1343.22	707.03	712.94	174.67	174.67	174.67	174.67	616.70
	8	277.48	133.47	140.56	79.27	79.27	79.27	79.27	169.00
	9	0.00	8.24	0.67	0.60	0.22	0.22	0.18	0.12
	10	125.86	149.98	0.00	0.00	0.00	0.00	0.00	84.73
	total	2877.51	1583.30	1390.42	699.18	682.72	652.40	599.46	1427.00
CO	1	218.46	144.02	0.00	0.00	0.00	0.00	0.00	134.60
	2	3628.47	763.37	0.00	0.00	0.00	0.00	0.00	1093.00
	3	793.92	185.43	0.00	0.00	0.00	0.00	0.00	680.60
	4	682.50	929.09	0.00	0.00	0.00	0.00	0.00	575.00
	5	27.16	0.00	0.00	0.00	0.00	0.00	0.00	8.30
	6	0.00	0.00	0.00	0.00	0.00	0.00	0.00	0.00
	7	6526.71	1549.74	0.00	0.00	0.00	0.00	0.00	1393.00
	8	242.98	151.35	0.00	0.00	0.00	0.00	0.00	159.20
	9	0.00	1.77	0.00	0.00	0.00	0.00	0.00	0.00
	10	0.00	0.00	0.00	0.00	0.00	0.00	0.00	0.00
	total	12120.21	3724.78	0.00	0.00	0.00	0.00	0.00	4043.00
NMVOC	1	8.28	11.25	14.23	13.78	13.78	13.78	13.78	8.55
	2	397.64	38.48	68.35	51.58	51.54	50.00	21.43	85.76
	3	11.13	5.06	5.71	4.67	4.67	4.67	4.67	3.19
	4	91.25	105.16	123.45	122.54	99.64	97.94	83.60	67.26
	5	277.23	78.45	26.31	18.71	18.71	18.71	17.46	34.36
	6	1160.00	742.62	762.77	656.68	576.72	516.07	367.58	723.80
	7	1408.99	154.67	234.56	60.04	60.04	60.04	60.04	135.70
	8	70.30	26.43	72.97	48.04	48.04	48.04	48.04	30.49
	9	0.00	0.31	17.00	17.00	16.32	16.32	16.32	0.00
	10	159.31	252.18	0.00	0.00	0.00	0.00	0.00	122.70
	total	3584.13	1414.61	1325.34	993.03	889.47	825.57	632.91	1212.00
NH3	1	3.64	2.93	2.61	3.42	3.41	3.73	4.85	2.98
	2	3.59	2.84	2.38	3.01	3.01	3.01	3.01	2.81
	3	2.24	1.00	0.71	0.56	0.53	0.53	0.81	1.35
	4	15.10	11.70	11.09	11.09	11.09	11.09	9.76	11.14
	5	0.60	0.00	0.00	0.00	0.00	0.00	0.00	0.00
	6	1.21	1.73	0.00	0.00	0.00	0.00	0.00	1.73
	7	4.01	9.89	22.87	13.23	13.23	13.23	13.23	9.62
	8	0.97	0.57	0.09	0.14	0.14	0.14	0.14	0.79
	9	0.00	0.00	10.87	10.87	10.87	10.87	10.87	0.00
	10	726.34	547.61	539.70	525.92	409.39	383.77	328.29	587.70
	total	757.70	578.26	590.31	568.24	451.67	426.37	370.96	618.10

Table A2.2 : Annual Emissions (National Totals) of Germany (kt yr^{-1}) cont'd

Germany	(kt yr^{-1})								
species	SNAP	1990 CEIP Retro	2005 CEIP Reference	2005 GAINS Baseline	2020 GAINS Baseline	2020 GAINS Low-star	2020 GAINS Mid	2020 GAINS MTFR	2006 TNO-MACC
PM2.5	1	0.00	10.49	8.51	6.97	6.97	6.97	6.64	9.84
	2	0.00	22.81	23.10	22.64	22.61	22.37	10.47	26.66
	3	0.00	3.39	2.72	1.72	1.72	1.66	1.42	1.74
	4	0.00	15.93	20.28	17.63	17.35	15.86	13.23	16.46
	5	0.00	0.00	1.53	1.01	1.01	1.01	1.01	0.15
	6	0.00	20.62	0.00	0.00	0.00	0.00	0.00	18.99
	7	0.00	31.27	30.56	8.56	8.56	8.56	8.56	30.20
	8	0.00	11.35	15.53	4.99	4.99	4.99	4.99	3.13
	9	0.00	0.01	12.75	12.52	10.59	10.59	9.97	0.01
	10	0.00	5.92	6.67	6.78	6.78	6.78	6.24	4.57
	total	0.00	121.78	121.65	82.83	80.59	78.81	62.53	111.70
PM10	1	0.00	11.90	9.70	7.86	7.86	7.86	7.30	11.12
	2	0.00	24.20	24.77	23.91	23.87	23.63	11.11	28.66
	3	0.00	3.91	3.41	2.05	2.05	1.99	1.61	1.99
	4	0.00	34.92	50.78	45.45	45.08	42.75	35.07	43.50
	5	0.00	0.00	12.47	8.22	8.22	8.22	8.22	0.46
	6	0.00	53.27	0.00	0.00	0.00	0.00	0.00	45.81
	7	0.00	40.07	43.43	22.55	22.55	22.55	22.55	39.35
	8	0.00	11.35	16.44	5.29	5.29	5.29	5.29	3.27
	9	0.00	0.01	13.02	12.80	10.59	10.59	9.97	0.01
	10	0.00	37.04	32.69	33.42	33.42	33.42	25.53	20.37
	total	0.00	216.67	206.71	161.55	158.94	156.30	126.65	194.50
PMcoarse	1	0.00	1.41	1.19	0.89	0.89	0.89	0.66	1.28
(PM10-PM2.5)	2	0.00	1.40	1.67	1.27	1.26	1.26	0.64	2.00
	3	0.00	0.52	0.69	0.33	0.33	0.33	0.19	0.25
	4	0.00	18.99	30.50	27.82	27.73	26.89	21.84	27.04
	5	0.00	0.00	10.94	7.21	7.21	7.21	7.21	0.31
	6	0.00	32.65	0.00	0.00	0.00	0.00	0.00	26.82
	7	0.00	8.80	12.87	13.99	13.99	13.99	13.99	9.15
	8	0.00	0.00	0.91	0.30	0.30	0.30	0.30	0.14
	9	0.00	0.00	0.27	0.28	0.00	0.00	0.00	0.00
	10	0.00	31.12	26.02	26.64	26.64	26.64	19.29	15.80
	total	0.00	94.89	85.06	78.72	78.35	77.49	64.12	82.80

Table A2.3 : Annual Emissions (National Totals) of Austria (kt yr^{-1})

Austria	(kt yr^{-1})								
species	SNAP	1990 CEIP Retro	2005 CEIP Reference	2005 GAINS Baseline	2020 GAINS Baseline	2020 GAINS Low-star	2020 GAINS Mid	2020 GAINS MTFR	2006 TNO-MACC
SO2	1	14.04	6.91	7.14	3.22	3.22	3.22	3.17	7.97
	2	32.39	7.86	8.70	5.10	5.10	5.10	5.10	7.87
	3	18.30	10.70	9.01	8.56	8.56	8.56	5.46	10.16
	4	2.22	1.22	1.55	1.60	1.60	1.60	1.60	1.22
	5	2.00	0.13	0.00	0.00	0.00	0.00	0.00	0.17
	6	0.00	0.00	0.00	0.00	0.00	0.00	0.00	0.00
	7	3.76	0.16	0.56	0.13	0.13	0.13	0.13	0.13
	8	1.44	0.25	0.14	0.13	0.13	0.13	0.13	0.54
	9	0.07	0.06	0.03	0.02	0.01	0.00	0.00	0.06
	10	0.00	0.00	0.00	0.00	0.00	0.00	0.00	0.00
	total	74.23	27.29	27.13	18.76	18.74	18.74	15.59	28.12
NOx	1	17.91	15.93	21.13	16.10	15.97	15.97	11.99	13.48
	2	17.57	16.52	17.07	15.98	15.98	14.71	11.61	15.98
	3	44.19	25.55	18.05	16.79	14.72	13.99	12.80	37.32
	4	4.80	1.75	1.57	1.28	1.01	1.01	1.01	1.34
	5	0.00	0.00	0.00	0.00	0.00	0.00	0.00	0.00
	6	0.00	0.00	0.00	0.00	0.00	0.00	0.00	0.00
	7	98.88	149.20	125.39	34.04	34.04	34.04	34.04	119.70
	8	22.06	22.11	23.38	10.97	10.97	10.97	10.97	23.04
	9	0.10	0.05	0.03	0.02	0.01	0.00	0.00	0.05
	10	6.08	5.65	0.00	0.00	0.00	0.00	0.00	5.21
	total	211.59	236.75	206.61	95.19	92.71	90.70	82.44	216.10
CO	1	6.10	3.63	0.00	0.00	0.00	0.00	0.00	4.62
	2	439.50	307.85	0.00	0.00	0.00	0.00	0.00	289.60
	3	236.60	151.29	0.00	0.00	0.00	0.00	0.00	175.90
	4	46.37	24.23	0.00	0.00	0.00	0.00	0.00	24.17
	5	0.00	0.00	0.00	0.00	0.00	0.00	0.00	0.00
	6	0.00	0.00	0.00	0.00	0.00	0.00	0.00	0.00
	7	420.53	279.41	0.00	0.00	0.00	0.00	0.00	138.20
	8	60.18	47.34	0.00	0.00	0.00	0.00	0.00	66.81
	9	11.37	6.39	0.00	0.00	0.00	0.00	0.00	6.02
	10	1.20	0.79	0.00	0.00	0.00	0.00	0.00	1.00
	total	1221.85	820.92	0.00	0.00	0.00	0.00	0.00	706.30
NMVOC	1	0.77	0.58	3.95	3.26	3.26	3.26	3.26	1.65
	2	52.03	33.18	30.20	13.50	13.41	13.41	2.95	31.68
	3	4.14	1.26	0.87	1.10	1.10	1.10	1.10	3.65
	4	17.69	5.65	25.00	23.69	20.84	20.59	18.77	4.55
	5	5.63	1.92	2.53	2.08	2.08	2.08	1.98	6.20
	6	116.95	89.31	70.78	53.47	52.22	49.52	31.23	85.40
	7	69.01	21.79	29.56	8.65	8.65	8.65	8.65	17.62
	8	16.15	8.83	7.50	6.65	6.65	6.65	6.65	11.89
	9	0.16	0.09	0.14	0.14	0.13	0.13	0.13	0.08
	10	1.85	1.86	0.12	0.01	0.01	0.01	0.01	1.80
	total	284.37	164.47	170.66	112.57	108.37	105.43	74.74	164.50
NH3	1	0.19	0.33	0.39	0.38	0.38	0.38	0.49	0.34
	2	0.63	0.72	0.77	0.78	0.78	0.78	0.71	0.69
	3	0.22	0.43	0.04	0.18	0.18	0.20	0.22	0.31
	4	0.27	0.07	0.18	0.18	0.18	0.18	0.02	0.07
	5	0.00	0.00	0.00	0.00	0.00	0.00	0.00	0.00
	6	0.00	0.00	0.00	0.00	0.00	0.00	0.00	0.00
	7	0.97	2.98	2.77	1.67	1.67	1.67	1.67	0.96
	8	0.01	0.01	0.01	0.02	0.02	0.02	0.02	0.05
	9	0.38	1.29	2.32	2.33	2.33	2.33	2.33	1.02
	10	65.98	56.86	54.63	55.87	45.78	44.90	32.06	60.65
	total	68.65	62.70	61.11	61.41	51.33	50.47	37.52	64.10

Table A2.3 : Annual Emissions (National Totals) of Austria (kt yr^{-1}) cont'd

Austria	(kt yr^{-1})								
species	SNAP	1990 CEIP Retro	2005 CEIP Reference	2005 GAINS Baseline	2020 GAINS Baseline	2020 GAINS Low-star	2020 GAINS Mid	2020 GAINS MTFR	2006 TNO-MACC
PM2.5	1	0.00	0.85	0.52	0.31	0.31	0.31	0.07	0.92
	2	0.00	7.55	8.15	4.99	4.89	4.89	1.63	6.19
	3	0.00	1.61	0.70	0.82	0.82	0.82	0.68	2.82
	4	0.00	1.24	2.39	2.23	2.10	2.10	1.68	4.28
	5	0.00	0.67	0.04	0.02	0.02	0.02	0.01	0.09
	6	0.00	0.44	0.00	0.00	0.00	0.00	0.00	0.00
	7	0.00	6.00	5.41	1.53	1.53	1.53	1.53	6.54
	8	0.00	2.98	2.13	0.79	0.79	0.79	0.79	2.88
	9	0.00	0.03	1.55	1.61	1.11	1.11	1.05	0.03
	10	0.00	1.32	1.24	1.16	1.16	1.16	1.08	2.12
	total	0.00	22.70	22.14	13.45	12.73	12.73	8.52	25.87
PM10	1	0.00	1.00	0.92	0.76	0.76	0.76	0.08	1.09
	2	0.00	8.38	8.69	5.26	5.16	5.16	1.77	6.96
	3	0.00	2.28	0.88	1.02	1.02	1.02	0.81	3.10
	4	0.00	3.54	6.94	6.83	6.66	6.66	4.98	14.28
	5	0.00	5.48	0.37	0.16	0.16	0.16	0.13	0.28
	6	0.00	0.44	0.00	0.00	0.00	0.00	0.00	0.00
	7	0.00	8.33	7.03	3.29	3.29	3.29	3.29	7.99
	8	0.00	3.50	2.25	0.83	0.83	0.83	0.83	3.31
	9	0.00	0.09	1.63	1.68	1.11	1.11	1.05	0.09
	10	0.00	5.56	5.63	5.56	5.56	5.56	4.40	9.34
	total	0.00	38.61	34.34	25.39	24.55	24.55	17.34	46.44
PMcoarse	1	0.00	0.15	0.40	0.45	0.45	0.45	0.01	0.18
(PM10-PM2.5)	2	0.00	0.83	0.54	0.27	0.27	0.27	0.14	0.77
	3	0.00	0.67	0.18	0.20	0.20	0.20	0.13	0.28
	4	0.00	2.30	4.55	4.60	4.56	4.56	3.30	10.00
	5	0.00	4.81	0.33	0.14	0.14	0.14	0.12	0.19
	6	0.00	0.00	0.00	0.00	0.00	0.00	0.00	0.00
	7	0.00	2.32	1.62	1.76	1.76	1.76	1.76	1.45
	8	0.00	0.52	0.12	0.04	0.04	0.04	0.04	0.43
	9	0.00	0.06	0.08	0.07	0.00	0.00	0.00	0.06
	10	0.00	4.24	4.39	4.40	4.40	4.40	3.32	7.22
	total	0.00	15.90	12.20	11.94	11.82	11.82	8.82	20.57

Table A2.4 : Annual Emissions (National Totals) of Italy (kt yr^{-1})

Italy	(kt yr^{-1})								
species	SNAP	1990 CEIP Retro	2005 CEIP Reference	2005 GAINS Baseline	2020 GAINS Baseline	2020 GAINS Low-star	2020 GAINS Mid	2020 GAINS MTFR	2006 TNO-MACC
SO2	1	1000.78	187.01	119.43	49.52	49.52	49.52	33.48	254.40
	2	95.63	19.71	22.45	9.22	9.22	9.22	5.32	16.90
	3	302.82	72.77	120.56	63.83	63.83	63.83	43.41	74.82
	4	155.87	59.28	57.36	53.23	53.23	53.23	20.84	26.15
	5	0.00	0.00	0.00	0.00	0.00	0.00	0.00	31.04
	6	0.00	0.00	0.00	0.00	0.00	0.00	0.00	0.00
	7	131.98	2.41	2.71	0.71	0.71	0.71	0.71	12.31
	8	94.70	50.51	54.38	57.21	57.21	57.21	13.23	55.43
	9	12.80	10.55	0.46	0.46	0.17	0.14	0.14	0.27
	10	0.00	0.00	0.15	0.15	0.00	0.00	0.00	0.16
	total	1794.58	402.24	377.50	234.32	233.89	233.85	117.13	471.50
NOx	1	457.37	117.16	106.31	84.49	81.30	79.67	46.12	141.00
	2	62.08	74.90	83.85	67.14	67.14	61.36	46.55	82.50
	3	289.26	148.24	161.37	125.56	91.79	74.58	57.86	168.60
	4	29.78	15.90	9.66	8.42	8.42	8.42	4.21	6.64
	5	0.00	0.00	0.00	0.00	0.00	0.00	0.00	5.25
	6	0.00	0.00	0.00	0.00	0.00	0.00	0.00	0.00
	7	893.40	610.80	596.35	229.91	229.91	229.91	229.91	528.60
	8	203.99	231.43	260.32	181.46	181.46	181.46	181.46	184.60
	9	8.67	15.99	0.83	0.83	0.17	0.14	0.14	15.72
	10	0.47	0.47	0.34	0.34	0.00	0.00	0.00	0.90
	total	1945.02	1214.90	1219.02	698.14	660.18	635.52	566.23	1134.00
CO	1	30.75	53.67	0.00	0.00	0.00	0.00	0.00	51.68
	2	256.23	358.27	0.00	0.00	0.00	0.00	0.00	483.30
	3	317.72	326.15	0.00	0.00	0.00	0.00	0.00	293.10
	4	215.89	144.16	0.00	0.00	0.00	0.00	0.00	122.30
	5	0.00	0.00	0.00	0.00	0.00	0.00	0.00	2.91
	6	0.00	0.00	0.00	0.00	0.00	0.00	0.00	0.00
	7	5495.02	1827.43	0.00	0.00	0.00	0.00	0.00	2243.00
	8	602.94	345.81	0.00	0.00	0.00	0.00	0.00	431.90
	9	308.72	295.74	0.00	0.00	0.00	0.00	0.00	321.00
	10	12.93	12.80	0.00	0.00	0.00	0.00	0.00	27.27
	total	7240.20	3364.03	0.00	0.00	0.00	0.00	0.00	3976.00
NMVOC	1	7.60	5.58	9.86	7.86	7.86	7.86	7.86	5.60
	2	22.73	79.78	71.32	55.70	55.70	55.70	14.20	53.73
	3	11.97	8.00	4.02	4.30	4.30	4.30	4.30	9.92
	4	99.31	76.06	57.53	55.24	50.06	47.78	37.40	48.31
	5	90.79	53.84	59.19	56.06	56.06	56.06	55.18	71.18
	6	617.21	494.72	472.38	377.87	364.47	352.30	258.19	489.70
	7	962.64	397.49	833.51	219.62	219.62	219.62	219.62	375.90
	8	192.20	130.44	247.27	133.14	133.14	133.14	133.14	143.60
	9	16.83	25.93	11.12	11.12	11.12	10.45	10.45	26.63
	10	1.30	1.22	1.17	1.17	0.42	0.42	0.42	3.40
	total	2022.58	1273.05	1767.38	922.08	902.74	887.63	740.77	1228.00
NH3	1	0.15	0.20	1.35	1.14	1.09	1.12	2.08	0.25
	2	0.00	0.35	0.96	0.87	0.87	0.87	0.78	0.00
	3	0.08	3.42	0.26	0.32	0.28	0.58	0.86	0.06
	4	0.76	0.53	0.22	0.08	0.08	0.08	0.08	0.17
	5	0.00	0.00	0.00	0.00	0.00	0.00	0.00	0.00
	6	0.00	0.00	0.00	0.00	0.00	0.00	0.00	0.00
	7	0.68	14.85	14.05	8.73	8.73	8.73	8.73	15.21
	8	0.03	0.04	0.13	0.16	0.16	0.16	0.16	0.03
	9	5.49	9.78	30.31	27.50	27.50	27.50	27.50	8.61
	10	397.35	386.63	357.61	346.71	275.79	265.04	215.16	397.50
	total	404.54	415.80	404.89	385.51	314.51	304.09	255.36	421.80

Table A2.4 : Annual Emissions (National Totals) of Italy (kt yr^{-1}) cont'd

Italy	(kt yr^{-1})								
species	SNAP	1990 CEIP Retro	2005 CEIP Reference	2005 GAINS Baseline	2020 GAINS Baseline	2020 GAINS Low-star	2020 GAINS Mid	2020 GAINS MTFR	2006 TNO-MACC
PM2.5	1	0.00	5.58	4.50	1.74	1.74	1.74	0.67	5.26
	2	0.00	38.60	34.16	27.34	27.34	27.34	8.84	14.64
	3	0.00	19.36	15.01	13.96	13.96	13.96	12.30	18.18
	4	0.00	8.38	12.39	12.13	12.13	10.61	8.01	13.95
	5	0.00	0.76	0.07	0.10	0.10	0.10	0.10	1.30
	6	0.00	0.02	0.00	0.00	0.00	0.00	0.00	0.01
	7	0.00	37.09	44.18	13.30	13.30	13.30	13.30	34.76
	8	0.00	23.70	23.16	12.77	12.77	12.77	12.77	12.34
	9	0.00	11.19	10.98	11.35	7.99	7.98	7.51	9.70
	10	0.00	5.70	6.18	6.34	5.24	5.24	4.81	3.64
	total	0.00	150.38	150.62	99.03	94.57	93.04	68.32	113.80
PM10	1	0.00	5.87	6.71	3.55	3.55	3.55	0.74	7.52
	2	0.00	39.03	35.39	28.24	28.24	28.24	9.13	20.90
	3	0.00	20.38	18.14	16.99	16.99	16.99	14.09	26.00
	4	0.00	19.86	28.16	29.02	29.02	26.64	20.52	19.54
	5	0.00	0.76	0.62	0.87	0.87	0.87	0.87	1.86
	6	0.00	0.02	0.00	0.00	0.00	0.00	0.00	0.02
	7	0.00	41.51	52.99	23.41	23.41	23.41	23.41	49.88
	8	0.00	23.74	24.62	13.55	13.55	13.55	13.55	17.62
	9	0.00	13.05	11.46	11.83	7.99	7.98	7.51	13.86
	10	0.00	17.59	25.10	25.90	24.65	24.65	18.76	5.11
	total	0.00	181.80	203.19	153.34	148.25	145.86	108.57	162.30
PMcoarse	1	0.00	0.29	2.21	1.81	1.81	1.81	0.07	2.26
(PM10-PM2.5)	2	0.00	0.43	1.23	0.90	0.90	0.90	0.29	6.26
	3	0.00	1.02	3.13	3.03	3.03	3.03	1.79	7.82
	4	0.00	11.48	15.77	16.89	16.89	16.03	12.51	5.59
	5	0.00	0.00	0.55	0.77	0.77	0.77	0.77	0.56
	6	0.00	0.00	0.00	0.00	0.00	0.00	0.00	0.01
	7	0.00	4.42	8.81	10.11	10.11	10.11	10.11	15.12
	8	0.00	0.03	1.46	0.78	0.78	0.78	0.78	5.28
	9	0.00	1.86	0.48	0.48	0.00	0.00	0.00	4.16
	10	0.00	11.89	18.92	19.56	19.41	19.41	13.95	1.48
	total	0.00	31.42	52.57	54.31	53.68	52.82	40.25	48.50

Table A2.5 : Annual Emissions (National Totals) of Switzerland (kt yr^{-1})

Switzerland	(kt yr^{-1})								
species	SNAP	1990 CEIP Retro	2005 CEIP Reference	2005 GAINS Baseline	2020 GAINS Baseline	2020 GAINS Low-star	2020 GAINS Mid	2020 GAINS MTFR	2006 TNO-MACC
SO2	1	4.03	1.99	1.88	1.95	1.95	1.95	1.87	1.93
	2	15.48	7.65	6.75	3.63	3.63	3.63	3.53	6.74
	3	11.60	4.93	6.02	6.22	6.22	6.22	3.69	3.57
	4	3.87	2.12	1.00	0.68	0.68	0.68	0.68	2.10
	5	0.00	0.31	0.00	0.00	0.00	0.00	0.00	0.34
	6	0.00	0.19	0.00	0.00	0.00	0.00	0.00	0.01
	7	3.79	0.08	0.09	0.08	0.08	0.08	0.08	0.08
	8	1.10	0.18	0.27	0.18	0.18	0.18	0.18	0.14
	9	2.44	0.08	0.02	0.03	0.00	0.00	0.00	1.34
	10	0.00	0.05	0.04	0.04	0.00	0.00	0.00	0.05
	total	42.30	17.59	16.09	12.82	12.75	12.75	10.03	16.30
NOx	1	6.53	3.03	4.28	4.52	4.44	4.24	3.03	2.92
	2	14.41	11.01	7.42	7.23	7.23	7.23	6.54	10.51
	3	15.82	8.34	8.37	8.67	7.28	6.95	6.57	7.88
	4	0.63	0.32	0.29	0.28	0.28	0.28	0.28	0.76
	5	0.23	0.27	0.00	0.00	0.00	0.00	0.00	0.28
	6	0.05	0.03	0.00	0.00	0.00	0.00	0.00	0.01
	7	93.62	50.38	48.41	19.41	19.41	19.41	19.41	40.72
	8	16.47	14.43	15.46	7.83	7.83	7.83	7.83	15.40
	9	1.29	0.35	0.05	0.06	0.00	0.00	0.00	0.49
	10	6.54	3.88	0.10	0.10	0.00	0.00	0.00	4.46
	total	155.59	92.03	84.38	48.10	46.47	45.94	43.66	83.43
CO	1	1.05	1.47	0.00	0.00	0.00	0.00	0.00	1.05
	2	42.45	64.41	0.00	0.00	0.00	0.00	0.00	52.89
	3	21.37	13.49	0.00	0.00	0.00	0.00	0.00	10.85
	4	16.25	10.21	0.00	0.00	0.00	0.00	0.00	10.58
	5	0.04	0.85	0.00	0.00	0.00	0.00	0.00	0.07
	6	0.83	0.26	0.00	0.00	0.00	0.00	0.00	0.02
	7	494.51	177.06	0.00	0.00	0.00	0.00	0.00	182.40
	8	54.24	49.41	0.00	0.00	0.00	0.00	0.00	51.29
	9	3.18	1.89	0.00	0.00	0.00	0.00	0.00	2.08
	10	7.28	8.01	0.00	0.00	0.00	0.00	0.00	7.28
	total	641.21	327.05	0.00	0.00	0.00	0.00	0.00	318.50
NMVOC	1	0.29	0.13	0.72	0.85	0.85	0.85	0.85	0.13
	2	2.27	7.23	12.30	5.02	4.89	4.89	1.59	2.14
	3	0.66	0.64	1.00	1.16	1.16	1.16	1.16	0.43
	4	14.89	10.89	13.80	14.09	9.46	9.46	5.65	10.05
	5	0.11	3.00	5.22	3.15	3.15	3.15	3.05	10.96
	6	140.84	43.54	50.40	40.06	34.54	34.54	23.89	49.98
	7	87.57	23.50	22.93	5.32	5.32	5.32	5.32	17.36
	8	9.23	6.65	9.78	7.48	7.48	7.48	7.48	6.49
	9	1.30	3.24	4.46	4.46	4.46	4.20	4.20	2.06
	10	4.63	4.70	0.59	0.59	0.06	0.06	0.06	4.64
	total	261.80	103.52	121.21	82.17	71.37	71.10	53.23	104.20
NH3	1	0.00	0.03	0.05	0.06	0.06	0.06	0.07	0.03
	2	0.12	0.22	0.24	0.25	0.25	0.25	0.25	0.22
	3	0.04	0.20	0.19	0.23	0.21	0.22	0.22	0.09
	4	0.30	0.21	1.32	1.27	1.27	1.27	1.20	0.11
	5	0.00	0.88	0.00	0.00	0.00	0.00	0.00	0.00
	6	0.05	0.11	0.00	0.00	0.00	0.00	0.00	0.04
	7	0.63	3.74	1.93	0.42	0.42	0.42	0.42	1.29
	8	0.01	0.01	0.01	0.01	0.01	0.01	0.01	0.01
	9	0.91	0.50	0.89	0.98	0.98	0.98	0.98	0.84
	10	65.73	58.08	57.16	61.27	53.25	51.81	45.36	52.66
	total	67.79	63.97	61.78	64.50	56.46	55.03	48.51	55.28

Table A2.5 : Annual Emissions (National Totals) of Switzerland (kt yr^{-1}) cont'd

Switzerland	(kt yr^{-1})								
species	SNAP	1990 CEIP Retro	2005 CEIP Reference	2005 GAINS Baseline	2020 GAINS Baseline	2020 GAINS Low-star	2020 GAINS Mid	2020 GAINS MTFR	2006 TNO-MACC
PM2.5	1	0.00	0.27	0.02	0.05	0.05	0.05	0.01	0.18
	2	0.00	3.03	2.95	1.91	1.59	1.59	0.73	1.27
	3	0.00	0.98	0.99	0.94	0.94	0.94	0.84	0.72
	4	0.00	0.81	1.07	1.18	1.18	1.18	0.66	0.83
	5	0.00	0.13	0.00	0.00	0.00	0.00	0.00	0.00
	6	0.00	0.24	0.00	0.00	0.00	0.00	0.00	0.26
	7	0.00	1.94	1.81	0.90	0.90	0.90	0.90	1.77
	8	0.00	2.01	1.79	0.63	0.63	0.63	0.63	2.63
	9	0.00	0.01	0.59	0.65	0.34	0.34	0.33	0.02
	10	0.00	1.34	0.80	0.82	0.38	0.38	0.34	1.24
	total	0.00	10.75	10.02	7.08	6.02	6.02	4.45	8.93
PM10	1	0.00	0.27	0.02	0.07	0.07	0.07	0.01	0.18
	2	0.00	3.03	3.11	2.03	1.70	1.70	0.79	1.29
	3	0.00	1.17	1.20	1.20	1.20	1.20	0.99	0.87
	4	0.00	1.95	3.06	3.33	3.33	3.33	1.75	1.94
	5	0.00	0.45	0.02	0.02	0.02	0.02	0.02	0.00
	6	0.00	0.35	0.00	0.00	0.00	0.00	0.00	0.41
	7	0.00	4.11	2.74	2.00	2.00	2.00	2.00	4.26
	8	0.00	6.75	1.89	0.67	0.67	0.67	0.67	6.72
	9	0.00	0.49	0.63	0.70	0.34	0.34	0.33	0.50
	10	0.00	3.34	2.26	2.35	1.86	1.86	1.30	3.17
	total	0.00	21.91	14.92	12.36	11.18	11.18	7.85	19.35
PMcoarse	1	0.00	0.00	0.00	0.02	0.02	0.02	0.00	0.00
(PM10-PM2.5)	2	0.00	0.00	0.16	0.12	0.11	0.11	0.06	0.02
	3	0.00	0.19	0.21	0.26	0.26	0.26	0.15	0.15
	4	0.00	1.14	1.99	2.15	2.15	2.15	1.09	1.11
	5	0.00	0.33	0.02	0.02	0.02	0.02	0.02	0.00
	6	0.00	0.11	0.00	0.00	0.00	0.00	0.00	0.15
	7	0.00	2.17	0.93	1.10	1.10	1.10	1.10	2.49
	8	0.00	4.74	0.10	0.04	0.04	0.04	0.04	4.09
	9	0.00	0.48	0.04	0.05	0.00	0.00	0.00	0.49
	10	0.00	2.00	1.46	1.53	1.48	1.48	0.96	1.93
	total	0.00	11.16	4.90	5.28	5.16	5.16	3.40	10.42

Table A2.6 : Annual Emissions of International Shipping (kt yr^{-1}). Atlantic (ATL), North Sea (NOS), Baltic Sea (BAS, Mediterranean Sea (MED), Black Sea (BLS). Scenario dependent [*Cofala et al.*, 2007]

Ships, scen. dep.	(kt yr-1)							
species	area	1990 CEIP Retro	2005 CEIP Reference	2005 GAINS Baseline	2020 GAINS Baseline	2020 GAINS Low-star	2020 GAINS Mid	2020 GAINS MTFR
SO2	ATL	383.73	558.30	558.30	804.10	800.90	165.10	152.00
NOX	ATL	564.64	795.60	795.60	1048.30	762.00	696.50	119.70
CO	ATL	54.84	79.59	0.00	0.00	0.00	0.00	0.00
PM2.5	ATL	0.00	64.90	64.90	91.30	91.30	73.50	73.50
PM10	ATL	0.00	68.50	0.00	0.00	0.00	0.00	0.00
PMcoarse	ATL	0.00	3.60	0.00	0.00	0.00	0.00	0.00
SO2	NOS	360.96	501.30	501.30	406.30	148.80	148.80	137.00
NOX	NOS	507.66	714.30	714.30	946.00	687.90	629.00	107.90
CO	NOS	51.77	75.44	0.00	0.00	0.00	0.00	0.00
PM2.5	NOS	0.00	58.30	58.30	67.90	66.30	66.30	66.30
PM10	NOS	0.00	61.60	0.00	0.00	0.00	0.00	0.00
PMcoarse	NOS	0.00	3.30	0.00	0.00	0.00	0.00	0.00
SO2	BAS	168.28	212.80	212.80	170.70	62.70	62.70	57.80
NOX	BAS	236.22	303.30	303.30	404.10	293.80	268.80	46.10
CO	BAS	24.21	35.20	0.00	0.00	0.00	0.00	0.00
PM2.5	BAS	0.00	24.80	24.80	28.60	27.90	27.90	27.90
PM10	BAS	0.00	26.20	0.00	0.00	0.00	0.00	0.00
PMcoarse	BAS	0.00	1.40	0.00	0.00	0.00	0.00	0.00
SO2	MED	857.94	1212.20	1212.20	1714.30	1664.10	363.00	334.30
NOX	MED	1234.49	1727.40	1727.40	2311.80	1681.90	1539.10	263.10
CO	MED	123.61	181.82	0.00	0.00	0.00	0.00	0.00
PM2.5	MED	0.00	141.00	141.00	198.40	198.00	161.60	161.60
PM10	MED	0.00	148.90	0.00	0.00	0.00	0.00	0.00
PMcoarse	MED	0.00	7.90	0.00	0.00	0.00	0.00	0.00
SO2	BLS	45.08	62.80	62.80	90.50	90.10	18.60	17.10
NOX	BLS	62.06	89.50	89.50	118.00	85.80	78.40	13.50
CO	BLS	6.44	9.35	0.00	0.00	0.00	0.00	0.00
PM2.5	BLS	0.00	7.30	7.30	10.30	10.30	8.30	8.30
PM10	BLS	0.00	7.70	0.00	0.00	0.00	0.00	0.00
PMcoarse	BLS	0.00	0.40	0.00	0.00	0.00	0.00	0.00

Table A2.7 : Annual Emissions of International Shipping (kt yr^{-1}). Atlantic (ATL), North Sea (NOS), Baltic Sea (BAS, Mediterranean Sea (MED), Black Sea (BLS). Scenario independent for 2020 [*Wagner et al.*, 2010]

Ships, scen. indep.	(kt yr-1)			
species	area	2000 CEIP / GAINS	2005 CEIP Reference	2020 GAINS
SO2	ATL	494.00	558.30	804.00
NOX	ATL	723.00	795.60	1015.00
NMVOC	ATL	24.00		52.00
PM2.5	ATL	56.00	64.90	91.00
SO2	NOS	443.00	501.30	28.00
NOX	NOS	649.00	714.30	915.00
NMVOC	NOS	23.00		49.00
PM2.5	NOS	50.00	58.30	13.00
SO2	BAS	188.00	212.80	12.00
NOX	BAS	276.00	303.30	387.00
NMVOC	BAS	10.00		22.00
PM2.5	BAS	21.00	24.80	6.00
SO2	MED	1070.00	1212.20	1714.00
NOX	MED	1564.00	1727.40	2231.00
NMVOC	MED	53.00		115.00
PM2.5	MED	121.00	141.00	198.00
SO2	BLS	56.00	62.80	90.00
NOX	BLS	81.00	89.50	114.00
NMVOC	BLS	3.00		6.00
PM2.5	BLS	6.00	7.30	10.00

References

Cofala, J., M. Amann, C. Heyes, F. Wagner, Z. Klimont, M. Posch, W. Schoepp, L. Tarasson, J. E. Jonson, C. Whall, and A. Stavrakaki (2007), Analysis of Policy Measures to Reduce Ship Emissions in the Context of the Revision of the National Emissions Ceilings Directive. Final Report*Rep.*, IIASA Contract No. 06-107.

Wagner, F., M. Amann, B. Imrich, J. Cofala, C. Heyes, Z. Klimont, P. Rafaj, and W. Schoepp (2010), Baseline Emission Projections and Further Cost-effective Reductions of Air Pollution Impacts in Europe - A 2010 Perspective*Rep.*, IIASA Contract No. 070307/2009/531887/SER/C4.

Appendix 3: Model results for the European domain

A3.1 Ozone

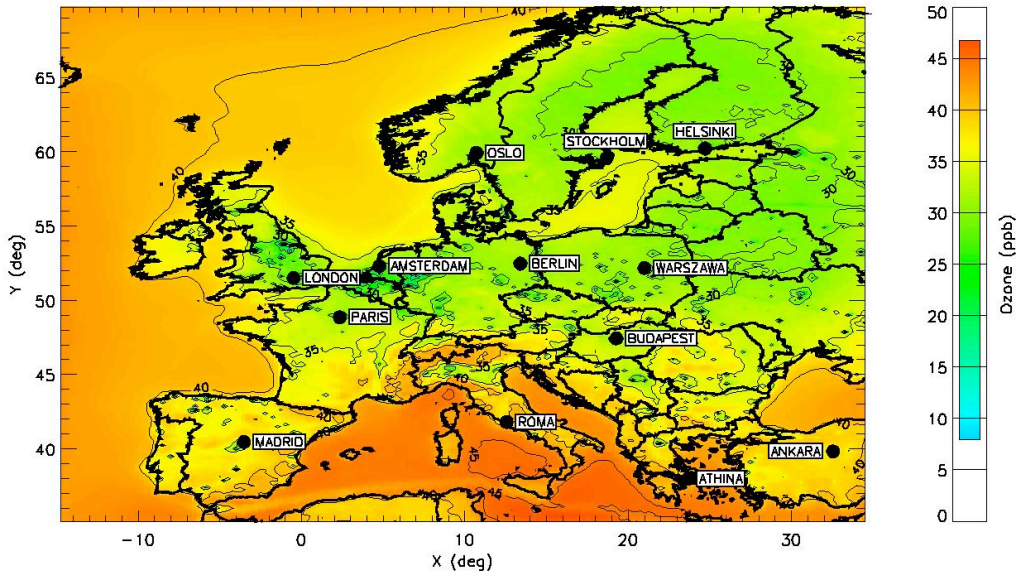

Figure A3.1.1: Annual average concentration of ozone (ppb) for RC 2005

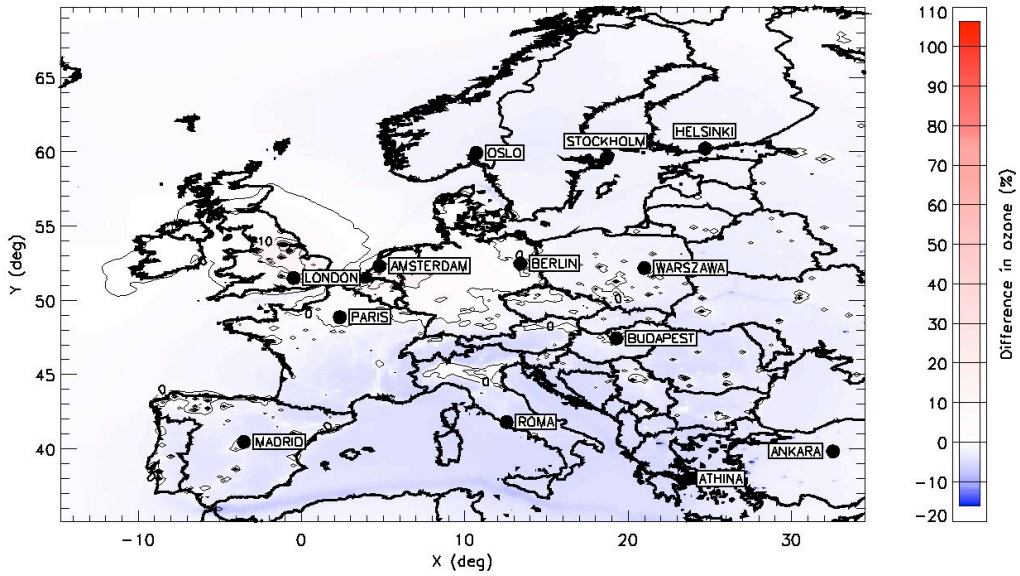

Figure A3.1.2: Difference in annual average of ozone (%), BL 2020- RC 2005.

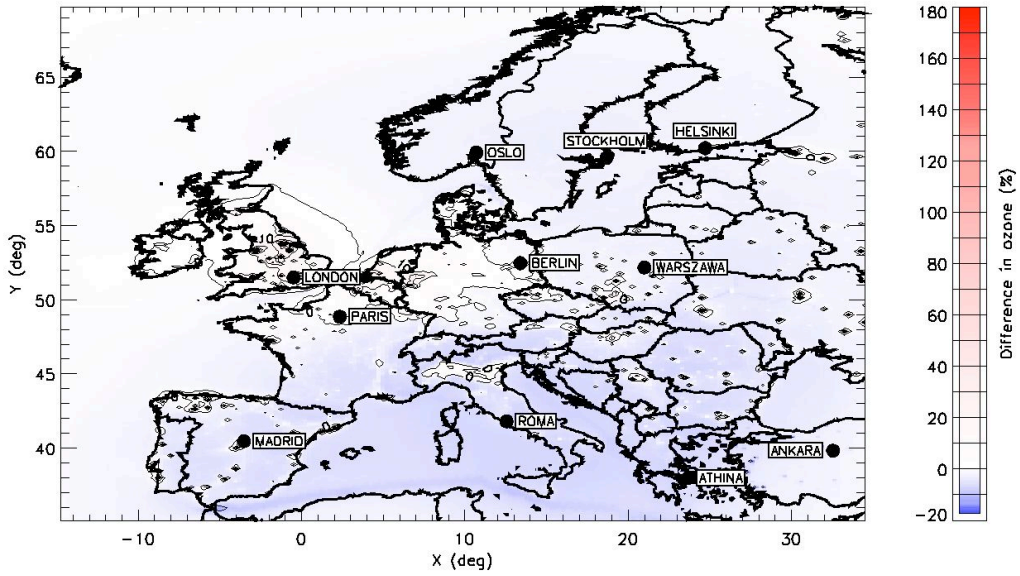

Figure A3.1.3: Difference in annual average of ozone (%), MTFR 2020- RC 2005.

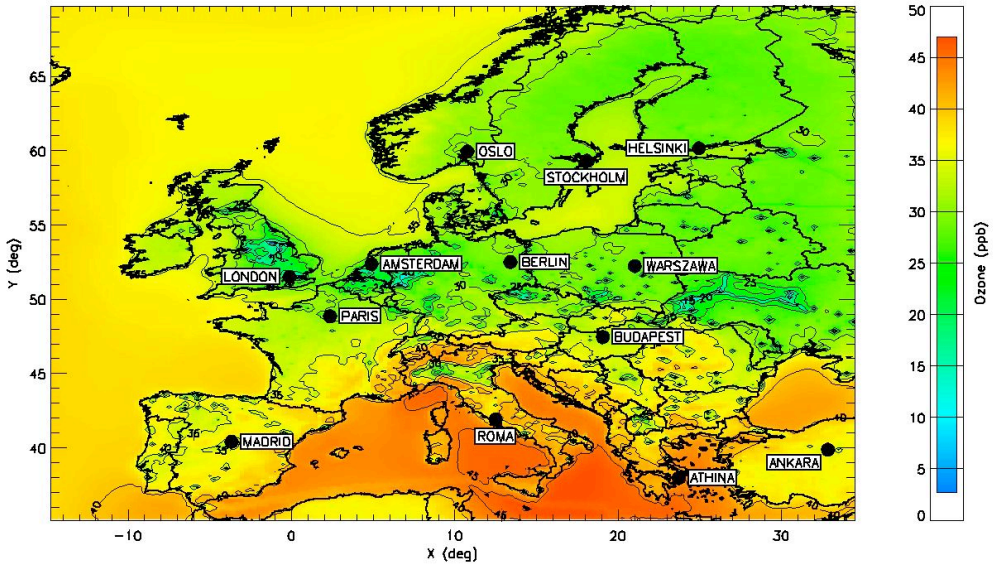

Figure A3.1.4: Annual average concentration of ozone (ppb) for Retro 1,1990

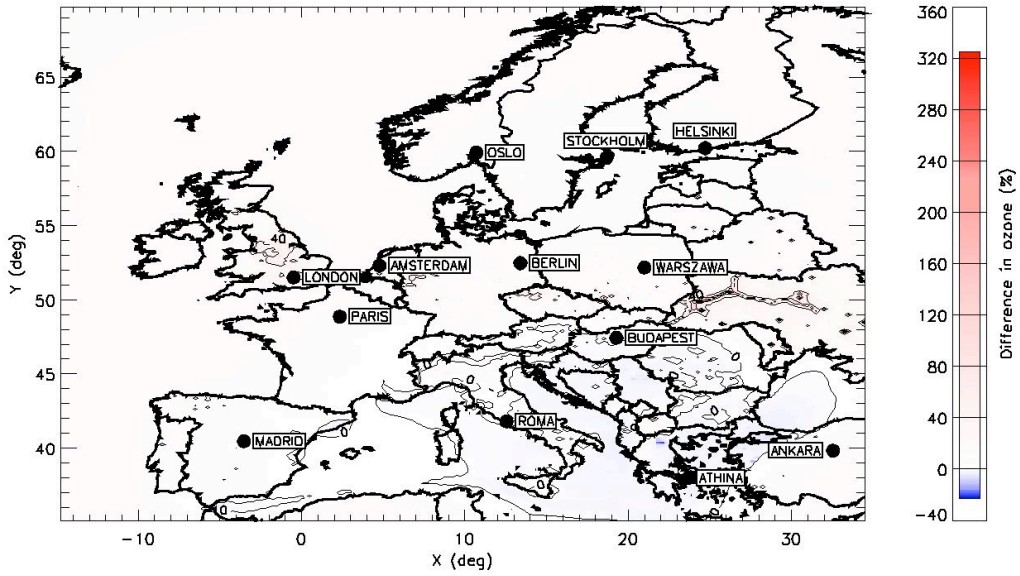

Figure A3.1.5: Difference in annual average of ozone (%), RC 2005 – Retro 1, 1990.

A3.2 AOT40

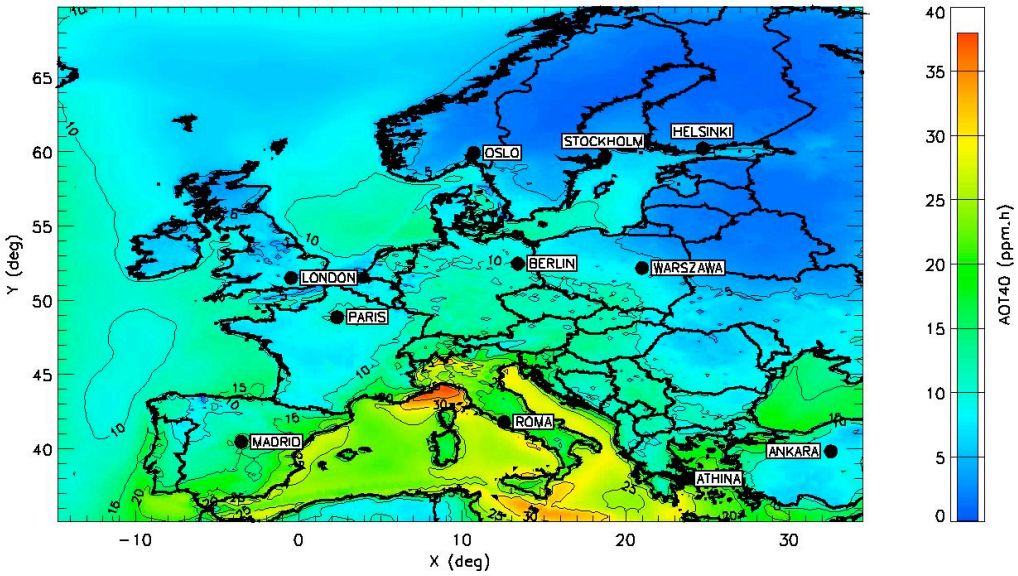

Figure A3.2.1: AOT40 (ppm.h) for RC 2005

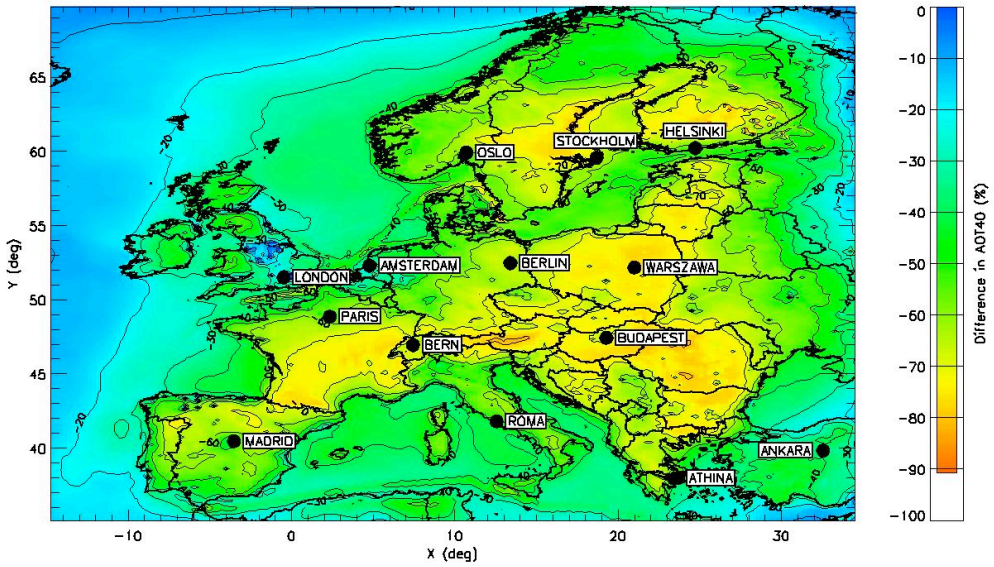

Figure A3.2.2: Difference in AOT40 (%), BL 2020- RC 2005.

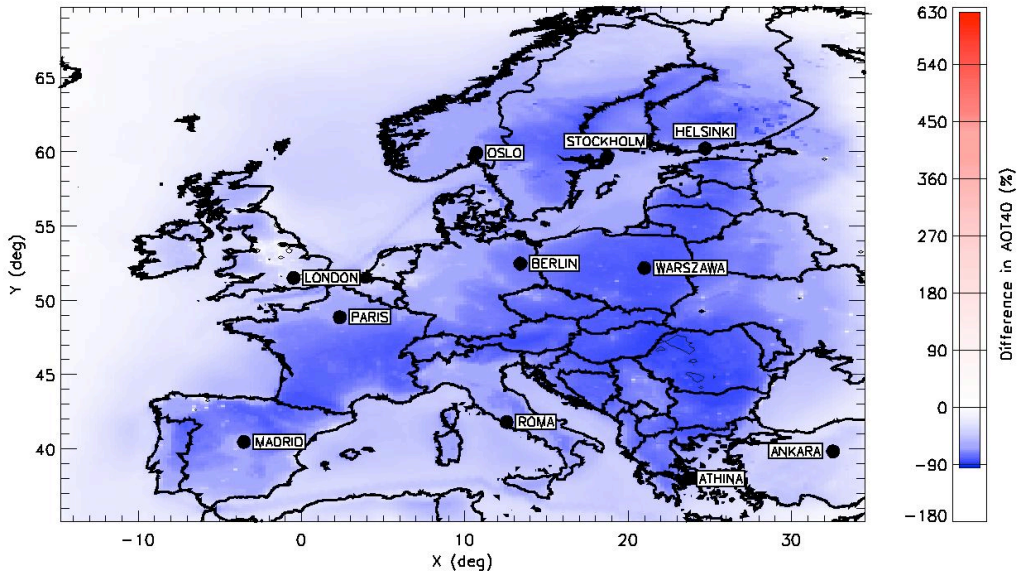

Figure A3.2.3: Difference in AOT40 (%), MTFR 2020- RC 2005.

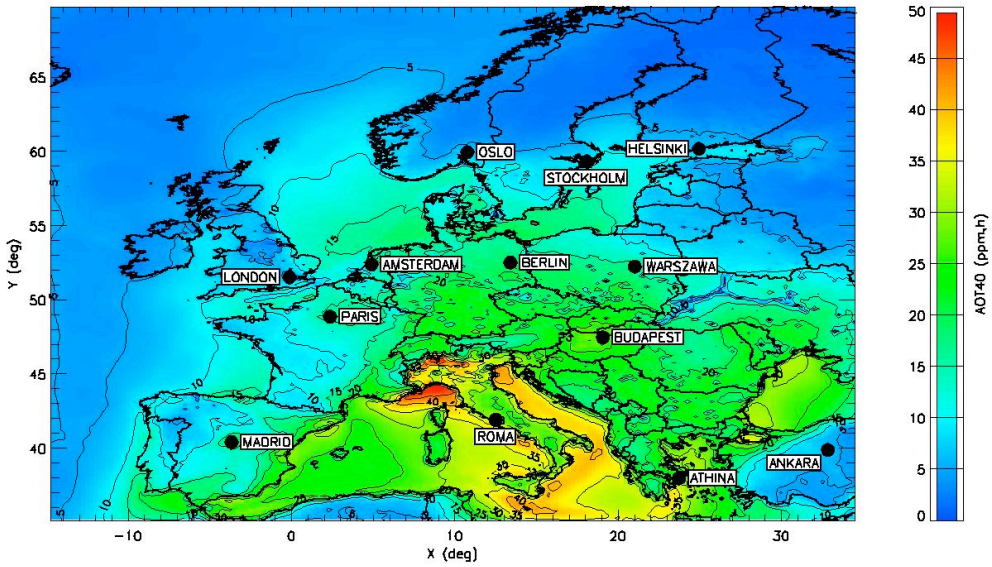

Figure A3.2.4: AOT40 (ppm.h) for Retro 1, 1990

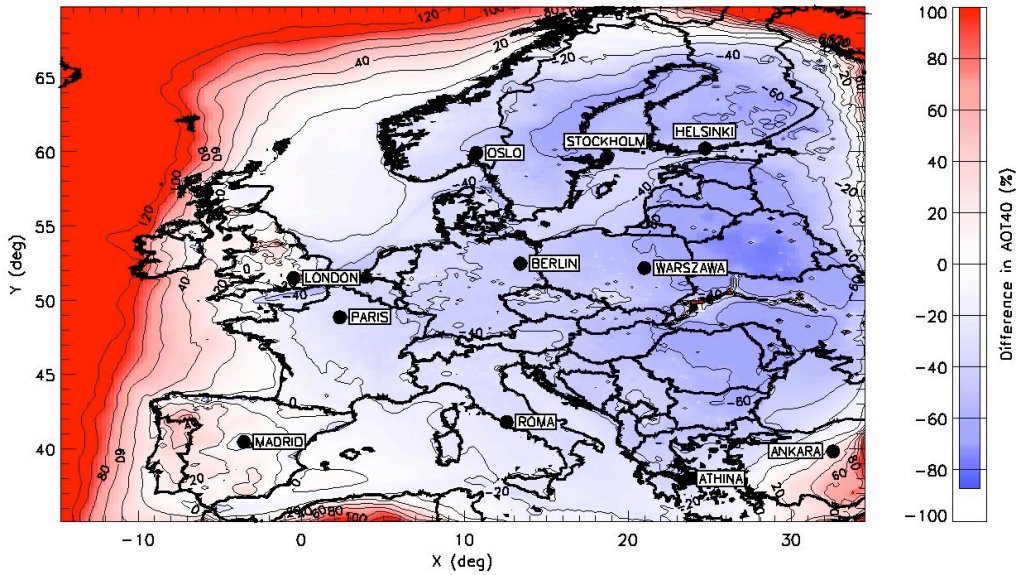

Figure A3.2.5: Difference in AOT40 (%), RC 2005 – Retro 1, 1990.

A3.3 SOMO35

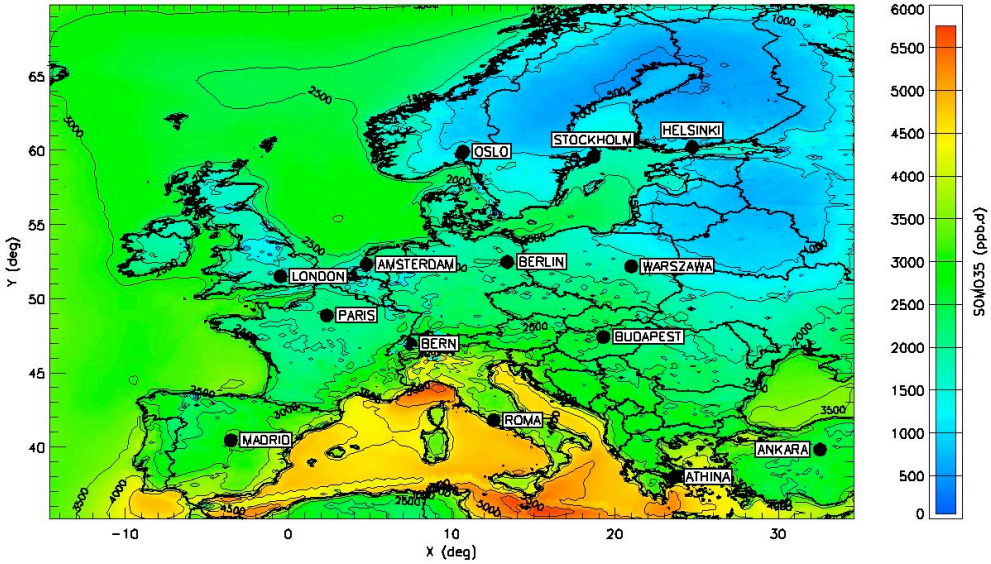

Figure A3.3.1: SOMO35 (ppb.d) for RC 2005

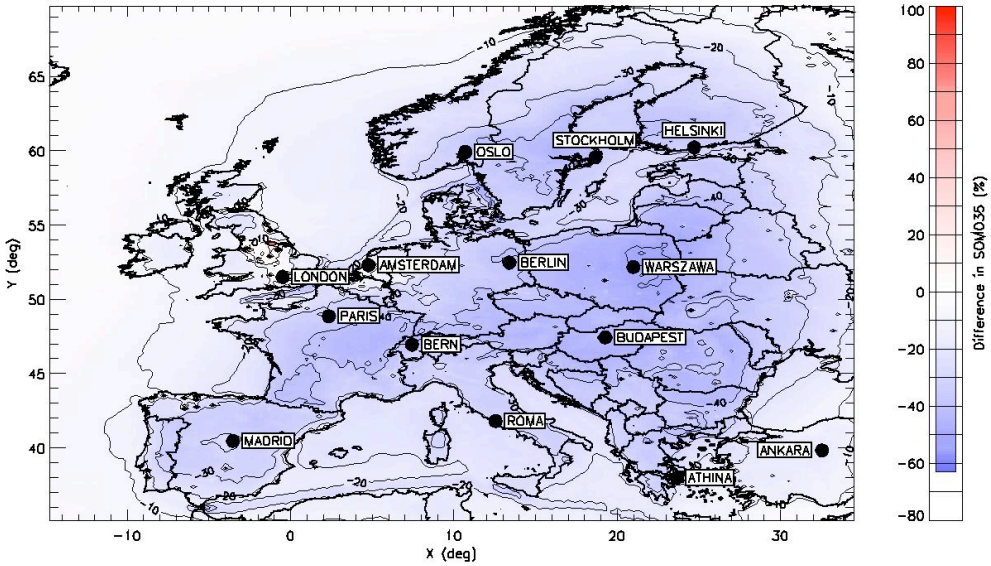

Figure A3.3.2: Difference in SOMO35 (%), BL 2020- RC 2005.

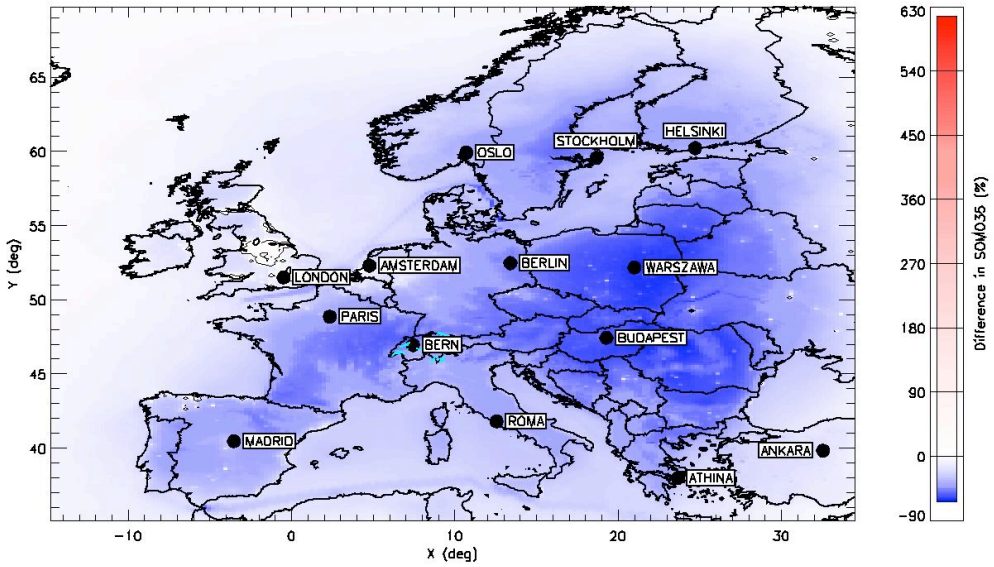

Figure A3.3.3: Difference in SOMO35 (%), MTFR 2020- RC 2005.

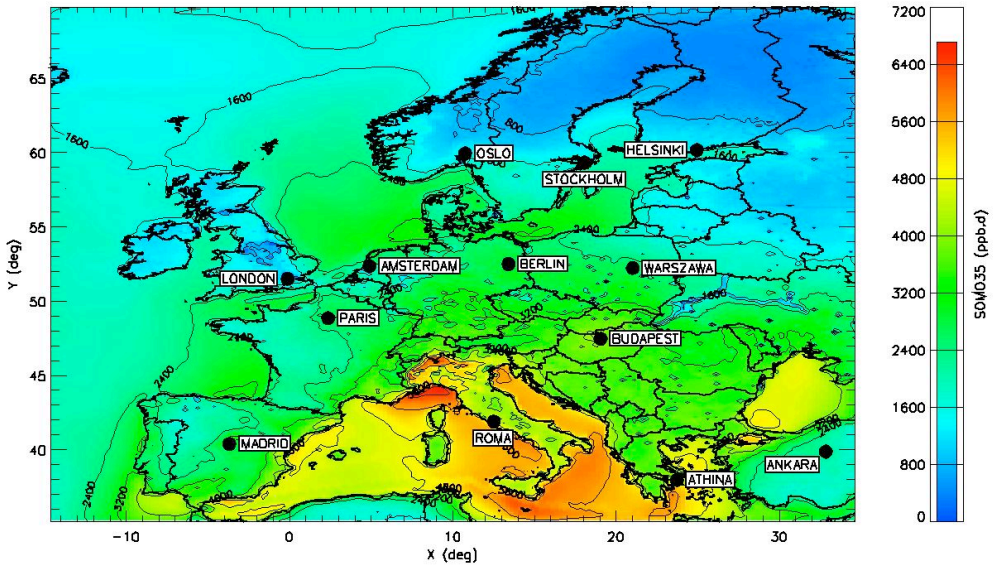

Figure A3.3.4: SOMO35 (ppb.d) for Retro 1, 1990.

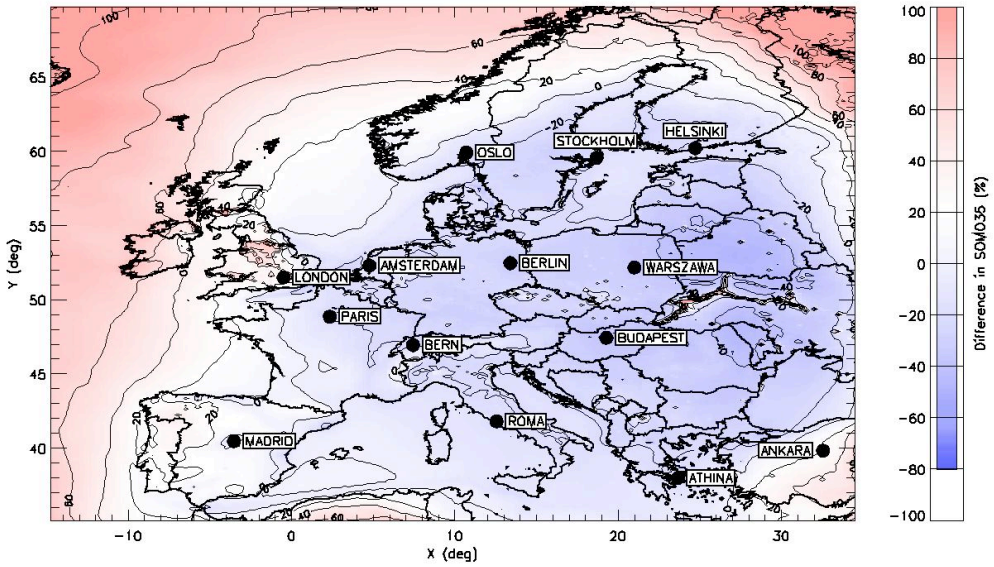

Figure A3.3.5: Difference in SOMO35 (%), RC 2005 – Retro 1, 1990.

A3.4 Particulate matter, PM2.5

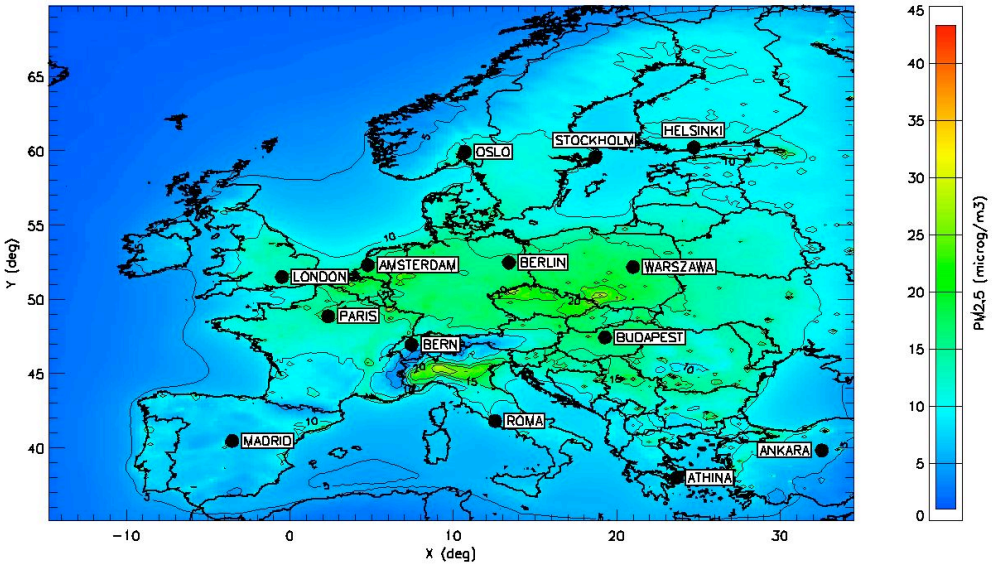

Figure A3.4.1: Annual average of PM2.5 ($\mu g.m^{-3}$) for RC 2005.

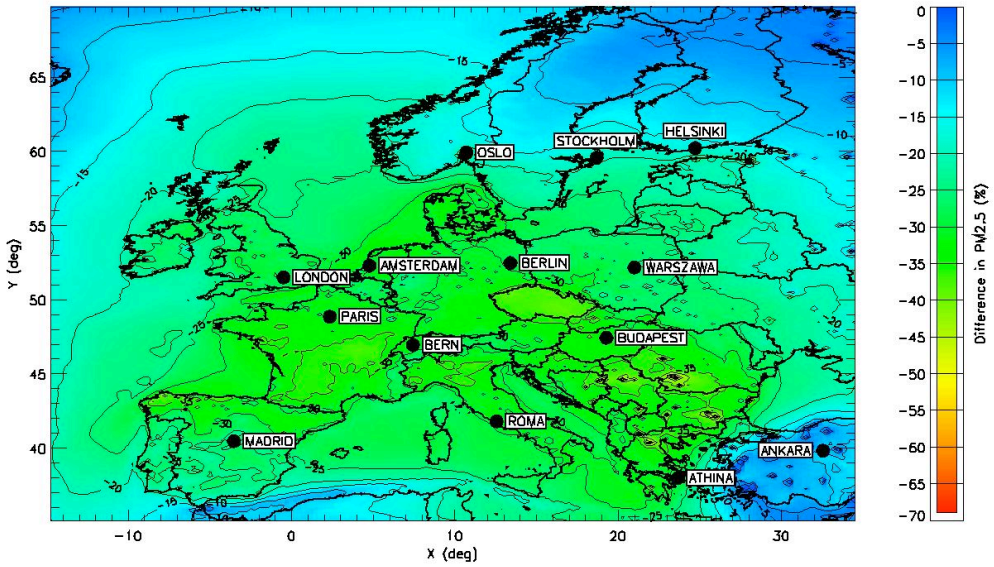

Figure A3.4.2: Difference in annual average of PM2.5 (%), BL 2020-RC 2005.

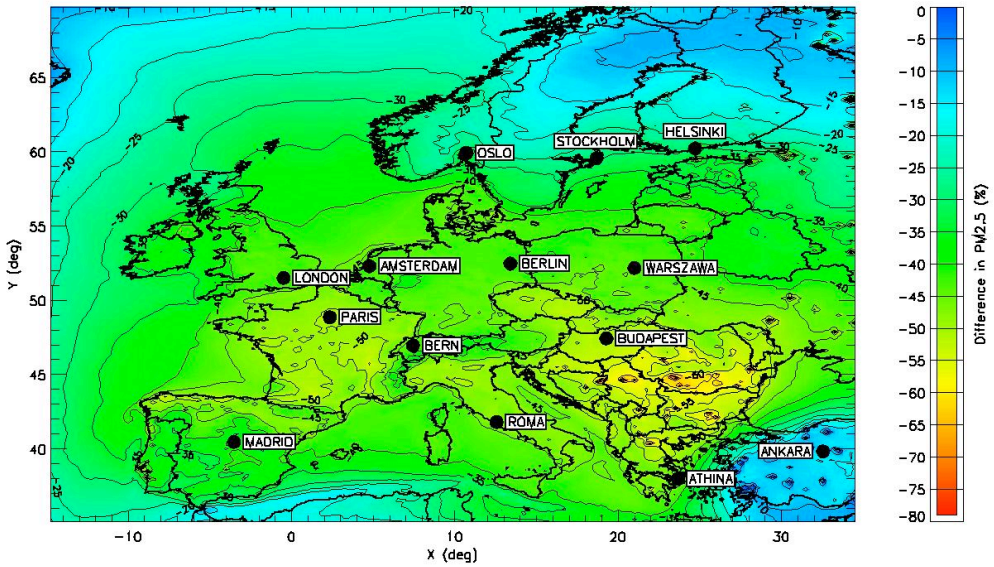

Figure A3.4.3: Difference in annual average of PM2.5 (%), MTFR 2020-RC 2005.

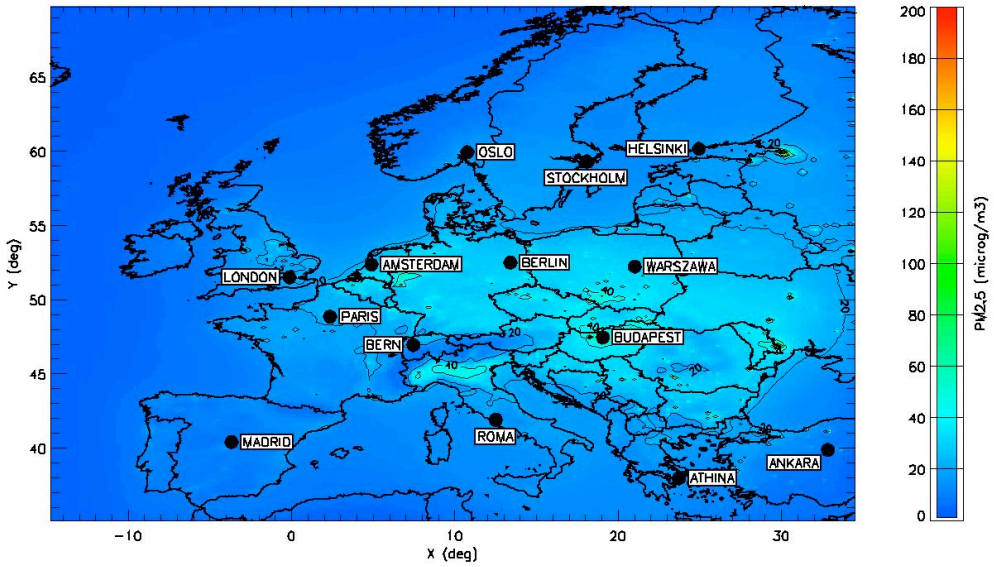

Figure A3.4.4: Annual average of PM2.5 ($\mu g.m^{-3}$) for Retro 1, 1990.

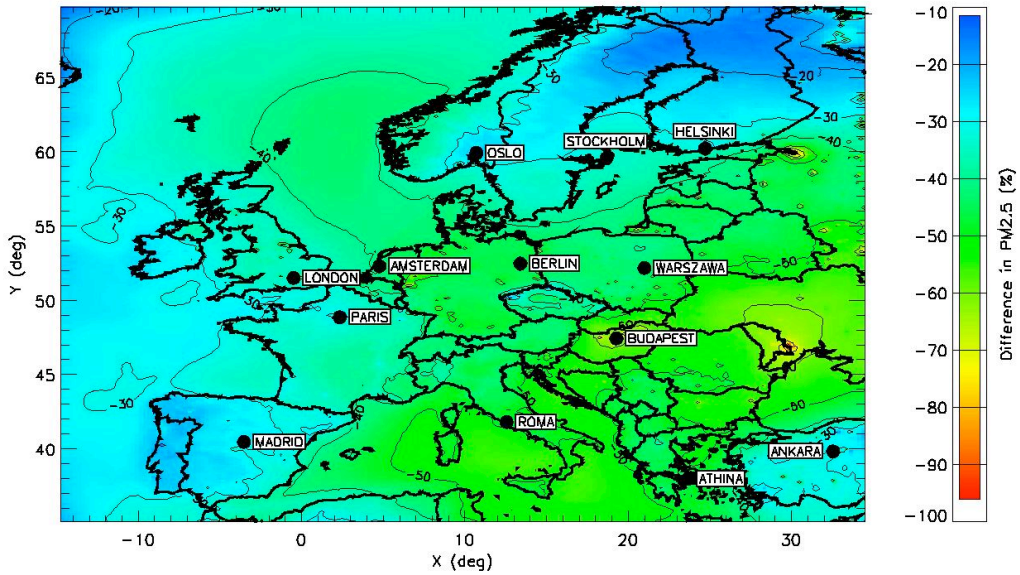

Figure A3.4.5: Difference in annual average of PM2.5 (%), RC 2005 – Retro 1, 1990.

A3.5 Particulate Matter, PM10

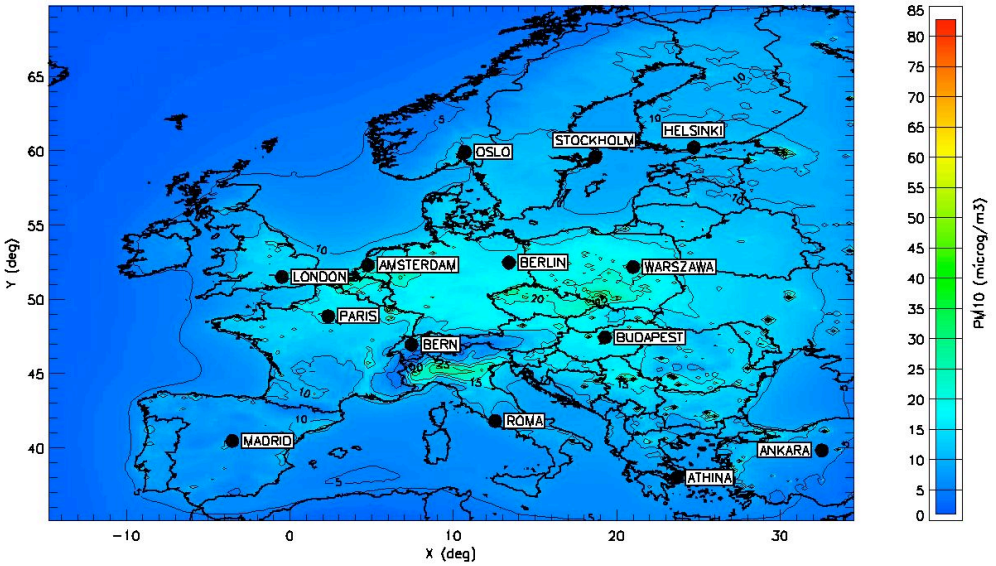

Figure A3.5.1: Annual average of PM10 ($\mu g.m^{-3}$) for the reference case (RC 2005).

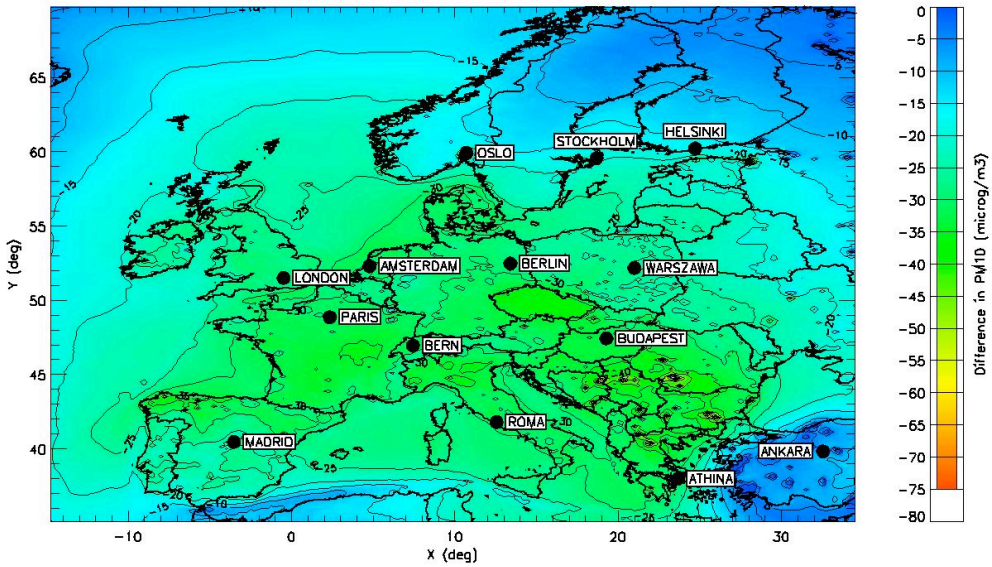

Figure A3.5.2: Difference in annual average of PM10 (%), BL 2020- RC 2005.

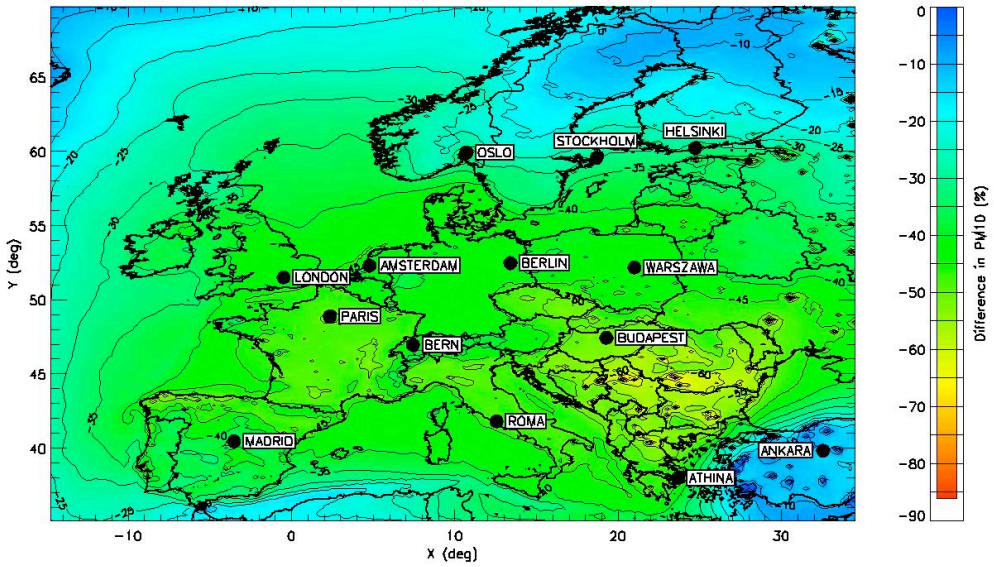

Figure A3.5.3: Difference in annual average of PM10 (%), MTFR 2020- RC 2005.